

UNCLASSIFIED

AD NUMBER

ADB103404

LIMITATION CHANGES

TO:

Approved for public release; distribution is unlimited.

FROM:

Distribution authorized to DoD and DoD contractors only; Critical Technology; APR 1986. Other requests shall be referred to Naval Ocean Research and Development Activity, NSTL, MI 39529-5004. This document contains export-controlled technical data.

AUTHORITY

NRL ltr, dtd 23 Aug 2007

THIS PAGE IS UNCLASSIFIED

UNCLASSIFIED

SECURITY CLASSIFICATION OF THIS PAGE

REPORT DOCUMENTATION PAGE																
1a. REPORT SECURITY CLASSIFICATION Unclassified		1b. RESTRICTIVE MARKINGS None														
2a. SECURITY CLASSIFICATION AUTHORITY		3. DISTRIBUTION/AVAILABILITY OF REPORT Distribution is limited to DoD and DoD contractors only.														
2b. DECLASSIFICATION/DOWNGRADING SCHEDULE																
4. PERFORMING ORGANIZATION REPORT NUMBER(S) NORDA Report 132		5. MONITORING ORGANIZATION REPORT NUMBER(S) NORDA Report 132														
6. NAME OF PERFORMING ORGANIZATION Naval Ocean Research and Development Activity		7a. NAME OF MONITORING ORGANIZATION Naval Ocean Research and Development Activity														
6c. ADDRESS (City, State, and ZIP Code) Ocean Science Directorate NSTL, Mississippi 39529-5004		7b. ADDRESS (City, State, and ZIP Code) Ocean Science Directorate NSTL, Mississippi 39529-5004														
8a. NAME OF FUNDING/SPONSORING ORGANIZATION Naval Ocean Research and Development Activity		8b. OFFICE SYMBOL (If applicable)		9. PROCUREMENT INSTRUMENT IDENTIFICATION NUMBER												
8c. ADDRESS (City, State, and ZIP Code) Ocean Science Directorate NSTL, Mississippi 39529-5004		10. SOURCE OF FUNDING NOS. <table border="1"><tr><td>PROGRAM ELEMENT NO. 62759N</td><td>PROJECT NO. SF59552C</td><td>TASK NO.</td><td>WORK UNIT NO.</td></tr></table>			PROGRAM ELEMENT NO. 62759N	PROJECT NO. SF59552C	TASK NO.	WORK UNIT NO.								
PROGRAM ELEMENT NO. 62759N	PROJECT NO. SF59552C	TASK NO.	WORK UNIT NO.													
11. TITLE (Include Security Classification) Environmental Support for High Frequency Acoustic Experiments Conducted at the Quinault Range, April-May 1983																
12. PERSONAL AUTHOR(S) M. D. Richardson, K. B. Briggs, R. I. Ray, and W. H. Jahn																
13a. TYPE OF REPORT Final		13b. TIME COVERED From _____ To _____		14. DATE OF REPORT (Yr., Mo., Day) April 1986												
15. PAGE COUNT 76																
16. SUPPLEMENTARY NOTATION																
17. COSATI CODES <table border="1"><thead><tr><th>FIELD</th><th>GROUP</th><th>SUB GR.</th></tr></thead><tbody><tr><td> </td><td> </td><td> </td></tr><tr><td> </td><td> </td><td> </td></tr><tr><td> </td><td> </td><td> </td></tr></tbody></table>			FIELD	GROUP	SUB GR.										18. SUBJECT TERMS (Continue on reverse if necessary and identify by block number) environmental support, geoacoustic properties, bottom roughness, bottom backscatter, grain size distribution, macrofauna distribution, high frequency acoustics	
FIELD	GROUP	SUB GR.														
19. ABSTRACT (Continue on reverse if necessary and identify by block number) Environmental data were gathered and analyzed that support the joint Naval Ocean Research and Development Activity, Naval Ocean Systems Center, Admiralty Underwater Weapons Establishment, and University of Washington/ Applied Physics Laboratory high-frequency acoustic experiment. The experiment was conducted 17 km west of the Washington coast in the Quinault Range (49-m water depth). An objective of this project was to provide the high-resolution acoustic and environmental data required to verify and develop high-frequency bottom scattering models. These models are required for developing new concepts in the design of naval weapon systems.																
20. DISTRIBUTION/AVAILABILITY OF ABSTRACT UNCLASSIFIED/UNLIMITED <input type="checkbox"/> SAME AS RPT. <input checked="" type="checkbox"/> DTIC USERS <input type="checkbox"/>			21. ABSTRACT SECURITY CLASSIFICATION Unclassified													
22a. NAME OF RESPONSIBLE INDIVIDUAL Kevin B. Briggs		22b. TELEPHONE NUMBER (Include Area Code) (601) 688-4692		22c. OFFICE SYMBOL Code 333												

LIBRARY
RESEARCH REPORTS DIVISION
NAVAL POSTGRADUATE SCHOOL
MONTEREY, CALIFORNIA 93940

Naval Ocean Research and Development Activity

April 1986

NORDA - Report-132



Environmental Support for High-Frequency Acoustic Experiments Conducted at the Quinault Range, April-May 1983

Michael D. Richardson

Kevin B. Briggs

Richard I. Ray

Oceanography Division

Ocean Science Directorate

Walter H. Jahn

Seafloor Geosciences Division

Ocean Science Directorate

Foreword

High-resolution acoustic and environmental data are required for developing new concepts in the design of weapon systems. These design concepts require statistical variability of acoustic and environmental data to model the effects that the ocean bottom and surface boundaries have on transmitted acoustic signals.

This report presents the biological, geoacoustic, and bottom roughness data required to model forward, back, and out-of-plane scattering from the sediment-water interface. Environmental and acoustic data were collected on a joint Naval Ocean Research and Development Activity, Naval Ocean Systems Center, Admiralty Underwater Weapons Establishment, University of Washington/Applied Physics Laboratory high-frequency acoustic experiment. This report, and other reports supported by the high-frequency acoustic block (NAVSEA Program Element 62759N), should provide the high-quality data required to improve the reliability of current Navy weapon systems that rely on bottom interaction models and will provide a basis for development of future systems.

A handwritten signature in dark ink, appearing to read 'R. P. Onorati', is positioned above the printed name and title.

R. P. Onorati, Captain, USN
Commanding Officer, NORDA

Executive summary

Environmental data were gathered and analyzed that support the joint Naval Ocean Research and Development Activity, Naval Ocean Systems Center, Admiralty Underwater Weapons Establishment, and University of Washington/Applied Physics Laboratory high-frequency acoustic experiment. The experiment was conducted 17 km west of the Washington coast in the Quinault Range (49-m water depth). An objective of this project was to provide the high-resolution acoustic and environmental data required to verify and develop high-frequency bottom scattering models. These models are required for developing new concepts in the design of naval weapon systems.

Surficial sediments in the Quinault Range were uniformly fine to very fine sand that had a mean porosity of 41.2% (coefficient of variation (CV) = 4.98) and mean grain size of 2.92ϕ (CV = 3.63). Compressional wave velocity ratio was 1.113 (CV = 1.19), and compressional wave attenuation was 148 dB/m at 400 kHz (CV = 33.08). Variability of sediment geoacoustic properties was approximately the same as reported for other shallow-water sandy sediments. Vertical variability of geoacoustic properties in the upper 22 cm of sediment was greater than horizontal variability over ranges of 100 m to 3 km. Bottom roughness (RMS, power spectral density) was determined from stereophotographs of the sediment. The strike of the largest sand ripples in the photographs ran perpendicular to the Washington coast. This resulted in higher values of RMS roughness (1.64 cm) and power spectral density for lines parallel to the coast than lines perpendicular to the coast (RMS = 1.20 cm). The greatest percentage of the bottom roughness variability, however, was associated with small-scale variations in bottom heights (over a distance of 10–500 m) rather than in azimuthal directionality. Sediment geoacoustic and roughness properties in the Quinault Range were primarily controlled by hydrodynamic, as opposed to biological, processes.

Bottom backscatter strengths were predicted from the environmental data using the semi-empirical model developed by D. R. Jackson of the University of Washington. Jackson's model is a simplification of composite-roughness and volume scattering models, and is supplemented by the Kirchhoff approximation for grazing angles near normal incidence. The range of variation of sediment geoacoustic properties had little impact on predicted bottom backscatter strengths. Both small-scale variations and azimuthal directionality of bottom roughness appeared to control predicted backscatter strengths. Small-scale horizontal variations (10–500 m) in roughness had a greater impact on predicted backscatter strengths than on azimuthal directionality.

If current models adequately predict bottom backscatter strength from environmental inputs, the range, the variability, and the distribution of bottom backscattering along the entire Washington continental shelf should be predictable from currently available environmental inputs. These inputs include depth, sediment type, dominant benthic communities, and past and present hydrodynamic conditions. These backscatter strength predictions could be made on both the spatial and the temporal scales required by current and future naval operational needs.

Acknowledgments

The authors particularly thank Dr. Darrell Jackson and his coworkers at the University of Washington, Applied Physics Laboratory (UW/APL) for logistics support. We also thank Dr. Jim Syck of the Naval Underwater Systems Center, New London, Connecticut, for advice on contouring bottom roughness features from paired stereophotographs, and Mr. Don Smith of Aerial Cartographic Technology, Cranston, Rhode Island, for making the actual contours. Drs. Darrell Jackson and Don Percival of UW/APL provided valuable information on bottom scattering models and analysis of bottom roughness data, respectively. This work was supported by NAVSEA Program Element 62759N, Dr. Robert L. Martin, program manager.

Contents

I. Introduction	1
II. Materials and methods	1
A. Description of study site	1
B. Field collection	2
C. Field analysis	2
D. Laboratory analysis	4
III. Results	6
A. Sediment geoacoustic properties	6
B. Bottom roughness	6
C. Biological data	11
IV. Discussion	11
A. Variability of sediment geoacoustic and bottom roughness properties	11
B. Prediction of in situ sediment geoacoustic properties	12
C. Prediction of acoustic bottom backscattering	13
V. Conclusions	15
VI. References	16
Appendix A. Sediment physical and geoacoustic data	19
Appendix B. Sediment grain size distribution data	
Appendix C. Sediment roughness contours and roughness profiles of cross-sectional lines	
Appendix D. Power spectral density functions from individual photographs	

Environmental support for high-frequency acoustic experiments conducted at the Quinault Range, April–May 1983

I. Introduction

Environmental data were gathered and analyzed that support the joint Naval Ocean Research and Development Activity (NORDA), Naval Ocean Systems Center (NOSC), Admiralty Underwater Weapons Establishment (AUWE), and University of Washington, Applied Physics Laboratory (UW/APL) high-frequency acoustic experiment. The experiment was conducted 17 km west of the Washington coast in the Quinault Tracking Range (49-m water depth).

The objective of this project was to provide the high-resolution acoustic and environmental data required for new concepts in designing weapon systems. These design concepts require statistical variability of acoustic and environmental data to model the effects that ocean bottom and surface boundaries have on transmitted acoustic signals.

In this report we provide the biological, geoacoustic, and bottom roughness data required to model forward, back, and out-of-plane scattering from the sediment-water interface. Using environmental data inputs we also predict acoustic bottom scattering for frequencies and grazing angles used in this experiment. These predicted results should be compared to bottom scattering data collected by D. R. Jackson (UW/APL).

The combined environmental and acoustic data will not only be important for weapon system design and performance prediction, but will be invaluable for acoustic sub-model development and verification (Sienkiewicz, 1985). Most of the empirical and quasi-theoretical submodels used today are based on limited data sets, have not been validated, or do not cover acoustic and environmental conditions of interest to weapon system developers. This and other projects supported by the high-frequency acoustic block (NAVSEA Program Element 62759N) should provide the high-quality environmental and acoustic data required to develop these bottom-scattering models.

II. Materials and methods

A. Description of study site

The Oregon-Washington continental shelf is characterized by three separate sedimentological regimes that parallel

the coastline (McManus, 1972; Kulm et al., 1975; Sternberg et al., 1977). At depths less than 60 m, modern sand from the Columbia and other rivers accumulates; a mid-shelf modern silt deposit is found between 60 and 150 m, and relict sand remains uncovered beyond 150 m. The Quinault Shallow Water Tracking Range is located on the modern sand facies in an approximately 50-m water depth (Fig. 1). Surficial sediments are fine sands that have less than 5% silt- and clay-sized particles (Krell, 1980). Most of the sand material is supplied by the Columbia River with minor inputs from the nearby Queets and Hoh Rivers (Stewart, 1980). Off the Washington coast, average bottom currents flow northward at 1–2 km/day at depths

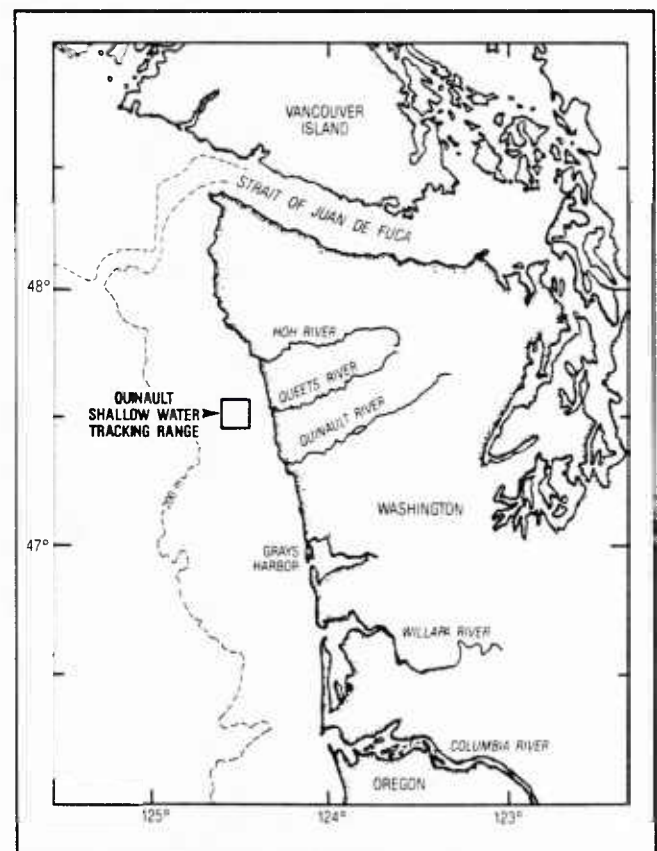


Figure 1. Location of Quinault Acoustic Shallow Water Tracking Range.

of 40–100 m (Barnes et al., 1972). These currents, coupled with storm events, are responsible for distributing Columbia River sediments on the Washington continental shelf. Sediments in the Quinault Range are in dynamic equilibrium with present hydrographic conditions. Average storm conditions are sufficient to produce sediment ripples at 100-m depths off the Washington coast, and occasional sand ripples are produced as deep as 200 m by major winter storms (Komar et al., 1972). Longer period ocean swells from distant storm sources are responsible for the variations in sand ripple length and height in deeper water, whereas locally produced ocean surface waves stir and rework the shallower shelf sediments (Komar et al., 1972).

The inner continental shelf along the Washington coast is characterized by a shallow-water sand-bottom benthic community (Lie, 1969; Lie and Kelley, 1970; Lie and Kisker, 1970). Dominant macrobenthic animals are the cumacean *Diastylopsis dawsoni*; the amphipods *Ampelisca macrocephala* and *Paraphoxus obtusidens*; the bivalves *Tellina salmonea*, *Macoma expansa*, and *Siliqua patula*; and the polychaetes *Owenia fusiformis*, *Chaetozone setosa*, and *Nephtys* spp. Extensive bioturbation by this low diversity, low biomass (1.4 g ash-free dry wt/m²) benthic assemblage should not be expected.

B. Field collection

The experiments were conducted at two sites in the Quinault Range (Fig. 2). The north site was the location for the UW/APL mobile V-fin acoustic backscatter measurements and the south site was located near the high-resolution, bottom-mounted acoustic arrays.

A 0.25 m² USNEL box corer was used to remotely collect relatively undisturbed sediment samples for determining the spatial variability of sediment geoaoustic properties and the abundance of macrobenthic animals (Fig. 3a–c). Four box cores each were collected from the north (Nos. 3–6) and south (Nos. 1, 2, 7, and 8) sites. Cylindrical subcores (6.1-cm inside diameter and 48-cm length) were used to collect the sediment subsamples, which were later used for determining sediment physical and acoustic properties (Fig. 3c). The remaining sediments from box cores 1, 6, 7, and 8 were rinsed through a 1.00-mm screen. Material retained on the screens was stained with rose bengal and preserved in 5% formalin buffered with NaH₂BO₃. Macrofaunal animals were later sorted from this debris in the laboratory.

Stereophotographs of the sediment surface were made with two Photosea 70D 70-mm underwater cameras mounted in tandem with two Photosea 15005D 150-W/sec underwater strobes on a balanced steel frame. Distance

between optical axes of the cameras was 37.8 cm. The cameras and strobes were simultaneously actuated by a bottom contact switch connected to a weighted compass vane. In separate instances, stereophotographs of the sediment surface were taken at distances of 3 and 6 ft from the bottom by changing the length of wire connecting the bottom contact switch to the compass vane. By alternately lowering and raising the apparatus while drifting, a series of paired photographs were taken of the bottom. Twenty-five pairs of stereophotographs were taken at the 3-ft focal distance (*f*/8, 1/125 s), and 50 pairs of stereophotographs were taken at the 6-ft focal distance (*f*/5.6, 1/125 s). All stereophotography was conducted at the north site (Fig. 2). The color film (Kodak 70-mm Ektachrome, ASA 64) was developed on return from the field, and paired photographs were subsequently used to determine bottom roughness.

C. Field analysis

Sediment compressional wave velocity and attenuation were measured after sediments equilibrated with laboratory temperature aboard ship. Temperature and salinity of the

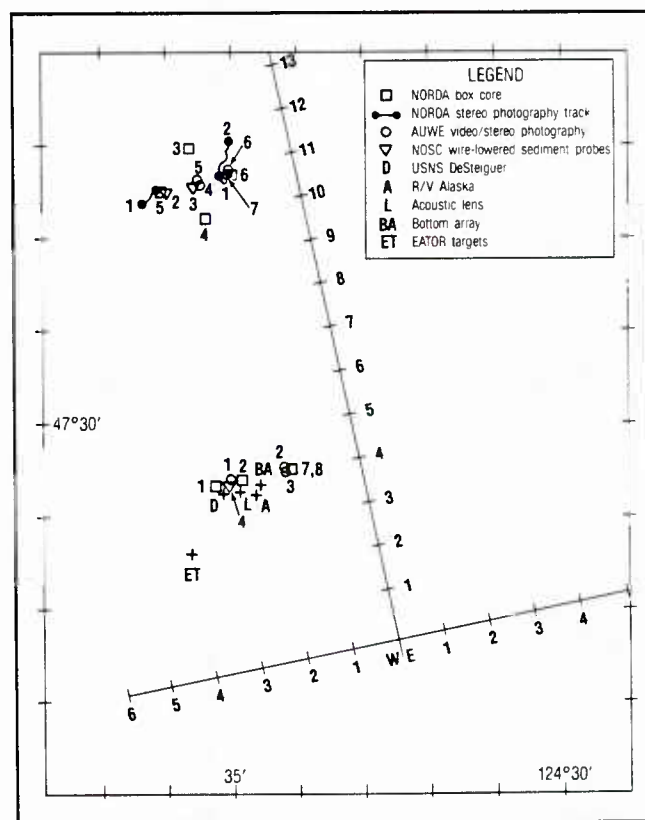


Figure 2. Location of box core and stereophotographic samples collected in the Quinault Range from 28 April to 1 May 1983.

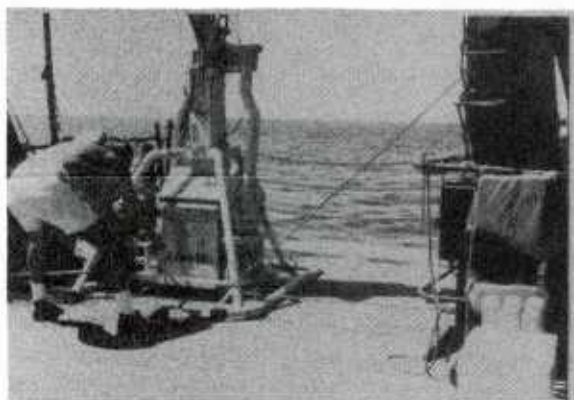
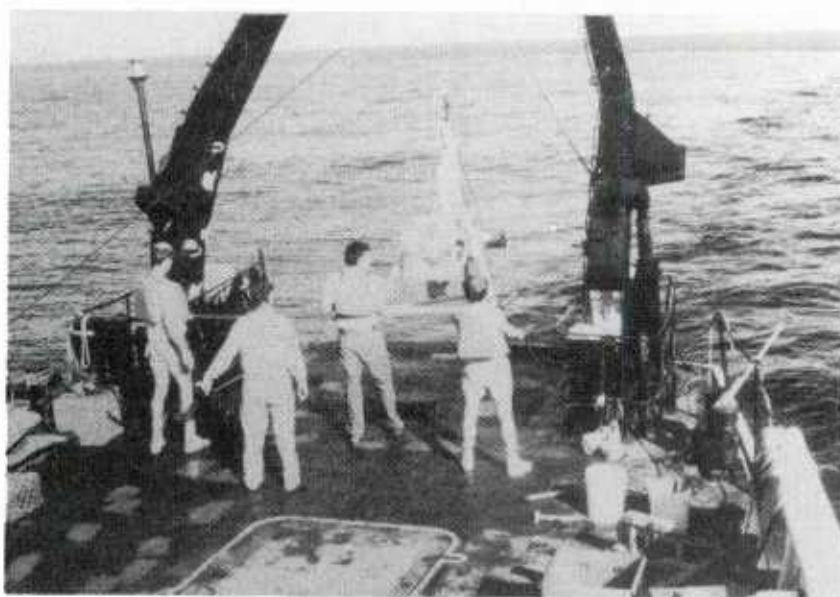


Figure 3. (a) Deployment, (b) recovery, and (c) subcore sampling of a 0.25 m Mk III box corer from the U-frame of a USN AGOR.

overlying water were measured with a YSI model 43TD temperature probe and an AO Goldberg temperature-compensated salinity refractometer. Compressional wave velocity and attenuation were measured at 1-cm intervals on sediments in subcores using a pulse technique.

Time delay measurements were made through sediments and a distilled water reference with a Hewlett-Packard 1743A dual time interval oscilloscope. Signals were generated by driving an Underwater Systems, Inc. (Model USI-103) transducer-receiver head with a 400-kHz, 20-V p-p sine wave triggered for 25 μ sec duration every 10 msec with a Tektronix PG 501 pulse generator and FG 504 function generator. Differences in time delay between distilled water and the sediment samples were used to calculate sediment compressional wave velocity (V_p). All sound velocities were calculated for the approximate in situ conditions at the time of the acoustic experiment (10°C, 32.5 ppt, 49 m). Compressional wave velocity was also expressed as the dimensionless ratio of measured sediment velocity divided by the velocity in the overlying water (both calculated for the same temperature, salinity, and depth; after Hamilton, 1971). This ratio is independent of sediment temperature, salinity, and depth, and is therefore ideal for comparison to other geoacoustic properties. Attenuation measurements were calculated as 20 log of the ratio of received voltage through distilled water to received voltage through sediment (Hamilton, 1972). Attenuation values were extrapolated to a 1-m pathlength and expressed as dB/m. Attenuation was also expressed as a sediment specific constant (k), which is reported to be independent of frequency or pathlength by Hamilton (1972). After acoustic measurements were made, all subcores were refrigerated for subsequent laboratory analysis of sediment porosity and mean grain size distribution.

D. Laboratory analysis

Cores were sectioned at 2-cm intervals by extruding the sediment with a plunger and slicing the exposed sediment off with a spatula. Immediately after sectioning, subsamples of extruded sediment for porosity determinations were placed in preweighed aluminum pans, weighed, dried in an oven at 105°C for 24 hours, cooled in a desiccator, and reweighed. Percent water was calculated by dividing the weight of evaporated water (difference between wet and dried sediment weights) by the weight of the dried solids and multiplying by 100. Using an average grain density value of 2.65 for sands, porosity values were determined from tables relating porosity to water content (Lambert and Bennett, 1972). The values were not corrected for the salinity of pore water.

Grain size analysis of sediment was done essentially as described by Folk (1965). The sediment samples were soaked overnight in 200 ml of dispersant solution (2.5 g of sodium hexametaphosphate per liter of distilled water), then disaggregated by sonicating the sample with a cell disruptor for 12 minutes, while simultaneously stirring the sample with a magnetic stirrer. The disaggregated sample was wet-sieved with dispersant through a 62- μ m screen to separate the sand-sized fraction from the silt- and clay-sized fraction. The finer fraction was collected in a 1000-ml graduated cylinder, and enough dispersant was added to fill the graduated cylinder to 1000 ml. The coarser fraction was rinsed off the screen with distilled water into a beaker and then dried.

The dried, coarser fraction was fractionated into whole phi intervals (-3 to 4ϕ) with a CE Tyler sieve shaker. Each fraction was individually weighed to determine the sand-sized particle distribution. The silt- and clay-sized fraction was thoroughly agitated by vigorous stirring and aeration. A 20-ml aliquot sample representative of the total distribution of particles in suspension was pipetted from the graduated cylinder, transferred to a preweighed beaker, dried in an oven, and weighed. After 85 minutes, 20-ml aliquot samples were pipetted from the appropriate depths in the graduated cylinder, transferred to preweighed beakers, dried, and weighed to estimate the weight of clay-sized particles ($>8\phi$).

Sediment grain size distributions were analyzed with an HP 9825A desktop computer and plotted with an HP 9862A plotter (unpublished program is available on request). Data were plotted as weight percent histograms and cumulative weight percent for all ϕ -sizes through 14ϕ . Because the sediment was predominantly sand ($<4\phi$), the silt fraction was equally divided between the whole phi intervals between 4 and 8ϕ ; the clay fraction was equally divided between whole phi intervals between 8 and 14ϕ . Percentages of gravel ($<-1.0\phi$), sand (-1.0 to 4.0ϕ), silt (4.0 to 8.0ϕ), and clay ($>8.0\phi$) were tabulated. The mean phi, standard deviation, skewness, kurtosis, and normalized kurtosis were calculated according to the graphic formula of Folk and Ward (1957).

Stereophotographs were analyzed by two methods to determine bottom roughness. First, wavelengths and orientation of sand ripples were measured using the known length (33 cm) and the displayed heading of the compass vane, which is visible in each photograph (Fig. 4). Values for wavelength and orientation were tabulated for both photographic sampling tracks and expressed as relative frequency histogram distributions.



Figure 4. Example of a seafloor photograph used to determine wavelength and orientation of dominant sand ripples at the Quinault Range. Compass and vane were 33 cm long.

Second, 14 pairs of stereophotographs were selected for bottom contouring based on picture clarity, presence of representative features, and parallel orientation with the bottom. Contours of bottom roughness features were made by Aerial Cartographic Technology of Cranston, Rhode Island, using a Kern-2AT stereoplotter. Spatial accuracies of better than 1 mm should be expected from the system used (Smith and Boyajian, 1984). Bottom roughness was calculated both as RMS roughness and as power spectral density function for six cross-sectional lines drawn on 11 of the contour plots. The orientation of these lines was chosen to parallel the two different ship's course headings maintained by Darrell Jackson (UW/APL) when he collected acoustic bottom scattering data. Figure 5 is an example of a bottom contour plot with six sampling cross-sectional lines, a compass rose, and the resultant bottom heights.

Relative sediment height was determined from not less than 64 equally spaced (at 0.5-cm intervals) points along a 31.5-cm pathlength for all 66 cross-sectional lines. RMS roughness was calculated as standard deviation about the mean height. No attempt was made to remove the effects of long wavelengths from these relatively short profiles. The power spectral density function was calculated for each set of 64 data points using manipulations suggested by Don Percival of UW/APL (personal communication, 1985). Actual data were prewhitened by taking differences of adjacent data points, and then possible leakage was eliminated by subtracting the sample mean from the prewhitened data. Data were tapered with a 20% cosine bell data taper. A fast Fourier transform was used to compute a periodogram from the first 64 data points. The periodogram was corrected for prewhitening by dividing each value by $4 \sin^2 \pi f_j \Delta$; where f_j is defined by $j/64 \Delta$; $j = 0, 1, 2, \dots, 32$; and Δ is the spacing between original data points (0.5 cm). The spectral density function was then averaged over the total number of cross-sectional lines taken for each azimuthal heading (i.e., 33 tracks for each heading).

III. Results

A. Sediment geoacoustic properties

The vertical distributions of sediment geoacoustic properties for 12 cores collected at the north site and 17 cores collected at the south site are presented in Appendix A. Although significant differences were found between the sites with respect to mean values of most geoacoustic properties (Table 1), these differences were so small that data for both sites were combined in Figures 6–9. Differences

of 10 m/sec, 22 dB/m and 0.07ϕ between mean values of compressional wave velocity, attenuation, and mean grain size at each site have little or no geoacoustic significance in bottom scattering models. Only the large number of samples collected allowed us to detect the small, yet real, differences in mean values of geoacoustic properties between the two sites.

Values of porosity ranged from 37.3 to 48.2% (mean 41.2%) in cores collected at the Quinault Range (Fig. 6). The slight increase in porosity with depth in the cores corresponded to an increase in the percent silt and clay. The highest values of porosity and percentages of silt and clay were found in the 12–18 cm depth intervals.

Sediment mean grain size ranged from 2.82 to 3.52ϕ (mean 2.94ϕ), with only two values (3.26ϕ and 3.52ϕ) outside an even smaller range of 2.82 – 3.07ϕ (Fig. 7). Sediments in the upper 12 cm were moderately to moderately well sorted, near-symmetrical to fine skewed, fine to very fine sands. Little downcore variation was evident in particle size distribution until the 12–14 cm depth interval, where a 6–8 cm thick layer with coarse shell relicts and a greater percentage of silt and clay began. Sediments in this deeper layer were poorly sorted, strongly fine-skewed, very leptokurtic fine sands. Core 5-1 was atypical in that the shell layer was not apparent at least to the maximum depth sampled (20 cm). Particle size frequency histograms for all sediment samples are presented in Appendix B.

Compressional wave velocities calculated for in situ conditions (10°C , 32.5 ppt, 49 m) ranged from 1572 to 1692 m/sec (mean 1655 m/sec) (Fig. 8). These values are equivalent to a range of 1616–1740 m/sec and a mean of 1702 m/sec at the standard laboratory conditions (23°C , 35 ppt, 0 m) defined by Hamilton (1971). Compressional wave velocity and velocity ratio decreased with depth (F-statistic = 54.5). The predicted velocity ratio, given the regression in Figure 8, is 1.119 at 1 cm and 1.102 at 20 cm.

Values of attenuation at 400 kHz ranged from 92 to 377 dB/m (mean 160 dB/m). These values are equivalent to sediment specific k values of attenuation of 0.230–0.942 (mean 0.40) calculated after Hamilton (1972). Compressional wave attenuation increased with depth (F-statistic = 389) from near 120 dB/m at 1 cm to 260 dB/m at a 20-cm core depth. Variability of values of attenuation was greatest below 12 cm depth in the cores.

B. Bottom roughness

The most striking feature in bottom photographs taken in the Quinault Range was the presence of large sand ripples. The strike of most large sand ripples ran west-southwest

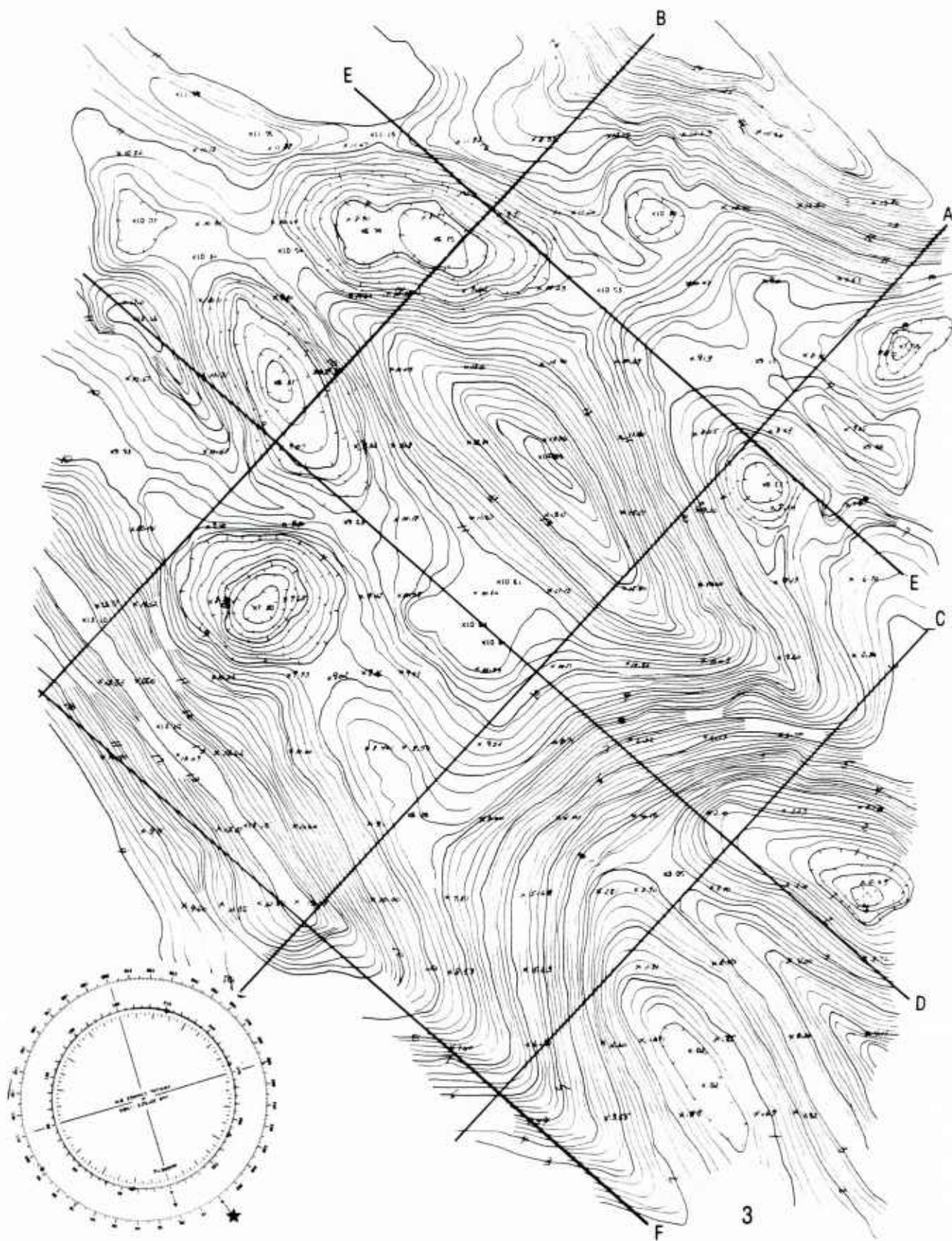


Figure 5. Bottom roughness contours and resultant bottom height profiles for a pair of stereophotographs taken in the Quinault Range. Included are six cross-sectional lines parallel and perpendicular to the azimuthal headings used by D. R. Jackson to obtain acoustic data.

Table 1. Mean values of sediment geoacoustic properties from north and south sites in the Quinault Range. Differences in means based on Mann-Whitney U-test.

Geoacoustic Property	North	South	Difference in Means
Compressional wave velocity (10°C, 32.5 ppt, 49 m)	1652	1662	***
Attenuation (dB/m @ 400 kHz)	162	140	*
Mean grain size (ϕ)	2.97	2.90	***
Porosity (%)	41.4	40.8	n.s.

* at 95% significance level

*** at 99.9% significance level

(257°) to east-northeast (77°) (Fig. 10), and the mean wavelength was 11.96 cm (Fig. 11).

Contour plots of relative bottom height for 11 paired stereophotographs are presented in Appendix C. Photographs 1, 2, 3, 10, 12, and 13 were obtained on photographic track 1; photographs 4, 5, 7, 8, and 9 were

obtained on photographic track 2. Superimposed on each contour plot are cross-sectional lines running parallel to the ship's azimuthal headings during Jackson's measurement of acoustic backscatter strength. For each contour plot, three cross-sectional lines run parallel to the Washington coastline (171–351°), and three cross-sectional lines are perpendicular to the coastline (81–261°). Waveheight versus distance over the bottom (31.5 cm) was plotted for each of these lines (Appendix C).

RMS roughness (calculated as standard deviation) along these cross-sectional lines ranged from 0.08 to 3.84 cm, and the mean was 1.42 cm (Table 2). Three photographs (4, 5, 7) exhibited low roughness values (mean 0.34 cm), but roughness values were higher at the other eight sites (means 1.31–2.51 cm). Mean RMS roughness was significantly higher for cross-sectional lines parallel to the coast (mean 1.64 cm) compared to cross-sectional lines perpendicular to the coast (mean 1.20 cm) (t-test, $\alpha < 0.05$).

Periodograms estimating power spectral density functions for the two orientations of cross-sectional lines are

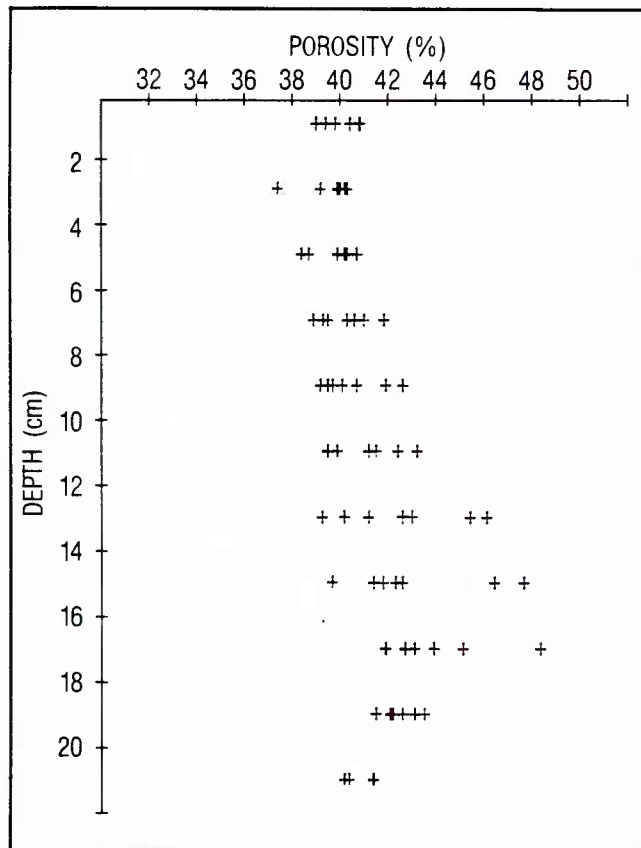


Figure 6. Vertical distribution of values of sediment porosity (%) determined from seven subcores collected at the Quinault Range.

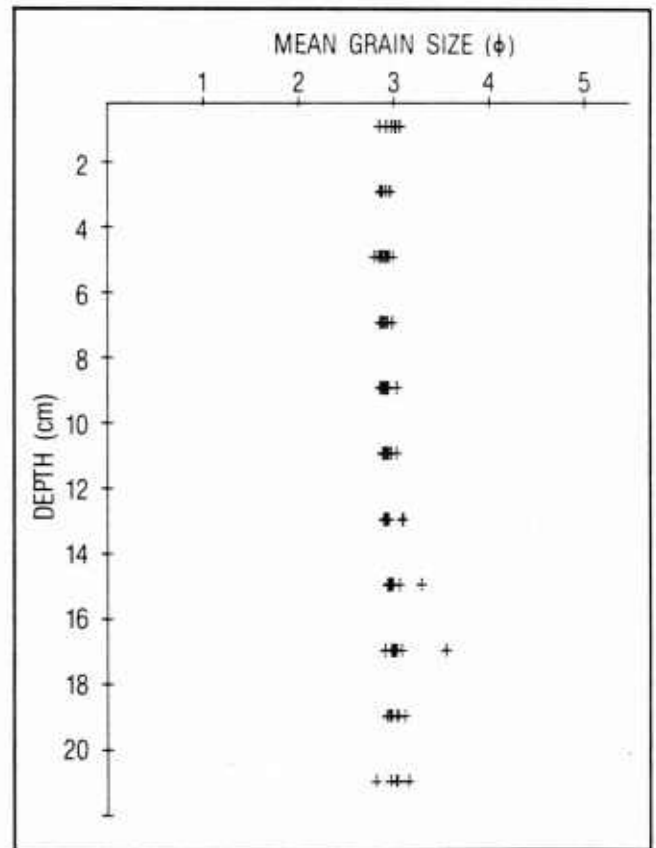


Figure 7. Vertical distribution of values of sediment mean grain size (ϕ) determined from seven subcores collected at the Quinault Range.

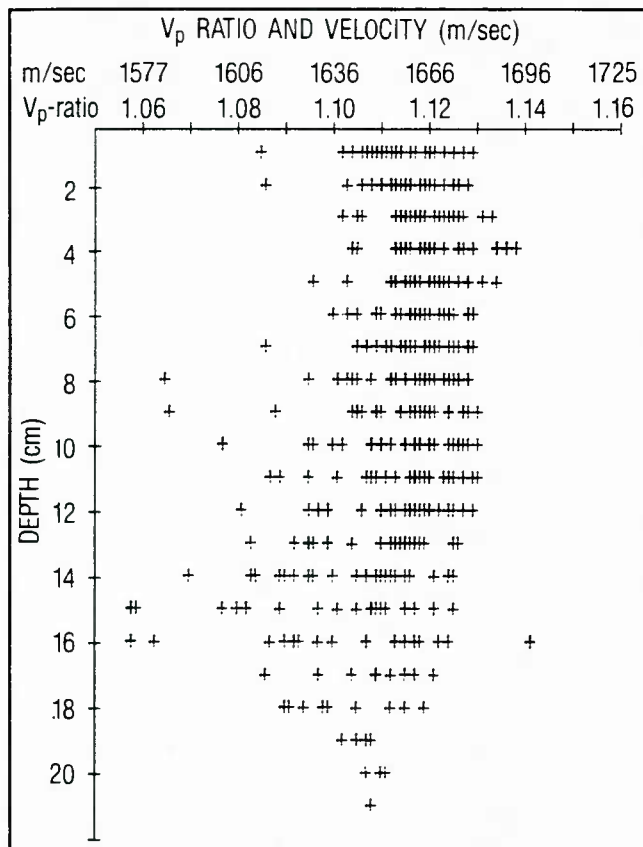


Figure 8. Vertical distribution of values of sediment compressional wave velocity (m/sec) and velocity ratio determined from 36 subcores collected at the Quinault Range. Compressional wave velocity calculated for experimental in situ conditions of 10°C, 32.5 ppt, and 49 m water depth. $V_p = 1665 - 1.32 \times \text{depth (cm)}$.

presented in Figure 12. Each periodogram represents an averaging of 33 spectral function ordinates (corresponding to 33 cross-sectional lines) for each orientation. The 95% confidence interval displayed on the plot is computed from tabulated chi-square values at 0.975 and 0.025 levels, with 66 (i.e., 2×33) degrees of freedom divided by an adjustment factor of 1.116 to account for the effects of tapering the data (Bloomfield, 1976). The upper confidence limit is calculated as $1.487 \times S(f)$; the lower limit is calculated as $0.719 \times S(f)$. The confidence interval is applicable to each point of the periodograms because, in this case, bandwidth is equal to the frequency interval (0.03125 cm^{-1}). Superimposing the confidence interval on each spectral value reveals that the sea bottom in the Quinault Range has no significant frequencies of roughness (Fig. 12); the power spectrum is concentrated in the low-frequency end. The 95% confidence intervals for the two periodograms in Figure 12 do not overlap throughout the entire fre-

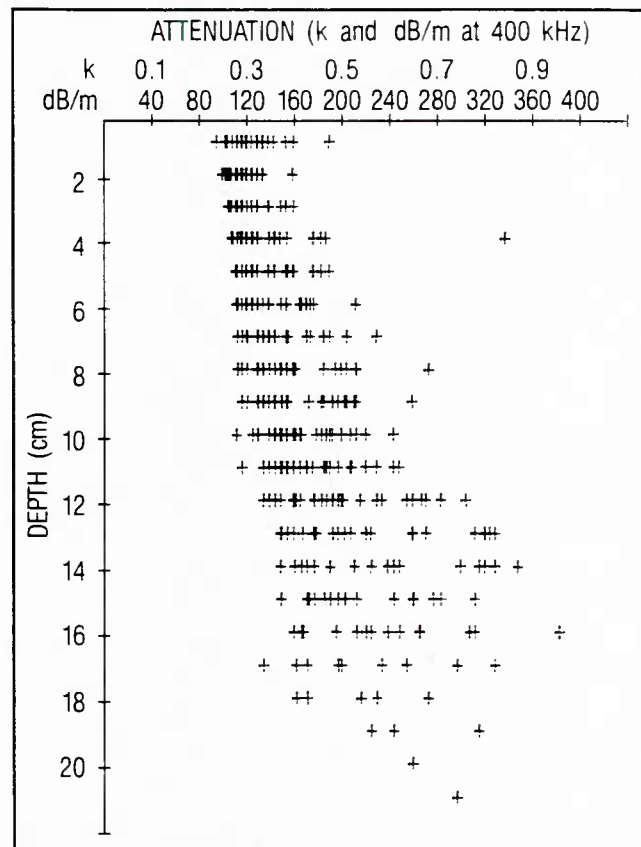


Figure 9. Vertical distribution of values of sediment compressional wave attenuation (k , $\alpha = \text{dB/m}$ @ 400 kHz) determined from 36 subcores collected at the Quinault Range. $\alpha = 92 + 8 \times \text{depth (cm)}$.

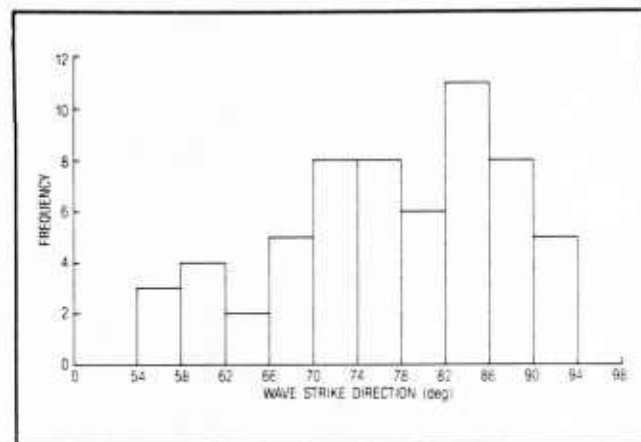


Figure 10. Frequency histogram of azimuthal directions of the strike of dominant sand ripples measured from 60 bottom photographs taken at the Quinault Range ($n = 60$).

quency spectrum. From this observation we conclude that the power spectral density functions of bottom roughness for orientations A-C and D-F were significantly different

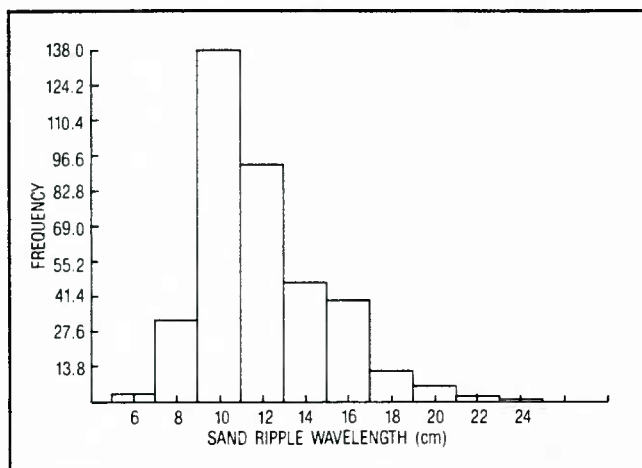


Figure 11. Frequency histogram of the wavelengths of dominant sand ripples measured from 60 bottom photographs taken at the Quinault Range ($n = 375$).

and that greater power spectral density roughness was found for tracks parallel to the Washington coastline (A–C).

Eleven periodograms, each representing an average of the six cross-sectional lines in each photograph, are presented in Appendix D. A comparison of individual photographs, regardless of azimuthal direction, reveals that all power spectral density functions fall within 95% confidence bounds of another function. Periodograms representing photographs 5 and 7 depict the outer limits of the ranges of power spectral density functions and, consequently, are significantly different at the 95% confidence level.

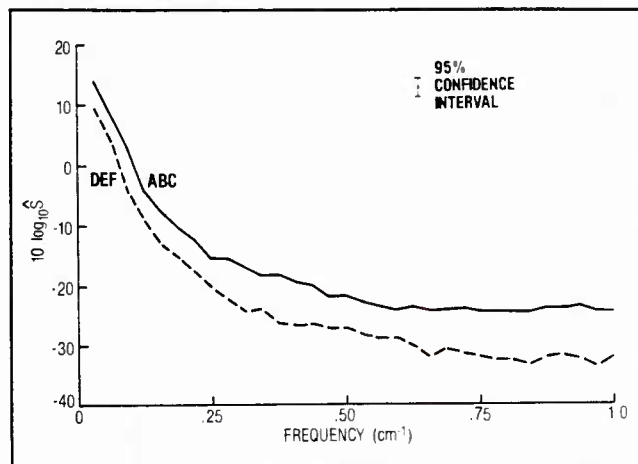


Figure 12. Power spectral density ($10 \log_{10} \hat{S}$) versus frequency (cm^{-1}) for relative bottom height measurements derived from stereophotographs of Quinault Range sediments. Data collected from cross-sectional lines perpendicular (DEF) and parallel (ABC) to the coast. The 95% confidence intervals are given for each point of the periodograms.

A plot of (log) power spectral values versus (log) frequency for each orientation yields regression slopes of -2.67 and -2.92 for A–C and D–F orientations, respectively. There is no significant difference in regression slopes of the two orientations by analysis of covariance ($F_s = 2.79$). We therefore conclude that despite differences in overall values of power spectral density between azimuthal directions, there was little difference in the relative

Table 2. Values of RMS roughness (cm) determined from stereophotographs of bottom sediments in the Quinault Range. Each of the 66 cross-sectional lines was 31.5 cm long. Lines A–C were parallel to the Washington coastline ($171\text{--}351^\circ$); lines D–F were perpendicular ($81\text{--}261^\circ$).

Photograph	Cross-Sectional Lines						Mean
	A	B	C	D	E	F	
1	3.315	3.842	3.380	0.490	0.583	0.557	2.03
2	2.662	1.416	3.726	1.988	1.530	3.752	2.51
3	1.684	1.945	1.984	3.709	1.314	3.708	2.39
4	0.573	0.557	0.601	0.157	0.207	0.378	0.41
5	0.435	0.230	0.215	0.424	0.443	0.495	0.37
7	0.247	0.251	0.293	0.077	0.273	0.292	0.24
8	1.625	1.678	1.254	1.062	1.969	1.921	1.58
9	1.073	2.235	1.886	1.069	0.910	1.485	1.44
10	2.005	2.756	1.931	0.415	1.280	2.250	1.77
12	1.160	1.941	1.502	1.087	1.470	0.733	1.31
13	1.742	1.749	2.324	0.645	1.748	1.155	1.56
Means	1.50	1.69	1.74	0.92	1.06	1.52	

distribution of power with respect to wavelength (frequency, cm^{-1}) between directions.

C. Biological data

Polychaetes were the numerically dominant taxa collected with box cores at all sites (Table 3). Density of macrofauna ($1271 \text{ individuals/m}^2$) was similar to that reported by Lie and Kisker (1970) for shallow-water sand bottom assemblages of the Washington coast. Bioturbation by the dominant macrofauna—which included surface deposit-feeding polychaetes, tube-dwelling polychaetes, and burrowing amphipods—probably had little impact on surficial sediment geoaoustic properties. The relatively undisturbed nature of the sediment surface observed in the bottom photographs also suggests macrofauna have little impact on bottom roughness.

IV. Discussion

A. Variability of sediment geoaoustic and bottom roughness properties

Sediment geoaoustic properties, such as compressional wave velocity and attenuation, sediment mean grain size, and sediment porosity, can be quite variable in shallow-water marine sediments (Richardson, in press). Table 4 presents a comparison of the coefficient of variation of

Table 3. Density of macrofauna collected with 0.25 m^2 box cores in the Quinault Range.

Taxa	Box Core			
	1	6	7	8
Polychaeta	245	219	183	337
Gastropoda	3	8	5	32
Pelecypoda	23	14	6	9
Mysidacea	4	2	1	1
Cumacea	2	1	10	3
Isopoda			1	
Amphipoda	24	30	49	32
Decapoda		2	4	2
Echinoidea	6		2	
Ophiuroidea	3	2	1	2
Holothuroidea	1	2	1	
Total	311	279	263	418
Nos./m ²	1244	1116	1052	1672

sediment geoaoustic properties among sediments collected for this study and those collected from Long Island Sound; the Atlantic Ocean, east of Montauk Point, New York; off Charleston, South Carolina; the Gulf of Mexico, south of Panama City, Florida; the Pacific Ocean, off San Diego, California; and the Arafura Sea, north of Australia.

The coefficients of variation of geoaoustic properties for sediment collected from the Quinault Range were in

Table 4. Coefficient of variation ($\text{SD}/\bar{X} \times 100$) of sediment geoaoustic properties calculated for nine shallow-water sediment types.

Site	Porosity	Grain Size	V_p -ratio	Attenuation
Quinault Range (this study)				
0-22 cm	4.98	3.63	1.19	33.08
0-10 cm	2.84	2.19	0.89	24.99
Long Island Sound ¹				
FOAM	7.33	11.53	0.82	*
NWC	1.50	1.91	0.35	*
Montauk Point, New York ²	3.36	6.45	0.93	15.72
San Diego, California ³				
fine sand	*	11.76	1.16	16.41
coarse sand	*	7.42	0.97	25.73
Charleston, South Carolina ⁴	6.28	18.84	1.03	37.76
Arafura Sea, Australia ⁵	5.81	14.56	0.62	47.26
Panama City, Florida ⁵	3.72	6.16	0.87	15.59

* Measurements not made

(1) Richardson et al., 1983a; (2) Richardson et al., 1983b; (3) Richardson et al., 1983c; (4) Briggs et al., 1986; (5) Richardson, in press.

the same range as those from other studies. At all sites compressional wave attenuation had the highest values of variation and compressional wave velocity the lowest values. The highest variability of attenuation values was associated with sites that had a high percentage of large-sized (>1.00 mm) shell fragments (Quinault Range, Charleston, and Arafura Sea). Attenuation at those sites included both intrinsic absorption (see Hamilton, 1972) and losses due to scattering from shell particles (Richardson, in press). The lowest variability of attenuation was found for hard-packed fine sands (San Diego, Montauk Point, and Panama City). The coefficient of variation for compressional wave velocity was lower at muddy sites (Long Island Sound and Arafura Sea) compared to sandy sites such as the Quinault Range.

As can be observed from Figures 6-9, sediment geoacoustic properties in the Quinault Range were less variable in the upper 10 cm of sediments compared to the 10-20 cm sediment depth interval. The coefficients of sediment at the Quinault Range are consistently lower of sediment at the Quinault Range are consistently higher than for the 0-22 cm depth interval (Table 4). The presence of whole and broken shell material, coupled with a higher percentage of silt and clay in sediments from the 10-20 cm depth interval, contributed to this higher variability.

The coefficients of variation of RMS roughness values for the two azimuthal directions used to make measurements were 62.80 for the cross-sectional lines parallel to the Washington coastline (171-351°) and 83.98 for those perpendicular to the coastline (81-261°). This variation is greater than the variation found in all other geoacoustic properties. A two-way analysis of variance of RMS roughness data found a greater degree of variability associated with between photograph differences ($SS = 36.7$) than between the two azimuthal directions ($SS = 3.4$).

B. Prediction of in situ sediment geoacoustic properties

Sediment physical properties, such as porosity and mean grain size, can be used to calculate or predict sediment bulk density, impedance, reflection coefficient, bottom loss at normal incidence, and critical angle. These values are required inputs for some submodels that predict acoustic backscatter at the sediment-water interface, and are often calculated as intermediate steps within other submodels. We calculated values of these sediment geoacoustic properties for the in situ conditions at the Quinault Range during the acoustic experiment (Table 5). Geoacoustic prop-

Table 5. Measured, calculated, and predicted environmental and geoacoustic properties for in situ conditions at the Quinault Range during May 1983.

Measured Properties	Sediment Depth Interval (cm)	
	0-22	0-10
Water depth (m)	49	49
Bottom water temperature (°C)	10	10
Bottom water salinity (ppt)	32.5	32.5
Sediment porosity (%)	41.2	40.1
Sediment mean grain size (ϕ)	2.94	2.91
Compressional wave velocity (m/sec)	1656	1659
Compressional wave velocity ratio	1.113	1.115
Attenuation (dB/m @ 400 kHz)	148	139
Attenuation (k)	0.37	0.35
<u>Calculated Properties</u>		
Sediment bulk density (g/cm^3)	1.981	1.998
Bottom water impedance ($\text{g/cm}^2 \text{ sec} \cdot 10^5$)	1.525	1.525
Sediment impedance ($\text{g/cm}^2 \text{ sec} \cdot 10^5$)	3.279	3.319
Rayleigh reflection coefficient	0.37	0.37
Bottom loss (dB)	8.7	8.6
Critical angle (deg)	26.1	26.3

erties were calculated from mean values of porosity, mean grain size, and compressional wave velocity for the upper 10 cm of sediments and for the upper 22 cm of sediments. Sediment bulk density (ρ) was calculated from the porosity (n) assuming a mean grain density for quartz sand of 2.65 g/cm^3 (ρ_s) and an interstitial water density of 1.0255 g/cm^3 (ρ_w).

$$\rho = n\rho_w + (1 - n)\rho_s$$

Seawater velocity (V_w) was calculated from in situ temperature, salinity, and depth, given the nine-term equation for sound speed developed by Mackenzie (1981). Seawater density (ρ_w) was calculated from the Knudsen hydrographic tables. Sediment impedance was calculated as the product of density (ρ) and compressional wave velocity (V_p). The Rayleigh reflection coefficient (R) for compressional waves at normal incidence to the sediment-water interface was calculated as the impedance mismatch between water and sediment (Hamilton, 1970), where impedance is the product of the compressional wave velocity and density of sediment or water.

$$R = \frac{\rho V_p - \rho_w V_w}{\rho V_p + \rho_w V_w}$$

Bottom loss (BL) was calculated in decibels (after Hamilton, 1970).

$$BL = -20 \log R$$

The critical angle (θ_c) was calculated as the arc cosine of the reciprocal of the compressional wave velocity ratio (V_p).

$$\theta_c = \cos^{-1} (1/V_p)$$

As previously suggested the occasional high or low outlying values of sediment geoaoustic properties (Figs. 6-9) are probably not important considerations for predicting acoustic backscatter. We have, therefore, calculated sediment geoaoustic properties using a range of measured geoaoustic properties contained within 80% of the mean (Table 6). These calculations show that sediment impedance, Rayleigh reflection coefficient, bottom loss, and critical angle vary little for most of the range of sediment conditions encountered in the Quinault Range.

Table 6. Range of measured, predicted, and calculated geoaoustic properties within 80% of the mean for in situ conditions at the Quinault Range during May 1983.

Measured Properties	10%	Mean	90%
Sediment porosity (%)	38.7	41.2	42.6
Sediment mean grain size (ϕ)	2.9	2.94	3.1
Compressional wave velocity (m/sec)	1676	1656	1630
Compressional wave velocity ratio	1.127	1.113	1.096
Attenuation (dB/m @ 400 kHz)	115	148	240
Attenuation (k)	0.29	0.37	0.60
Calculated Properties			
Sediment bulk density (g/cm ³)	2.02	1.981	1.96
Sediment impedance (g/cm ² sec $\cdot 10^5$)	3.387	3.280	3.191
Rayleigh reflection coefficient	0.379	0.365	0.353
Bottom loss (dB)	8.4	8.7	9.0
Critical angle (deg)	27.4	26.1	24.1

C. Prediction of acoustic bottom backscattering

One of the important objectives of this program was to collect and analyze sufficient environmental data to make accurate predictions of acoustic bottom backscatter strength. We used the semi-empirical model developed by Jackson et al. (1986) to predict high-frequency bottom back-

scattering from the environmental data. Jackson's model is a simplification of composite-roughness and volume scattering models supplemented by the Kirchhoff approximation for grazing angles near normal incidence (Sienkiewicz, 1985). The model generates bottom backscatter strength (dB) versus grazing angle plots for different acoustic frequencies, given the required environmental inputs.

Backscattering predictions using this model require four environmental inputs: compressional wave velocity ratio, sediment density ratio, sediment volume backscattering parameter, and RMS roughness over a 100-cm pathlength. The mean, range, and variability of all inputs, except the volume scattering parameter, can be readily calculated from data in Figures 6, 7, and 8 or in Tables 1, 2, 5, and 6. Values of sediment compressional wave velocity ratio are given in Table 1, 5, and 6. Sediment density ratio is the ratio of the sediment density to bottom water density (1.0255 g/cm³). Values of RMS roughness over a 100-cm pathlength (RMS_{100}) were calculated from the following relationship:

$$RMS_{100} = \left(\frac{100}{L} \right)^{0.625} \times RMS_L,$$

where L was the pathlength of the known roughness profile (31.5 cm in our data) and RMS_L was the RMS roughness (cm) over a pathlength of 31.5 cm. This formula reduced to $RMS_{100} = 2.0585 RMS_{31.5}$ for a constant pathlength.

Jackson made acoustic bottom backscatter strength measurements in the Quinault Range over the frequency range of 20-85 kHz and for grazing angles of 2-30°. Measurements were made at two azimuthal headings (171 or 351° versus 81 or 261°). We therefore performed a sensitivity analysis to determine the effects of the variability of the four environmental input parameters on backscatter predictions generated by Jackson's model for given acoustic frequencies, grazing angles, and azimuthal headings used to obtain acoustic data.

In the first series of calculations the volume backscattering parameter (0.002) and bottom roughness (2.92 cm) were assumed to be constant over the range of values of the compressional wave velocity and sediment density ratios reported in Table 6. At none of the frequencies between 20 and 85 kHz were the differences in predicted backscatter strength greater than 1 dB for any given grazing angle (Fig. 13). The largest differences in predicted backscatter strength were at grazing angles above the critical angle (24.1 to 27.4°) where sediment volume scattering, not sediment surface scattering, dominates bottom

backscattering. Apparently, differences in values of velocity and density ratios encountered in the Quinault Range have little impact on acoustic backscatter predictions.

In the second set of predictions, the velocity ratio (1.113), density ratio (1.932), and RMS roughness (2.92 cm) were assumed to be constant as the volume backscattering parameter was allowed to vary between 0.0001 and 0.003. These are the minimum and maximum values of that parameter suggested as inputs for the model by Jackson et al. (1986). These differences in predicted backscatter strength

resulted from changes in the volume backscattering parameter and were large only above the critical angle of 26.1° (Fig. 14). The emphasis of these experiments was on low grazing angles; therefore, we assumed a value of 0.002 for the volume backscattering parameter for the remaining backscatter predictions. This value is suggested by Jackson for sandy substrates.

The third set of analyses compared backscatter strength predictions for the two different azimuthal headings used by Jackson to collect acoustic data. Mean values of the

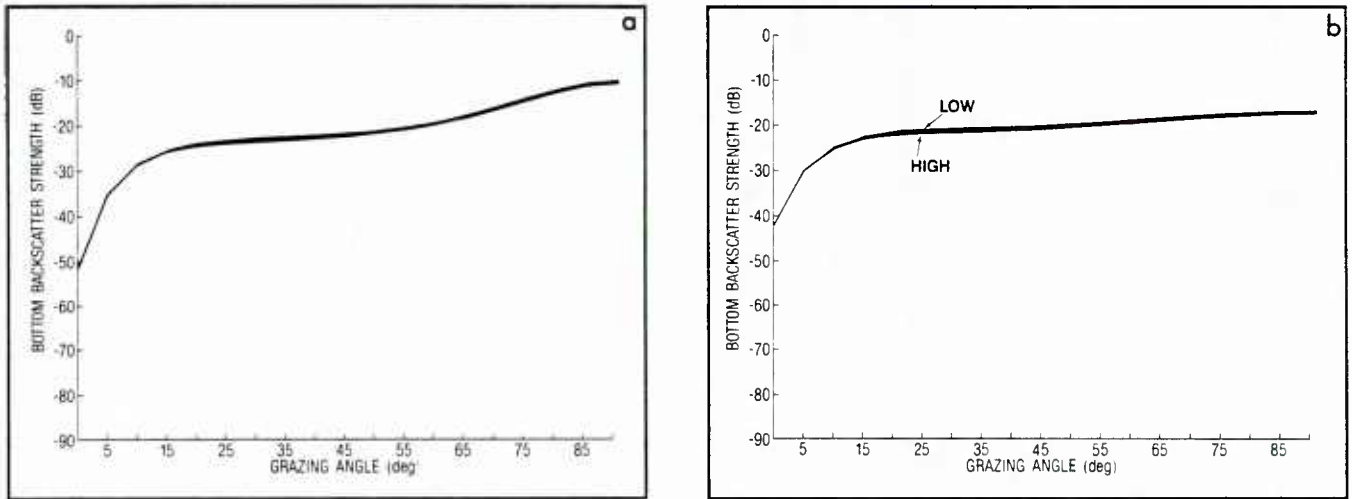


Figure 13. Predicted bottom backscatter strength (dB) versus grazing angle for the range of velocity ratio values (1.096–1.127) and density ratio values (1.909–1.971) encountered at the Quinault Range. Backscatter strengths calculated for acoustic frequencies of (a) 20 kHz and (b) 85 kHz. Other model inputs included bottom backscatter parameter = 0.002 and RMS bottom roughness = 2.92 cm. Low and high designations pertain to relative magnitudes of values of velocity and density ratios.

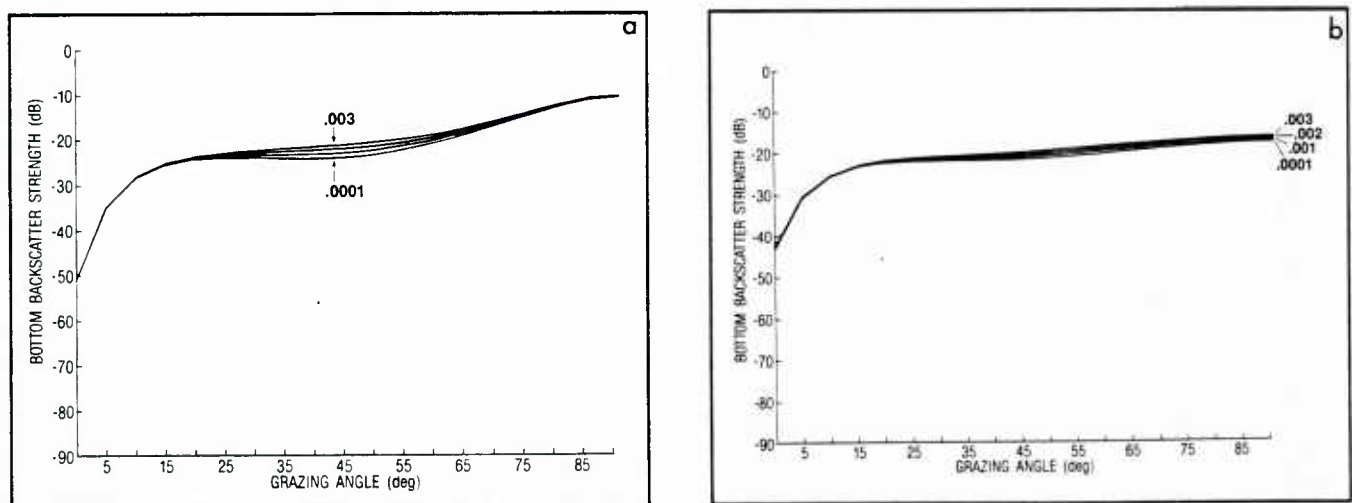


Figure 14. Predicted bottom backscatter strength (dB) versus grazing angle for the possible range of values of the volume backscattering parameter (0.0001–0.003) for Quinault Range sediments. Backscatter strengths calculated for acoustic frequencies of (a) 20 kHz and (b) 85 kHz. Other model inputs included velocity ratio = 1.113, density ratio = 1.932, and RMS bottom roughness = 2.92 cm.

velocity ratio (1.113) and density ratio (1.932) from Table 6, together with a volume backscattering parameter value of 0.002, were used as inputs for these analyses. As depicted in Figure 15a, the model predicts a 2–6 dB higher bottom backscatter strength at low grazing angles for bottom roughness values on tracks parallel to the Washington coastline ($RMS_{100} = 3.38$ cm) compared to tracks perpendicular to the coast ($RMS_{100} = 2.40$ cm). At higher frequencies (85 kHz) these differences are less pronounced (Fig. 15b). As stated, the variability of bottom roughness was much greater between photographs taken 10–500 m apart than between the two azimuthal headings (Table 2).

In the fourth set of analyses we compared predicted backscatter strength for the range of mean values of roughness for any single direction in each photograph ($RMS = 0.44$ – 6.82 cm for the 100-cm pathlength). Other geoacoustic inputs were the same as in the third set of analyses. Comparisons of backscattering plots for these roughness values predict a 17–52 dB difference in backscatter strength at 20 kHz and a 13–49 dB difference at 85 kHz (Figs. 16a and 16b) for grazing angles less than the critical angle.

This sensitivity analysis suggests that the Quinault Range bottom roughness is the most important factor controlling bottom backscattering at angles below the critical angle, whereas the volume-scattering parameter controls bottom backscattering at higher grazing angles. In Figure 17 bottom backscatter strength is predicted over the range of frequencies used in the acoustic experiment for the mean environmental conditions encountered at the Quinault Range.

V. Conclusions

- The variability of sediment geoacoustic properties in the Quinault Range was approximately the same as for other shallow-water sandy sediments. Vertical variability in the upper 22 cm was greater than horizontal variability over 100 m to 3 km distances.
- Values of bottom roughness exhibited a higher variability than sediment geoacoustic properties. A greater percentage of the variability in bottom roughness was associated with small-scale horizontal variations (over 10–500 m) rather than with azimuthal direction.
- Sediment geoacoustic and roughness properties are primarily controlled by hydrodynamic, as opposed to biological, processes in the Quinault Range.
- The range of variation of sediment mean grain size, porosity, and compressional wave velocity has little impact on predicted bottom backscatter strengths.
- Both the small-scale horizontal variation and azimuthal directionality of bottom roughness appear to control predicted bottom backscatter strengths. Small-scale horizontal variations (10–500 m) in roughness have a greater impact on predicted scattering strengths than azimuthal directionality.
- Sediment bottom roughness on the Washington continental shelf is probably predictable on spatial and temporal scales. The required environmental inputs for prediction are depth, sediment type, dominant benthic (animal) communities, and the past and present hydrodynamic conditions.

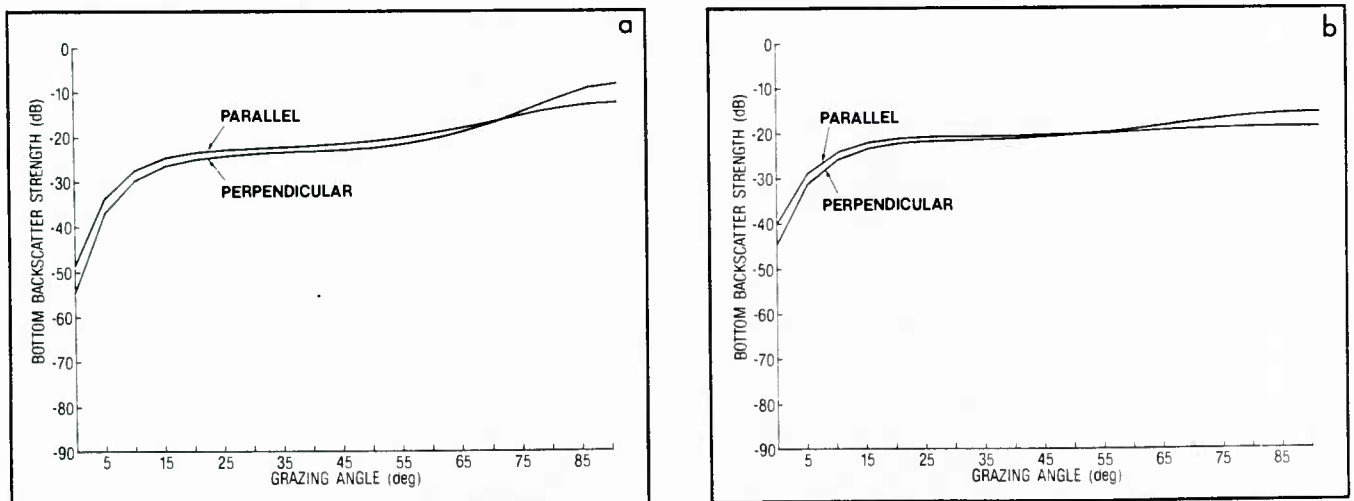


Figure 15. Predicted bottom backscatter strength (dB) versus grazing angle for values of RMS bottom roughness calculated for 100-cm tracks parallel to the coast (RMS height = 3.38 cm) and perpendicular to the coast (RMS height = 2.47 cm) in the Quinault Range. Backscatter strengths calculated for acoustic frequencies of (a) 20 kHz and (b) 85 kHz. Other model inputs included velocity ratio = 1.113, density ratio = 1.932, and volume backscattering parameter = 0.002.

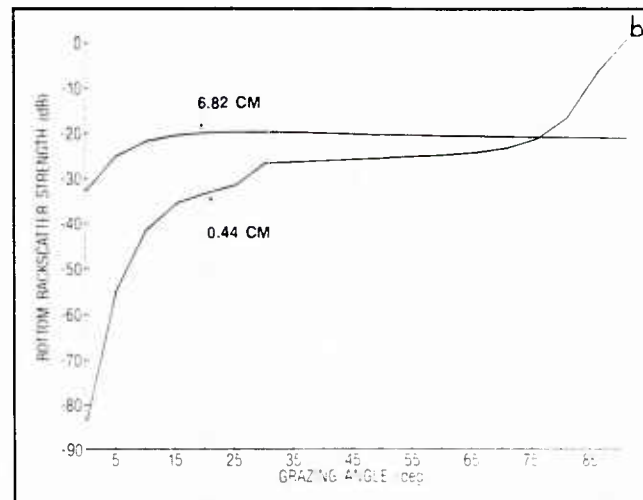
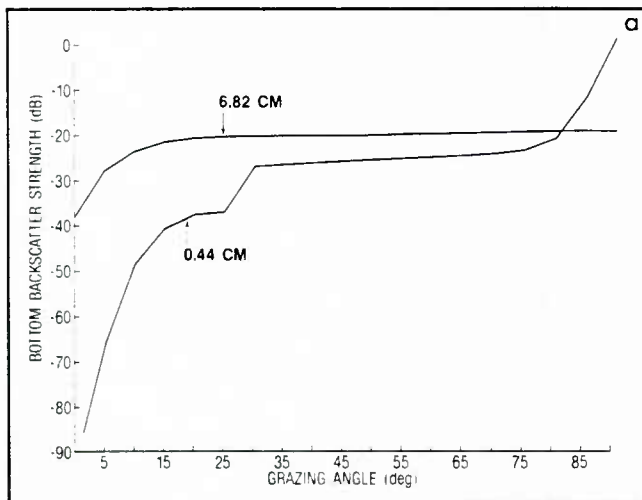


Figure 16. Predicted bottom backscatter strength (dB) versus grazing angle for the range of values of RMS bottom roughness (0.44–6.82 cm over 100-cm tracks) calculated for Quinault Range sediments. Backscatter strengths calculated for acoustic frequencies of (a) 20 kHz and (b) 85 kHz. Other model inputs included velocity ratio = 1.113, density ratio = 1.932, and volume backscattering parameter = 0.002.

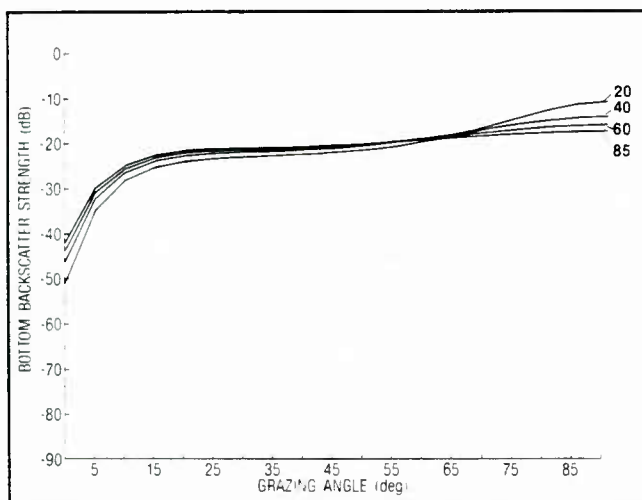


Figure 17. Predicted bottom backscatter strength (dB) versus grazing angle for the range of acoustic frequencies used by D. R. Jackson to collect bottom backscatter data. All environmental inputs are average values from this study. Velocity ratio = 1.113, density ratio = 1.932, volume backscattering parameter = 0.002, and RMS bottom roughness = 2.92.

- If current models are adequate to predict bottom backscatter strength from environmental inputs, then the range, the variability, and the distribution of bottom backscattering along the entire Washington continental shelf can be predictable from readily available environmental inputs.

VI. References

- Barnes, C. A., A. C. Duxbury, and B. A. Morse (1972). Circulation and Selected Properties of the Columbia River Effluent at Sea. In: *The Columbia River Estuary and Adjacent Ocean Waters, Bioenvironmental Studies*. A. T. Pruter and D. L. Alverson (eds.), University of Washington Press, Seattle, Washington, pp. 41–80.
- Bloomfield, P. (1976). *Fourier Analysis of Time Series: An Introduction*. John Wiley and Sons, New York. 258 pp.
- Briggs, K. B., P. Fleischer, R. I. Ray, W. B. Sawyer, D. K. Young, M. D. Richardson, and S. Stanic (1986). *Environmental Support for a High Frequency Bottom Backscatter Experiment off Charleston, South Carolina, 17–28 June 1983*. Naval Ocean Research and Development Activity, NSTL, Mississippi, NORDA Report 130, 86 pp.
- Folk, R. L. (1965). *Petrology of Sedimentary Rocks*. Hemphill's, Austin, Texas.
- Folk, R. L. and W. C. Ward (1957). Brazos River Bar. A Study in the Significance of Grain Size Parameters. *Journal of Sedimentary Petrology*, v. 27, pp. 3–26.
- Hamilton, E. L. (1970). Reflection Coefficients and Bottom Losses at Normal Incidence Computed from Pacific Sediment Properties. *Geophysics*, v. 35, pp. 995–1004.
- Hamilton, E. L. (1971). Elastic Properties of Marine Sediments. *Journal of Geophysical Research*, v. 76, pp. 579–604.

- Hamilton, E. L. (1972). Compressional-Wave Attenuation in Marine Sediments. *Geophysics*, v. 37, pp. 620-646.
- Jackson, D. R., D. P. Winebrenner, and A. Ishimaru (1986). Application of the Composite Roughness Model to High-Frequency Bottom Backscattering. *Journal of the Acoustical Society of America*, v. 75, p. S30.
- Komar, P. D., R. H. Neudeck, and L. D. Kulm (1972). Observations and Significance of Deep-Water Oscillatory Ripple Marks on the Oregon Continental Shelf. In: *Shelf Sediment Transport: Process and Pattern*, D. J. P. Swift, D. B. Duane, and O. H. Pilkey (eds.), Dowden, Hutchinson, and Ross, Stroudsburg, Pennsylvania.
- Krell, R. M. (1980). *Shallow Water Range Region Bottom Sediment Characteristics: Summarization of Investigations and Facts Obtained to Date*. Applied Research Division Memorandum 19-80, NUWES, Keyport, Washington, 114 pp.
- Kulm, L. D., R. C. Roush, J. C. Harlett, R. H. Neudeck, D. M. Chambers, and E. J. Runge (1975). Oregon Continental Shelf Sedimentation: Interrelations of Facies Distribution and Sedimentary Process. *Journal of Geology*, v. 83, pp. 145-175.
- Lambert, D. N. and R. H. Bennett (1972). *Tables for Determining Porosity of Deep-Sea Sediments from Water Content and Average Grain Density Measurements*. NOAA Technical Memo. ERL AOML-17.
- Lie, U. (1969). Standing Crop of Benthic Infauna in Puget Sound and off the Coast of Washington. *Journal of the Fisheries Research Board of Canada*, v. 26, pp. 55-62.
- Lie, U. and J. C. Kelley (1970). Benthic Infauna Communities off the Coast of Washington and in Puget Sound: Identification and Distribution of Communities. *Journal of the Fisheries Research Board of Canada*, v. 27, pp. 621-651.
- Lie, U. and D. S. Kisker (1970). Species Composition and Structure of Benthic Infauna Communities off the Coast of Washington. *Journal of the Fisheries Research Board of Canada*, v. 27, pp. 2273-2285.
- Mackenzie, K. V. (1981). Nine-Term Equation for Sound Speed in the Oceans. *Journal of the Acoustical Society of America*, v. 70, pp. 807-812.
- McManus, D. A. (1972). Bottom Topography and Sediment Texture near the Columbia River Mouth. In: *The Columbia River Estuary and Adjacent Ocean Waters. Bioenvironmental Studies*, A. T. Pruter and D. L. Alverson (eds.), University of Washington Press, Seattle. Washington, pp. 241-253.
- Richardson, M. D. (in press). Spatial Variability of Surficial Shallow Water Sediment Geoacoustic Properties. In: *Ocean Seismo-Acoustics*, T. Akal and J. M. Berkson (eds.), Plenum Press, New York, New York.
- Richardson, M. D., D. K. Young, and K. B. Briggs (1983a). Effects of Hydrodynamic and Biological Processes on Sediment Geoacoustic Properties in Long Island Sound, USA. *Marine Geology*, v. 52, pp. 201-226.
- Richardson, M. D., D. K. Young, and R. I. Ray (1983b). *Environmental Support for High Frequency Acoustic Measurements at NOSC Oceanographic Tower. 26 April-7 May. Part I: Sediment Geoacoustic Properties*. Naval Ocean Research and Development Activity, NSTL, Mississippi, NORDA Technical Note 219, 68 pp.
- Richardson, M. D., J. H. Tietjen, and R. I. Ray (1983c). *Environmental Support for Project WEAP East of Montauk Point, New York, 7-28 May 1982*. Naval Ocean Research and Development Activity, NSTL, Mississippi, NORDA Report 40, 52 pp.
- Sienkiewicz, C. G. (1985). An Overview of Outstanding Problems in Ocean Boundary Scattering at High Frequencies. *Proceedings, Institute of Acoustics*, v. 7, pp. 1-9.
- Smith, D. A. and M. M. Boyajian (1984). Stereo Photography for Vertical and Horizontal Measurements. In: *Underwater Photography, Scientific and Engineering Applications*, P. F. Smith (ed.), Van Nostrand Reinhold, New York, New York, pp. 205-214.
- Sternberg, R. W., J. S. Creager, W. Glassley, and J. Johnson (1977). *Aquatic Disposal Field Investigations Columbia River Disposal Site, Oregon*. Appendix A: Investigation of the Hydraulic Regime and Physical Nature of Bottom Sedimentation. Dredged Material Research Program Technical Report D-77-30, Environmental Effects Laboratory, U. S. Army Engineer Waterways Experiment Station CE, Vicksburg, Mississippi.
- Stewart, R. (1980). *Mineralogy of NUWES Cores from the Washington and Continental Shelf*. Applied Research Division Memorandum 19-80, Enclosure 4, NUWES, Keyport, Washington, 4 pp.

Appendix A. Sediment physical and geoacoustic data

Cruise: 1206-83 Station: DeS 1-1 Date: 4/28/83
 Position: 47-30N;124-35W Depth: 49m

Calculated for: 23.0 Deg-C 35.00 o/oo 0 m 400 kHz

Depth (cm)	Vp (m/sec)	Vp Ratio	Alpha (dB/m)	Attenu- ation k	Mean Grain Size(0)	% Pors.	Depth (cm)
WATER	1528.6	0.999	19.7	0.049			WATER
0.0	1535.8	1.004	179.3	0.448			0.0
1.0	1716.2	1.122	150.1	0.375			1.0
2.0	1719.5	1.124	121.6	0.304			2.0
3.0	1719.1	1.124	126.0	0.315			3.0
4.0	1711.5	1.119	145.0	0.362			4.0
5.0	1711.0	1.119	173.0	0.432			5.0
6.0	1694.1	1.108	166.9	0.417			6.0
7.0	1699.7	1.111	166.9	0.417			7.0
8.0	1708.6	1.117	155.5	0.389			8.0
9.0	1710.5	1.118	150.1	0.375			9.0
10.0	1708.6	1.117	161.1	0.403			10.0
11.0	1709.1	1.118	166.9	0.417			11.0
12.0	1706.8	1.116	173.0	0.432			12.0
13.0	1703.0	1.114	173.0	0.432			13.0
14.0	1690.9	1.106	185.9	0.465			14.0
15.0	1688.6	1.104	185.9	0.465			15.0
16.0	1743.3	1.140	291.6	0.729			16.0

Cruise: 1206-83 Station: DeS 1-2 Date: 4/28/83
 Position: 47-30N;124-35W Depth: 49m

Calculated for: 23.0 Deg-C 35.00 o/oo 0 m 400 kHz

Depth (cm)	Vp (m/sec)	Vp Ratio	Alpha (dB/m)	Attenu- ation k	Mean Grain Size(0)	% Pors.	Depth (cm)
WATER	1528.2	0.999	0.0	0.000			WATER
0.0	1638.6	1.071	130.5	0.326			0.0
1.0	1719.5	1.124	125.8	0.315			1.0
2.0	1720.5	1.125	116.9	0.292			2.0
3.0	1721.9	1.126	125.8	0.315			3.0
4.0	1710.0	1.118	125.8	0.315			4.0
5.0	1703.0	1.114	140.3	0.351			5.0
6.0	1704.9	1.115	145.5	0.364			6.0
7.0	1703.9	1.114	135.3	0.338			7.0
8.0	1700.7	1.112	156.4	0.391			8.0
9.0	1706.8	1.116	188.2	0.471			9.0
10.0	1706.8	1.116	188.2	0.471			10.0

Cruise: 1206-83 Station: DeS 1-3 Date: 4/28/83
Position: 47-30N;124-35W Depth: 49m

Calculated for: 23.0 Deg-C 35.00 o/oo 0 m 400 kHz

Depth (cm)	Vp (m/sec)	Vp Ratio	Alpha (dB/m)	Attenu- ation k	Mean Grain Size(°)	% Pors.	Depth (cm)
WATER	1527.4	0.999	0.0	0.000			WATER
0.0	1532.3	1.002	14.5	0.036			0.0
1.0	1725.3	1.128	109.2	0.273	2.82	39.3	1.0
2.0	1724.3	1.127	109.2	0.273			2.0
3.0	1728.2	1.130	113.2	0.283	2.83	37.3	3.0
4.0	1732.5	1.133	109.2	0.273			4.0
5.0	1728.2	1.130	113.2	0.283	2.85	38.3	5.0
6.0	1723.9	1.127	109.2	0.273			6.0
7.0	1723.9	1.127	117.3	0.293	2.87	39.2	7.0
8.0	1723.9	1.127	126.0	0.315			8.0
9.0	1722.4	1.126	130.5	0.326	2.86	39.4	9.0
10.0	1719.5	1.124	150.1	0.375			10.0
11.0	1716.7	1.122	155.5	0.389	2.86	39.8	11.0
12.0	1711.0	1.119	155.5	0.389			12.0
13.0	1701.1	1.112	216.0	0.540	2.90	40.1	13.0
14.0	1688.1	1.104	233.8	0.585			14.0
15.0	1681.7	1.100	278.0	0.695	2.92	41.7	15.0
16.0	1680.4	1.099	376.7	0.942			16.0
17.0	1694.1	1.108	291.6	0.729	2.88	41.8	17.0
18.0	1703.5	1.114	370.4	0.926			18.0
19.0					2.95	42.1	19.0
20.0							20.0
21.0					2.79	40.1	21.0

Cruise: 1206-83 Station: DeS 1-4 Date: 4/28/83
Position: 47-30N;124-35W Depth: 49m

Calculated for: 23.0 Deg-C 35.00 o/oo 0 m 400 kHz

Depth (cm)	Vp (m/sec)	Vp Ratio	Alpha (dB/m)	Attenu- ation k	Mean Grain Size(°)	% Pors.	Depth (cm)
WATER	1527.8	0.999	4.7	0.012			WATER
0.0	1535.4	1.004	147.5	0.369			0.0
1.0	1706.8	1.116	126.0	0.315	2.94	40.4	1.0
2.0	1709.6	1.118	101.5	0.254			2.0
3.0	1713.8	1.121	113.2	0.283			3.0
4.0	1712.4	1.120	126.0	0.315			4.0
5.0	1703.5	1.114	135.1	0.338			5.0
6.0	1706.3	1.116	150.1	0.375			6.0
7.0	1713.8	1.121	135.1	0.338			7.0
8.0	1713.4	1.120	145.0	0.362			8.0
9.0	1696.0	1.109	192.9	0.482			9.0
10.0	1703.5	1.114	179.3	0.448			10.0
11.0	1706.3	1.116	161.1	0.403			11.0
12.0	1705.8	1.115	179.3	0.448			12.0
13.0	1687.2	1.103	254.2	0.636			13.0
14.0	1655.2	1.082	342.4	0.856			14.0
15.0	1616.3	1.057	254.2	0.636			15.0

Cruise: 1206-83 Station: DeS 2-1 Date: 4/28/83
Position: 47-30N;124-35W Depth: 49m

Calculated for: 23.0 Deg-C 35.00 o/oo 0 m 400 kHz

Depth (cm)	Vp (m/sec)	Vp Ratio	Alpha (dB/m)	Attenu- ation k	Mean Grain Size(0)	% Pors.	Depth (cm)
WATER	1528.9	1.000	0.0	0.000			WATER
0.0	1638.6	1.071	145.0	0.362			0.0
1.0	1722.4	1.126	117.3	0.293	2.89	38.9	1.0
2.0	1721.0	1.125	103.4	0.258			2.0
3.0	1720.0	1.125	101.5	0.254	2.85	39.1	3.0
4.0	1721.0	1.125	113.2	0.283			4.0
5.0	1722.9	1.127	121.6	0.304	2.82	38.6	5.0
6.0	1724.8	1.128	121.6	0.304			6.0
7.0	1724.8	1.128	109.2	0.273	2.83	39.4	7.0
8.0	1719.5	1.124	109.2	0.273			8.0
9.0	1726.7	1.129	130.5	0.326	2.86	39.1	9.0
10.0	1726.3	1.129	140.0	0.350			10.0
11.0	1727.2	1.129	150.1	0.375	2.86	39.4	11.0
12.0	1718.1	1.123	224.6	0.562			12.0
13.0	1708.2	1.117	254.2	0.636	2.88	41.1	13.0
14.0	1712.9	1.120	238.7	0.597			14.0
15.0	1706.3	1.116	271.7	0.679	2.91	41.3	15.0
16.0	1714.8	1.121	306.6	0.766			16.0
17.0	1574.0	1.029	390.3	0.976	3.52	48.2	17.0
18.0							18.0
19.0					2.91	43.4	19.0

Cruise: 1206-83 Station: DeS 2-2 Date: 4/28/83
Position: 47-30N;124-35W Depth: 49m

Calculated for: 23.0 Deg-C 35.00 o/oo 0 m 400 kHz

Depth (cm)	Vp (m/sec)	Vp Ratio	Alpha (dB/m)	Attenu- ation k	Mean Grain Size(0)	% Pors.	Depth (cm)
WATER	1528.6	0.999	0.0	0.000			WATER
0.0	1738.9	1.137	352.9	0.882			0.0
1.0	1712.9	1.120	135.1	0.338			1.0
2.0	1720.0	1.125	117.3	0.293			2.0
3.0	1730.6	1.132	117.3	0.293			3.0
4.0	1735.9	1.135	105.3	0.263			4.0
5.0	1733.5	1.133	135.1	0.338			5.0
6.0	1725.8	1.128	135.1	0.338			6.0
7.0	1724.3	1.127	135.1	0.338			7.0
8.0	1721.0	1.125	126.0	0.315			8.0
9.0	1723.4	1.127	126.0	0.315			9.0
10.0	1723.4	1.127	145.0	0.362			10.0
11.0	1706.3	1.116	216.0	0.540			11.0
12.0	1713.8	1.121	254.2	0.636			12.0
13.0	1703.9	1.114	306.6	0.766			13.0
14.0	1694.1	1.108	314.7	0.787			14.0
15.0	1694.1	1.108	306.6	0.766			15.0
16.0	1707.2	1.116	259.8	0.650			16.0
17.0	1706.3	1.116	323.3	0.808			17.0
18.0	1679.9	1.098	587.7	1.469			18.0

Cruise: 1206-83 Station: DeS 2-3 Date: 4/28/83
 Position: 47-30N;124-35W Depth: 49m

Calculated for: 23.0 Deg-C 35.00 o/oo 0 m 400 kHz

Depth (cm)	Vp (m/sec)	Vp Ratio	Alpha (dB/m)	Attenu- ation k	Mean Grain Size(Ø)	% Pors.	Depth (cm)
WATER	1528.6	0.999	0.0	0.000			WATER
0.0	1533.1	1.002	-26.0	-0.065			0.0
1.0	1705.3	1.115	31.8	0.079	2.95	39.9	1.0
2.0	1719.5	1.124	104.5	0.261			2.0
3.0	1719.5	1.124	112.6	0.282			3.0
4.0	1721.5	1.126	112.6	0.282			4.0
5.0	1721.0	1.125	121.3	0.303			5.0
6.0	1723.9	1.127	125.8	0.315			6.0
7.0	1723.9	1.127	125.8	0.315			7.0
8.0	1722.9	1.127	145.5	0.364			8.0
9.0	1717.2	1.123	168.3	0.421			9.0
10.0	1720.0	1.125	162.2	0.406			10.0
11.0	1718.6	1.124	150.8	0.377			11.0
12.0	1711.5	1.119	195.5	0.489			12.0
13.0	1703.9	1.114	188.2	0.471			13.0
14.0	1700.7	1.112	220.0	0.550			14.0
15.0	1697.9	1.110	484.3	1.211			15.0
16.0	1624.0	1.062	301.9	0.755			16.0

Cruise: 1206-83 Station: DeS 2-4 Date: 4/28/83
 Position: 47-30N;124-35W Depth: 49m

Calculated for: 23.0 Deg-C 35.00 o/oo 0 m 400 kHz

Depth (cm)	Vp (m/sec)	Vp Ratio	Alpha (dB/m)	Attenu- ation k	Mean Grain Size(Ø)	% Pors.	Depth (cm)
WATER	1527.1	0.999	0.0	0.000			WATER
0.0	1534.7	1.003	142.9	0.357			0.0
1.0	1702.6	1.113	121.3	0.303			1.0
2.0	1715.4	1.122	104.5	0.261			2.0
3.0	1715.4	1.122	108.5	0.271			3.0
4.0	1720.1	1.125	104.5	0.261			4.0
5.0	1723.5	1.127	108.5	0.271			5.0
6.0	1724.5	1.128	121.3	0.303			6.0
7.0	1724.0	1.127	125.8	0.315			7.0
8.0	1720.6	1.125	130.5	0.326			8.0
9.0	1716.8	1.123	140.3	0.351			9.0
10.0	1720.6	1.125	140.3	0.351			10.0
11.0	1725.4	1.128	145.5	0.364			11.0
12.0	1725.4	1.128	211.3	0.528			12.0
13.0	1710.2	1.118	417.4	1.043			13.0

Cruise: 1206-83 Station: DeS 3-1 Date: 4/29/83
Position: 47-34N;124-35W Depth: 49m

Calculated for: 23.0 Deg-C 35.00 o/oo 0 m 400 kHz

Depth (cm)	Vp (m/sec)	Vp Ratio	Alpha (dB/m)	Attenu- ation k	Mean Grain Size(ϕ)	% Pors.	Depth (cm)
WATER	1525.6	0.998	0.0	0.000			WATER
0.0	1536.2	1.004	80.9	0.202			0.0
1.0	1696.1	1.109	116.9	0.292	3.03	40.3	1.0
2.0	1696.1	1.109	112.6	0.282			2.0
3.0	1700.3	1.112	121.3	0.303	2.93	39.9	3.0
4.0	1703.1	1.114	125.8	0.315			4.0
5.0	1705.0	1.115	121.3	0.303	2.92	40.1	5.0
6.0	1707.8	1.117	116.9	0.292			6.0
7.0	1711.1	1.119	116.9	0.292	2.90	40.2	7.0
8.0	1711.1	1.119	112.6	0.282			8.0
9.0	1712.0	1.119	112.6	0.282	2.89	40.6	9.0
10.0	1712.0	1.119	108.5	0.271			10.0
11.0	1712.0	1.119	112.6	0.282	2.89	41.4	11.0
12.0	1708.7	1.117	140.3	0.351			12.0
13.0	1702.1	1.113	174.6	0.437	2.92	42.5	13.0
14.0	1697.9	1.110	162.2	0.406			14.0
15.0	1704.5	1.114	168.3	0.421	2.94	42.2	15.0
16.0	1703.1	1.114	162.2	0.406			16.0
17.0	1694.7	1.108	195.5	0.489	2.98	42.6	17.0
18.0	1689.1	1.104	211.3	0.528			18.0
19.0	1693.7	1.107	239.0	0.597	3.01	42.1	19.0
20.0	1697.0	1.110	417.4	1.043			20.0
21.0					3.01	41.3	21.0

Cruise: 1206-83 Station: DeS 3-2 Date: 4/29/83
Position: 47-34N;124-35W Depth: 49m

Calculated for: 23.0 Deg-C 35.00 o/oo 0 m 400 kHz

Depth (cm)	Vp (m/sec)	Vp Ratio	Alpha (dB/m)	Attenu- ation k	Mean Grain Size(ϕ)	% Pors.	Depth (cm)
WATER	1526.4	0.998	0.0	0.000			WATER
0.0	1532.0	1.002	37.8	0.095			0.0
1.0	1657.4	1.084	156.4	0.391	3.07	44.1	1.0
2.0	1660.1	1.085	130.5	0.326			2.0
3.0	1684.0	1.101	156.4	0.391			3.0
4.0	1701.2	1.112	121.3	0.303			4.0
5.0	1706.4	1.116	116.9	0.292			5.0
6.0	1707.3	1.116	112.6	0.282			6.0
7.0	1707.3	1.116	116.9	0.292			7.0
8.0	1704.0	1.114	125.8	0.315			8.0
9.0	1706.8	1.116	135.3	0.338			9.0
10.0	1710.6	1.119	125.8	0.315			10.0
11.0	1708.3	1.117	140.3	0.351			11.0
12.0	1704.0	1.114	239.0	0.597			12.0

Cruise: 1206-83 Station: DeS 3-3 Date: 4/29/83
Position: 47-34N;124-35W Depth: 49m

Calculated for: 23.0 Deg-C 35.00 o/oo 0 m 400 kHz

Depth (cm)	Vp (m/sec)	Vp Ratio	Alpha (dB/m)	Attenu- ation k	Mean Grain Size(0)	% Pors.	Depth (cm)
WATER	1527.5	0.999	-4.7	-0.012			WATER
0.0	1535.1	1.004	121.3	0.303			0.0
1.0	1693.7	1.107	130.5	0.326			1.0
2.0	1703.5	1.114	121.3	0.303			2.0
3.0	1710.1	1.118	108.5	0.271			3.0
4.0	1715.3	1.122	112.6	0.282			4.0
5.0	1718.2	1.123	108.5	0.271			5.0
6.0	1718.2	1.123	108.5	0.271			6.0
7.0	1713.4	1.120	125.8	0.315			7.0
8.0	1710.6	1.118	125.8	0.315			8.0
9.0	1710.1	1.118	125.8	0.315			9.0
10.0	1706.3	1.116	125.8	0.315			10.0
11.0	1706.3	1.116	130.5	0.326			11.0
12.0	1705.9	1.115	135.3	0.338			12.0
13.0	1696.0	1.109	150.8	0.377			13.0
14.0	1673.1	1.094	286.9	0.717			14.0

Cruise: 1206-83 Station: DeS 3-4 Date: 4/29/83
Position: 47-34N;124-35W Depth: 49m

Calculated for: 23.0 Deg-C 35.00 o/oo 0 m 400 kHz

Depth (cm)	Vp (m/sec)	Vp Ratio	Alpha (dB/m)	Attenu- ation k	Mean Grain Size(0)	% Pors.	Depth (cm)
WATER	1526.9	0.998	0.0	0.000			WATER
0.0	1534.1	1.003	117.7	0.294			0.0
1.0	1694.9	1.108	139.7	0.349			1.0
2.0	1701.0	1.112	113.7	0.284			2.0
3.0	1702.4	1.113	113.7	0.284			3.0
4.0	1702.4	1.113	121.8	0.305			4.0
5.0	1700.5	1.112	121.8	0.305			5.0
6.0	1700.5	1.112	126.1	0.315			6.0
7.0	1702.8	1.113	126.1	0.315			7.0
8.0	1703.8	1.114	130.5	0.326			8.0
9.0	1705.2	1.115	139.7	0.349			9.0
10.0	1709.0	1.117	144.5	0.361			10.0
11.0	1705.2	1.115	171.4	0.429			11.0
12.0	1705.2	1.115	197.4	0.493			12.0
13.0	1704.7	1.115	311.1	0.778			13.0

Cruise: 1206-83 Station: DeS 4-1 Date: 4/29/83
Position: 47-33N;124-35W Depth: 49m

Calculated for: 23.0 Deg-C 35.00 o/oo 0 m 400 kHz

Depth (cm)	Vp (m/sec)	Vp Ratio	Alpha (dB/m)	Attenu- ation k	Mean Grain Size(0)	% Pors.	Depth (cm)
WATER	1527.0	0.998	0.0	0.000			WATER
0.0	1533.1	1.002	113.2	0.283			0.0
1.0	1701.1	1.112	113.2	0.283	2.98	41.0	1.0
2.0	1705.3	1.115	109.2	0.273			2.0
3.0	1708.6	1.117	117.3	0.293			3.0
4.0	1711.0	1.119	121.6	0.304			4.0
5.0	1714.8	1.121	135.1	0.338			5.0
6.0	1708.6	1.117	135.1	0.338			6.0
7.0	1704.4	1.114	140.0	0.350			7.0
8.0	1699.7	1.111	155.5	0.389			8.0
9.0	1694.1	1.108	179.3	0.448			9.0
10.0	1674.0	1.095	216.0	0.540			10.0
11.0	1682.6	1.100	243.7	0.609			11.0
12.0	1678.5	1.098	265.6	0.664			12.0
13.0	1674.4	1.095	405.3	1.013			13.0

Cruise: 1206-83 Station: DeS 4-2 Date: 4/29/83
Position: 47-33N;124-35W Depth: 49m

Calculated for: 23.0 Deg-C 35.00 o/oo 0 m 400 kHz

Depth (cm)	Vp (m/sec)	Vp Ratio	Alpha (dB/m)	Attenu- ation k	Mean Grain Size(0)	% Pors.	Depth (cm)
WATER	1525.0	0.997	0.0	0.000			WATER
0.0	1531.8	1.002	135.1	0.338			0.0
1.0	1694.7	1.108	126.0	0.315			1.0
2.0	1693.3	1.107	126.0	0.315			2.0
3.0	1689.1	1.104	150.1	0.375			3.0
4.0	1688.2	1.104	173.0	0.432			4.0
5.0	1674.9	1.095	185.9	0.465			5.0
6.0	1688.2	1.104	207.9	0.520			6.0
7.0	1658.7	1.085	224.6	0.562			7.0
8.0	1626.9	1.064	207.9	0.520			8.0
9.0	1628.2	1.065	254.2	0.636			9.0
10.0	1645.1	1.076	238.7	0.597			10.0
11.0	1660.5	1.086	204.0	0.510			11.0
12.0	1672.7	1.094	229.2	0.573			12.0
13.0	1678.6	1.098	323.3	0.808			13.0
14.0	1681.3	1.099	587.7	1.469			14.0

Cruise: 1206-83
Position: 47-33N;124-35W

Station: DeS 4-3

Date: 4/29/83
Depth: 49m

Calculated for: 23.0 Deg-C 35.00 o/oo 0 m 400 kHz

Depth (cm)	Vp (m/sec)	Vp Ratio	Alpha (dB/m)	Attenu- ation k	Mean Grain Size(0)	% Pors.	Depth (cm)
WATER	1526.7	0.998	4.7	0.012			WATER
0.0	1534.3	1.003	291.6	0.729			0.0
1.0	1699.5	1.111	113.2	0.283			1.0
2.0	1705.2	1.115	121.6	0.304			2.0
3.0	1709.4	1.118	135.1	0.338			3.0
4.0	1710.3	1.118	140.0	0.350			4.0
5.0	1706.1	1.116	150.1	0.375			5.0
6.0	1705.2	1.115	173.0	0.432			6.0
7.0	1692.1	1.106	185.9	0.465			7.0
8.0	1686.1	1.102	207.9	0.520			8.0
9.0	1694.9	1.108	200.2	0.500			9.0
10.0	1696.7	1.109	207.9	0.520			10.0
11.0	1700.0	1.112	224.6	0.562			11.0
12.0	1679.2	1.098	298.9	0.747			12.0
13.0	1672.9	1.094	314.7	0.787			13.0
14.0	1666.1	1.089	243.7	0.609			14.0
15.0	1664.3	1.088	207.9	0.520			15.0
16.0	1670.2	1.092	216.0	0.540			16.0
17.0	1659.4	1.085	229.2	0.573			17.0
18.0	1666.1	1.089	390.3	0.976			18.0

Cruise: 1206-83
Position: 47-33N;124-35W

Station: DeS 4-4

Date: 4/29/83
Depth: 49m

Calculated for: 23.0 Deg-C 35.00 o/oo 0 m 400 kHz

Depth (cm)	Vp (m/sec)	Vp Ratio	Alpha (dB/m)	Attenu- ation k	Mean Grain Size(0)	% Pors.	Depth (cm)
WATER	1526.0	0.998	0.0	0.000			WATER
0.0	1636.1	1.070	181.3	0.453			0.0
1.0	1687.0	1.103	125.8	0.315			1.0
2.0	1690.7	1.105	130.5	0.326			2.0
3.0	1690.7	1.105	145.5	0.364			3.0
4.0	1687.5	1.103	150.8	0.377			4.0
5.0	1685.6	1.102	156.4	0.391			5.0
6.0	1685.6	1.102	162.2	0.406			6.0
7.0	1688.9	1.104	181.3	0.453			7.0
8.0	1687.5	1.103	181.3	0.453			8.0
9.0	1687.0	1.103	181.3	0.453			9.0
10.0	1683.3	1.101	174.6	0.437			10.0
11.0	1682.0	1.100	181.3	0.453			11.0
12.0	1676.0	1.096	188.2	0.471			12.0
13.0	1672.4	1.094	220.0	0.550			13.0
14.0	1669.3	1.091	310.0	0.775			14.0
15.0	1649.7	1.079	372.0	0.930			15.0

Cruise: 1206-83 Station: DeS 4-5 Date: 4/29/83
Position: 47-33N;124-35W Depth: 49m

Calculated for: 23.0 Deg-C 35.00 o/oo 0 m 400 kHz

Depth (cm)	Vp (m/sec)	Vp Ratio	Alpha (dB/m)	Attenu- ation k	Mean Grain Size(°)	% Pors.	Depth (cm)
WATER	1525.2	0.997	-4.7	-0.012			WATER
0.0	1645.5	1.076	249.5	0.624			0.0
1.0	1700.7	1.112	130.5	0.326	2.98	40.7	1.0
2.0	1705.4	1.115	116.9	0.292			2.0
3.0	1708.7	1.117	121.3	0.303	2.89	39.8	3.0
4.0	1708.3	1.117	140.3	0.351			4.0
5.0	1703.5	1.114	140.3	0.351	2.91	40.6	5.0
6.0	1700.3	1.112	162.2	0.406			6.0
7.0	1694.2	1.108	181.3	0.453	2.95	41.7	7.0
8.0	1689.1	1.104	195.5	0.489			8.0
9.0	1689.1	1.104	188.2	0.471	3.00	42.5	9.0
10.0	1680.8	1.099	195.5	0.489			10.0
11.0	1663.6	1.088	203.2	0.508	3.00	43.1	11.0
12.0	1651.2	1.080	249.5	0.624			12.0
13.0	1655.2	1.082	318.7	0.797	3.07	46.0	13.0
14.0	1657.0	1.083	294.2	0.736			14.0
15.0	1653.8	1.081	255.1	0.638	3.03	46.3	15.0
16.0	1661.4	1.086	260.9	0.652			16.0
17.0	1660.1	1.085	249.5	0.624	3.05	45.0	17.0
18.0	1677.6	1.097	267.0	0.668			18.0
19.0	1688.2	1.104	310.0	0.775	3.02	42.5	19.0
20.0	1696.5	1.109	470.7	1.177			20.0
21.0					3.00	40.3	21.0
22.0							22.0
23.0					3.11	42.2	23.0

Cruise: 1206-83 Station: DeS 4-6 Date: 4/29/83
Position: 47-33N;124-35W Depth: 49m

Calculated for: 23.0 Deg-C 35.00 o/oo 0 m 400 kHz

Depth (cm)	Vp (m/sec)	Vp Ratio	Alpha (dB/m)	Attenu- ation k	Mean Grain Size(°)	% Pors.	Depth (cm)
WATER	1526.4	0.998	4.7	0.012			WATER
0.0	1650.3	1.079	233.8	0.585			0.0
1.0	1691.9	1.106	130.5	0.326			1.0
2.0	1705.9	1.115	126.0	0.315			2.0
3.0	1706.4	1.116	150.1	0.375			3.0
4.0	1700.3	1.112	179.3	0.448			4.0
5.0	1700.3	1.112	179.3	0.448			5.0
6.0	1705.0	1.115	166.9	0.417			6.0
7.0	1697.5	1.110	200.2	0.500			7.0
8.0	1682.7	1.100	200.2	0.500			8.0
9.0	1688.6	1.104	207.9	0.520			9.0
10.0	1698.4	1.111	185.9	0.465			10.0
11.0	1697.5	1.110	192.9	0.482			11.0
12.0	1700.7	1.112	192.9	0.482			12.0
13.0	1698.9	1.111	173.0	0.432			13.0
14.0	1698.9	1.111	185.9	0.465			14.0
15.0	1693.3	1.107	238.7	0.597			15.0
16.0	1668.1	1.091	405.3	1.013			16.0

Cruise: 1206-83 Station: DeS 5-1 Date: 4/29/83
Position: 47-33N;124-36W Depth: 49m

Calculated for: 23.0 Deg-C 35.00 o/oo 0 m 400 kHz

Depth (cm)	Vp (m/sec)	Vp Ratio	Alpha (dB/m)	Attenu- ation k	Mean Grain Size(°)	% Pors.	Depth (cm)
WATER	1526.4	0.998	0.0	0.000			WATER
0.0	1681.8	1.100	248.8	0.622			0.0
1.0	1691.4	1.106	105.3	0.263	2.99	40.7	1.0
2.0	1701.7	1.113	113.2	0.283			2.0
3.0	1703.5	1.114	126.0	0.315	2.93	40.2	3.0
4.0	1700.7	1.112	140.0	0.350			4.0
5.0	1698.4	1.111	155.5	0.389	2.96	40.2	5.0
6.0	1701.7	1.113	161.1	0.403			6.0
7.0	1705.4	1.115	150.1	0.375	2.95	40.5	7.0
8.0	1709.7	1.118	150.1	0.375			8.0
9.0	1712.0	1.119	150.1	0.375	2.91	40.0	9.0
10.0	1716.8	1.123	150.1	0.375			10.0
11.0	1716.8	1.123	150.1	0.375	2.91	39.4	11.0
12.0	1719.2	1.124	155.5	0.389			12.0
13.0	1719.2	1.124	155.5	0.389	2.91	39.2	13.0
14.0	1719.7	1.124	166.9	0.417			14.0
15.0	1719.7	1.124	166.9	0.417	2.93	39.6	15.0
16.0	1716.8	1.123	207.9	0.520			16.0
17.0	1712.5	1.120	383.3	0.958	2.97	41.8	17.0
18.0							18.0
19.0					2.94	41.4	19.0

Cruise: 1206-83 Station: DeS 5-2 Date: 4/29/83
Position: 47-33N;124-36W Depth: 49m

Calculated for: 23.0 Deg-C 35.00 o/oo 0 m 400 kHz

Depth (cm)	Vp (m/sec)	Vp Ratio	Alpha (dB/m)	Attenu- ation k	Mean Grain Size(°)	% Pors.	Depth (cm)
WATER	1524.1	0.997	0.0	0.000			WATER
0.0	1530.5	1.001	37.8	0.095			0.0
1.0	1694.2	1.108	112.6	0.282	3.00	39.7	1.0
2.0	1695.6	1.109	112.6	0.282			2.0
3.0	1702.1	1.113	121.3	0.303			3.0
4.0	1710.2	1.118	121.3	0.303			4.0
5.0	1713.9	1.121	121.3	0.303			5.0
6.0	1719.2	1.124	121.3	0.303			6.0
7.0	1717.3	1.123	125.8	0.315			7.0
8.0	1715.4	1.122	130.5	0.326			8.0
9.0	1717.8	1.123	130.5	0.326			9.0
10.0	1713.0	1.120	135.3	0.338			10.0
11.0	1711.6	1.119	135.3	0.338			11.0
12.0	1711.6	1.119	130.5	0.326			12.0
13.0	1706.8	1.116	145.5	0.364			13.0
14.0	1703.1	1.114	156.4	0.391			14.0
15.0	1675.8	1.096	181.3	0.453			15.0
16.0	1676.3	1.096	220.0	0.550			16.0

Cruise: 1206-83 Station: DeS 5-3 Date: 4/29/83
Position: 47-33N;124-36W Depth: 49m

Calculated for: 23.0 Deg-C 35.00 o/oo 0 m 400 kHz

Depth (cm)	Vp (m/sec)	Vp Ratio	Alpha (dB/m)	Attenu- ation k	Mean Grain Size(0)	% Pors.	Depth (cm)
WATER	1522.2	0.995	14.5	0.036			WATER
0.0	1527.5	0.999	117.3	0.293			0.0
1.0	1689.6	1.105	117.3	0.293			1.0
2.0	1699.3	1.111	113.2	0.283			2.0
3.0	1706.8	1.116	113.2	0.283			3.0
4.0	1712.5	1.120	113.2	0.030			4.0
5.0	1712.0	1.119	126.0	0.315			5.0
6.0	1711.1	1.119	135.1	0.338			6.0
7.0	1710.2	1.118	140.0	0.350			7.0
8.0	1710.2	1.118	150.1	0.375			8.0
9.0	1708.3	1.117	150.1	0.375			9.0
10.0	1708.3	1.117	150.1	0.375			10.0
11.0	1706.8	1.116	166.9	0.417			11.0
12.0	1696.1	1.109	161.1	0.403			12.0
13.0	1672.6	1.094	265.6	0.664			13.0
14.0	1635.5	1.069	173.0	0.432			14.0
15.0	1618.7	1.058	173.0	0.432			15.0
16.0	1616.2	1.057	143.7	0.609			16.0
17.0	1699.3	1.111	561.7	1.404			17.0
18.0	1667.2	1.090	224.6	0.562			18.0
19.0	1684.0	1.101	220.3	0.551			19.0
20.0	1691.4	1.106	254.2	0.636			20.0
21.0	1693.7	1.107	291.6	0.729			21.0

Cruise: 1206-83 Station: DeS 5-4 Date: 4/29/83
Position: 47-33N;124-36W Depth: 49m

Calculated for: 23.0 Deg-C 35.00 o/oo 0 m 400 kHz

Depth (cm)	Vp (m/sec)	Vp Ratio	Alpha (dB/m)	Attenu- ation k	Mean Grain Size(0)	% Pors.	Depth (cm)
WATER	1523.7	0.996	0.0	0.000			WATER
0.0	1536.2	1.004	147.5	0.369			0.0
1.0	1684.0	1.101	185.9	0.465			1.0
2.0	1704.5	1.114	155.5	0.389			2.0
3.0	1717.8	1.123	135.1	0.338			3.0
4.0	1721.1	1.125	140.0	0.350			4.0
5.0	1716.8	1.123	150.1	0.375			5.0
6.0	1717.3	1.123	150.1	0.375			6.0
7.0	1719.7	1.124	150.1	0.375			7.0
8.0	1717.3	1.123	150.1	0.375			8.0
9.0	1717.3	1.123	150.1	0.375			9.0
10.0	1721.6	1.126	155.5	0.389			10.0
11.0	1721.6	1.126	155.5	0.389			11.0
12.0	1721.6	1.126	145.0	0.362			12.0
13.0	1720.6	1.125	145.0	0.362			13.0
14.0	1717.3	1.123	145.0	0.362			14.0
15.0	1713.0	1.120	145.0	0.362			15.0
16.0	1707.8	1.117	155.5	0.389			16.0
17.0	1703.5	1.114	166.9	0.417			17.0
18.0	1698.9	1.111	166.9	0.417			18.0
19.0	1691.0	1.106	376.7	0.942			19.0

Cruise: 1206-83 Station: DeS 6-1 Date: 4/29/83
Position: 47-33N;124-36W Depth: 49m

Calculated for: 23.0 Deg-C 35.00 o/oo 0 m 400 kHz

Depth (cm)	Vp (m/sec)	Vp Ratio	Alpha (dB/m)	Attenu- ation k	Mean Grain Size(0)	% Pors.	Depth (cm)
WATER	1524.9	0.997	0.0	0.000			WATER
0.0	1533.6	1.003	103.4	0.258			0.0
1.0	1695.6	1.109	109.2	0.273	3.03	41.0	1.0
2.0	1699.8	1.111	117.3	0.293			2.0
3.0	1703.5	1.114	109.2	0.273			3.0
4.0	1704.5	1.114	105.3	0.263			4.0
5.0	1706.8	1.116	109.2	0.273			5.0
6.0	1706.8	1.116	109.2	0.273			6.0
7.0	1712.5	1.120	113.2	0.283			7.0
8.0	1715.8	1.122	117.3	0.293			8.0
9.0	1712.5	1.120	117.3	0.293			9.0
10.0	1711.1	1.119	121.6	0.304			10.0
11.0	1707.3	1.116	145.0	0.362			11.0
12.0	1690.5	1.105	173.0	0.432			12.0
13.0	1679.5	1.098	192.9	0.482			13.0

Cruise: 1206-83 Station: DeS 6-2 Date: 4/29/83
Position: 47-33N;124-36W Depth: 49m

Calculated for: 23.0 Deg-C 35.00 o/oo 0 m 400 kHz

Depth (cm)	Vp (m/sec)	Vp Ratio	Alpha (dB/m)	Attenu- ation k	Mean Grain Size(0)	% Pors.	Depth (cm)
WATER	1520.4	0.994	0.0	0.000			WATER
0.0	1529.0	1.000	94.2	0.235			0.0
1.0	1712.0	1.119	117.3	0.293	3.03	40.7	1.0
2.0	1713.0	1.120	113.2	0.283			2.0
3.0	1713.0	1.120	109.2	0.273	2.93	40.1	3.0
4.0	1739.5	1.137	117.3	0.293			4.0
5.0	1713.9	1.121	121.6	0.304	2.88	39.8	5.0
6.0	1715.8	1.122	109.2	0.273			6.0
7.0	1720.1	1.125	117.3	0.293	2.90	38.8	7.0
8.0	1720.1	1.125	126.0	0.315			8.0
9.0	1718.2	1.123	130.5	0.326	2.91	39.6	9.0
10.0	1708.3	1.117	155.5	0.389			10.0
11.0	1692.4	1.107	185.9	0.465	2.94	41.1	11.0
12.0	1676.3	1.096	278.0	0.695			12.0
13.0	1668.6	1.091	314.7	0.787	3.06	45.3	13.0
14.0	1674.9	1.095	323.3	0.808			14.0
15.0	1693.3	1.107	192.9	0.482	2.96	42.5	15.0
16.0	1691.9	1.106	233.8	0.585			16.0
17.0	1687.3	1.103	192.9	0.482	3.00	43.0	17.0
18.0	1672.2	1.093	364.3	0.911			18.0
19.0					3.09	43.0	19.0
20.0							20.0
21.0					3.13	41.3	21.0

Cruise: 1206-83 Station: DeS 6-3 Date: 4/29/83
Position: 47-33N;124-36W Depth: 49m

Calculated for: 23.0 Deg-C 35.00 o/oo 0 m 400 kHz

Depth (cm)	Vp (m/sec)	Vp Ratio	Alpha (dB/m)	Attenu- ation k	Mean Grain Size(0)	% Pors.	Depth (cm)
WATER	1523.0	0.996	-4.7	-0.012			WATER
0.0	1530.5	1.001	89.5	0.224			0.0
1.0	1711.6	1.119	100.6	0.252			1.0
2.0	1707.8	1.117	96.8	0.242			2.0
3.0	1707.8	1.117	104.5	0.261			3.0
4.0	1708.7	1.117	121.3	0.303			4.0
5.0	1712.5	1.120	121.3	0.303			5.0
6.0	1709.7	1.118	121.3	0.303			6.0
7.0	1703.1	1.114	130.5	0.326			7.0
8.0	1698.4	1.111	140.3	0.351			8.0
9.0	1702.6	1.113	150.8	0.377			9.0
10.0	1692.4	1.107	203.2	0.508			10.0
11.0	1673.1	1.094	239.0	0.597			11.0
12.0	1710.2	1.118	188.2	0.471			12.0
13.0	1706.8	1.116	203.2	0.508			13.0
14.0	1705.4	1.115	372.0	0.930			14.0

Cruise: 1206-83 Station: DeS 7-1 Date: 5/1/83
Position: 47-30N;124-34W Depth: 49m

Calculated for: 23.0 Deg-C 35.00 o/oo 0 m 400 kHz

Depth (cm)	Vp (m/sec)	Vp Ratio	Alpha (dB/m)	Attenu- ation k	Mean Grain Size(0)	% Pors.	Depth (cm)
WATER	1527.8	0.999	0.0	0.000			WATER
0.0	1532.0	1.002	39.3	0.098			0.0
1.0	1709.5	1.118	99.7	0.249	2.93	40.0	1.0
2.0	1709.5	1.118	107.8	0.270			2.0
3.0	1706.6	1.116	107.8	0.270			3.0
4.0	1704.7	1.115	135.5	0.339			4.0
5.0	1703.3	1.114	151.6	0.379			5.0
6.0	1681.5	1.099	169.8	0.425			6.0
7.0	1691.6	1.106	169.8	0.425			7.0
8.0	1693.0	1.107	157.4	0.394			8.0
9.0	1694.9	1.108	146.0	0.365			9.0
10.0	1693.5	1.107	146.0	0.365			10.0
11.0	1691.2	1.106	146.0	0.365			11.0
12.0	1676.5	1.096	262.2	0.655			12.0

Cruise: 1206-83 Station: DeS 7-2 Date: 5/1/83
 Position: 47-30N;124-34W Depth: 49m
 Calculated for: 23.0 Deg-C 35.00 o/oo 0 m 400 kHz

Depth (cm)	Vp (m/sec)	Vp Ratio	Alpha (dB/m)	Attenu- ation k	Mean Grain Size(Ø)	% Pors.	Depth (cm)
WATER	1526.1	0.998	5.0	0.012			WATER
0.0	1652.9	1.081	297.1	0.743			0.0
1.0	1691.0	1.106	116.5	0.291			1.0
2.0	1685.4	1.102	116.5	0.291			2.0
3.0	1683.1	1.101	135.5	0.339			3.0
4.0	1702.2	1.113	183.4	0.458			4.0
5.0	1704.1	1.114	125.6	0.314			5.0
6.0	1695.6	1.109	130.5	0.326			6.0
7.0	1703.6	1.114	151.6	0.379			7.0
8.0	1673.1	1.094	268.5	0.671			8.0
9.0	1662.7	1.087	206.5	0.516			9.0
10.0	1673.1	1.094	354.8	0.887			10.0

Cruise: 1206-83 Station: DeS 7-3 Date: 5/1/83
 Position: 47-30N;124-34W Depth: 49m
 Calculated for: 23.0 Deg-C 35.00 o/oo 0 m 400 kHz

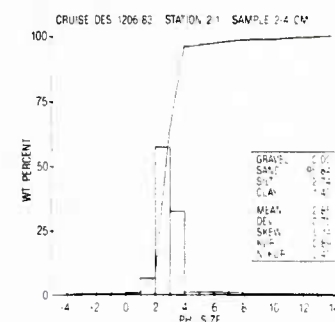
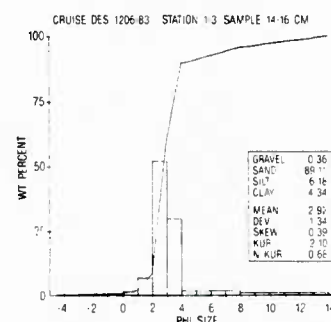
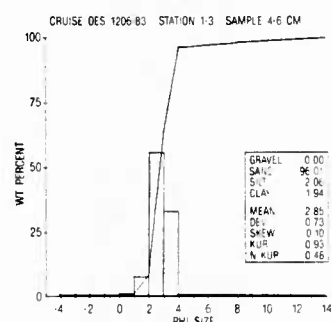
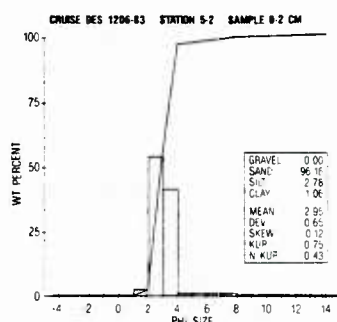
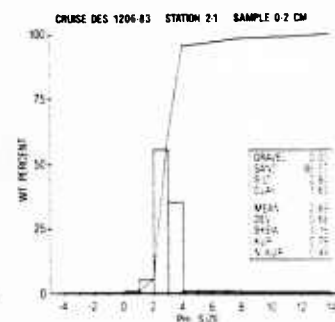
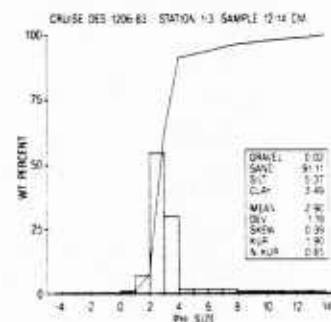
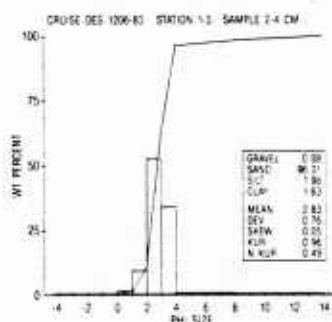
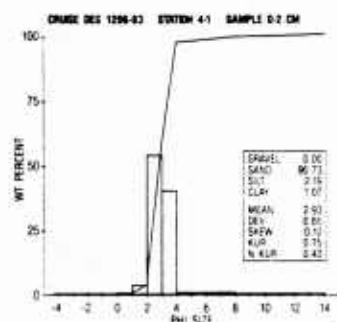
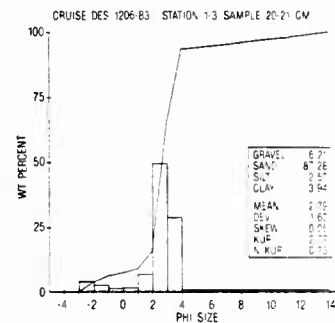
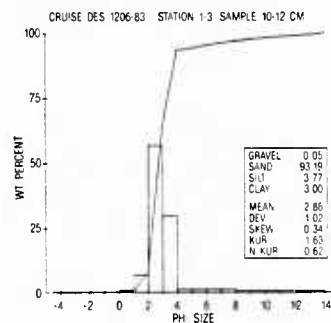
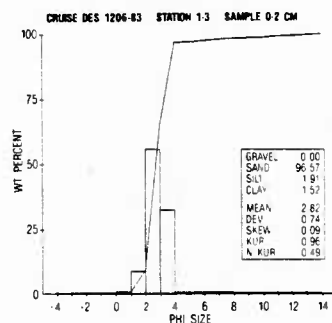
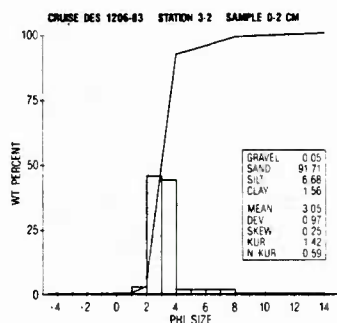
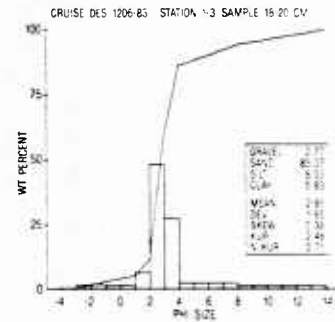
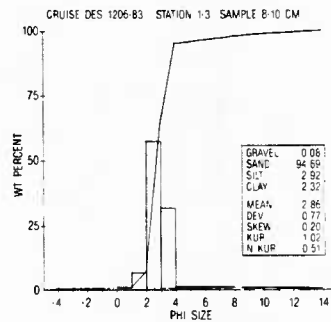
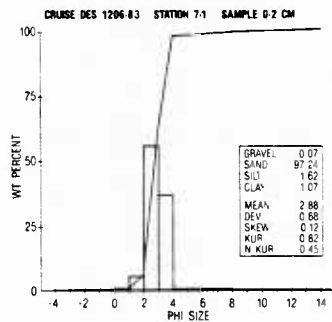
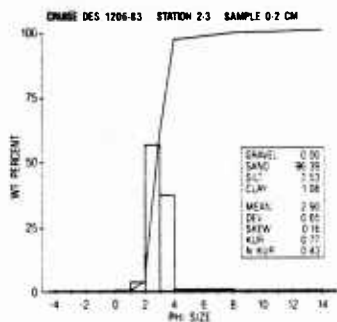
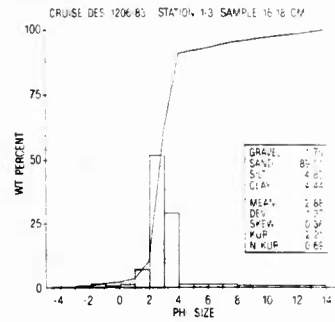
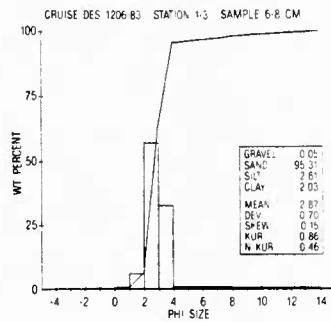
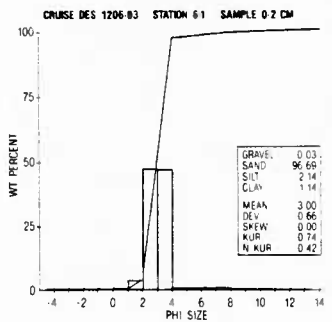
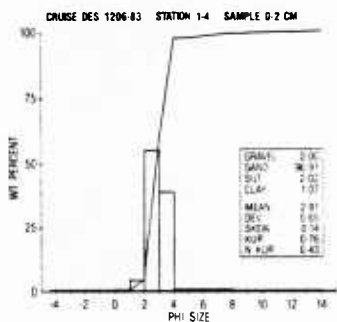
Depth (cm)	Vp (m/sec)	Vp Ratio	Alpha (dB/m)	Attenu- ation k	Mean Grain Size(Ø)	% Pors.	Depth (cm)
WATER	1527.6	0.999	0.0	0.000			WATER
0.0	1682.7	1.100	215.2	0.538			0.0
1.0	1701.7	1.113	116.5	0.291			1.0
2.0	1710.7	1.119	99.7	0.249			2.0
3.0	1720.7	1.125	103.7	0.259			3.0
4.0	1724.5	1.128	116.5	0.291			4.0
5.0	1716.4	1.122	116.5	0.291			5.0
6.0	1714.5	1.121	116.5	0.291			6.0
7.0	1713.5	1.120	135.5	0.339			7.0
8.0	1703.1	1.114	190.7	0.477			8.0
9.0	1690.5	1.105	198.4	0.496			9.0
10.0	1703.1	1.114	183.4	0.458			10.0
11.0	1706.9	1.116	183.4	0.458			11.0
12.0	1706.4	1.116	183.4	0.458			12.0
13.0	1701.7	1.113	163.5	0.409			13.0
14.0	1696.5	1.109	206.5	0.516			14.0
15.0	1696.5	1.109	198.4	0.496			15.0
16.0	1700.8	1.112	190.7	0.477			16.0
17.0	1694.7	1.108	130.5	0.326			17.0

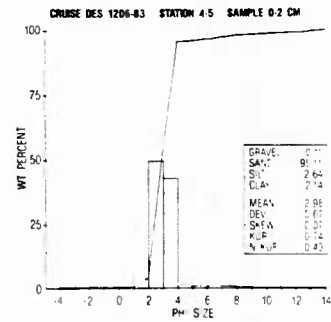
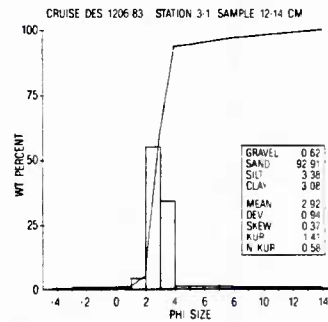
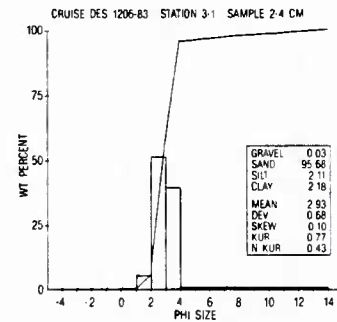
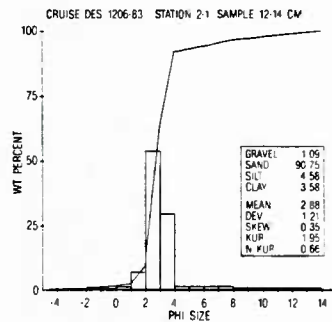
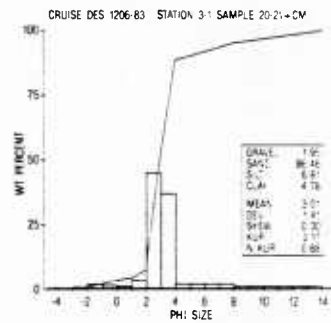
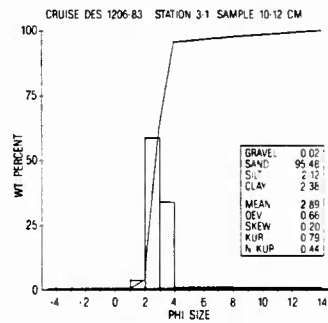
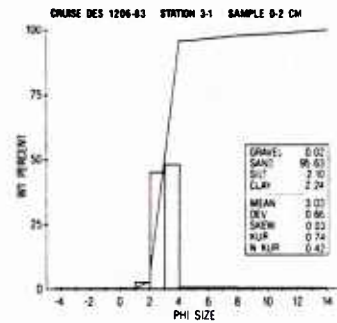
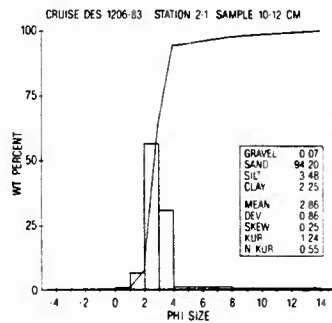
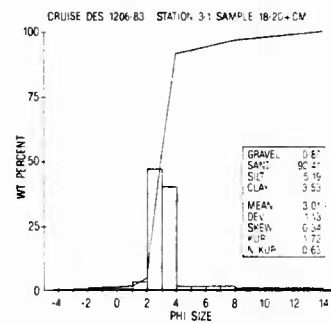
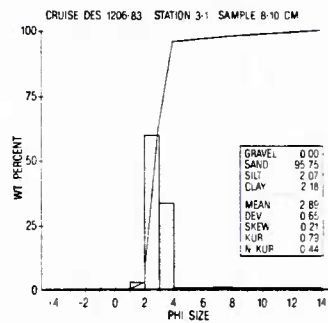
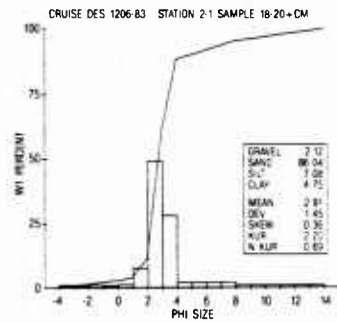
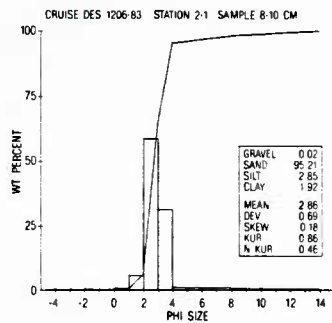
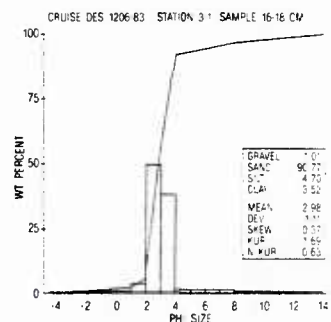
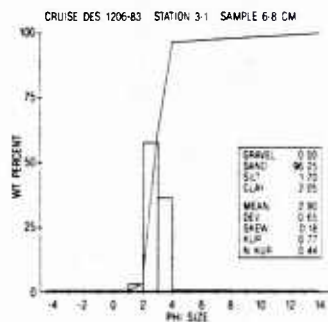
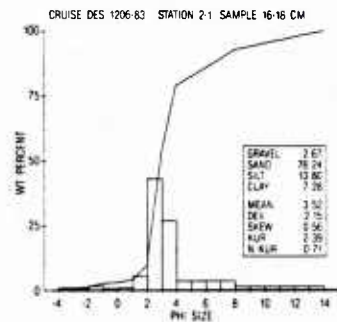
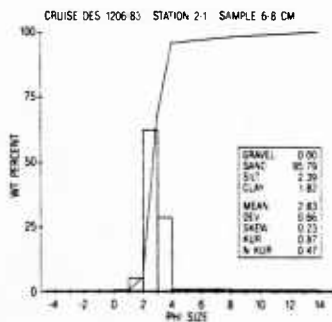
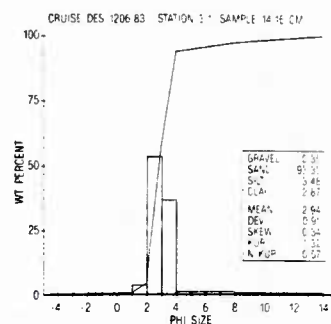
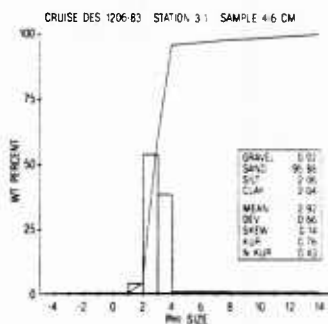
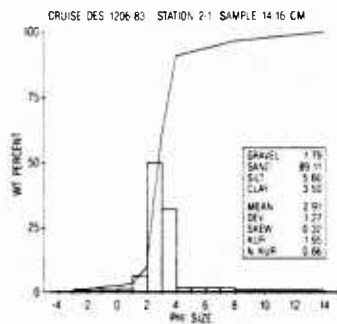
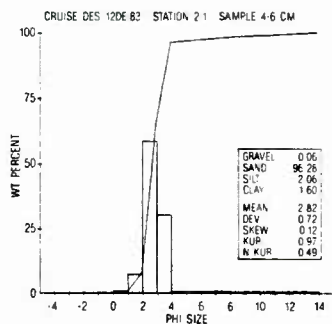
Cruise: 1206-83 Station: DeS 7-4 Date: 5/1/83
 Position: 47-30N;124-34W Depth: 49m

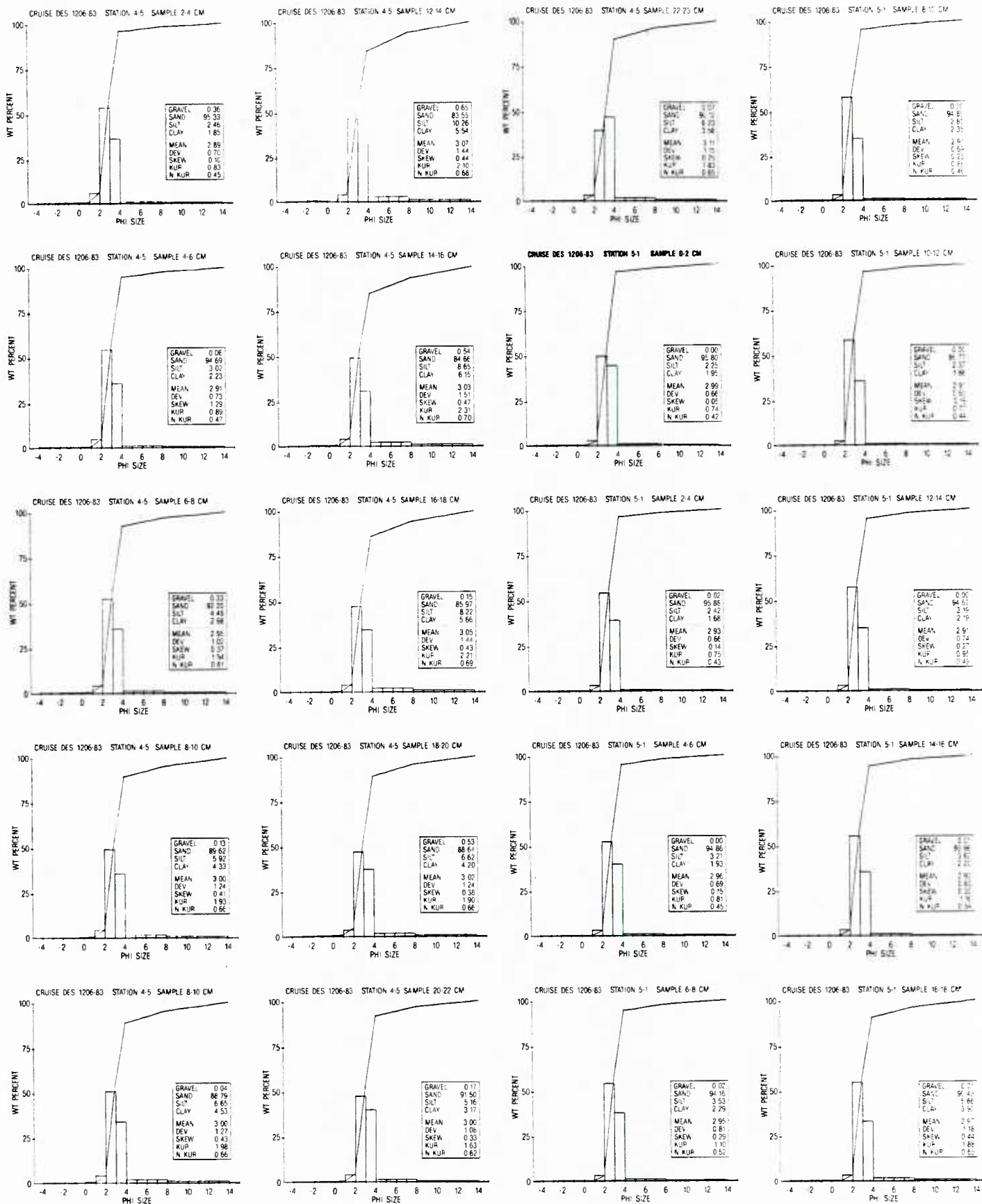
Calculated for: 23.0 Deg-C 35.00 o/oo 0 m 400 kHz

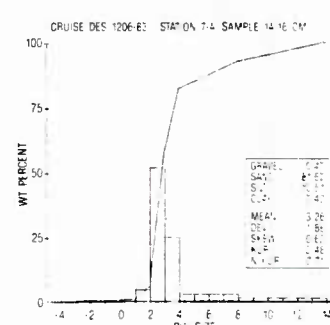
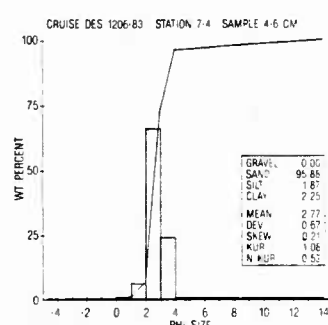
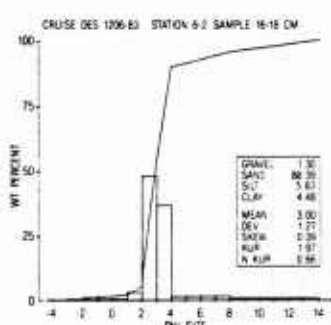
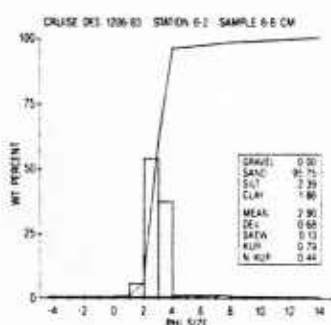
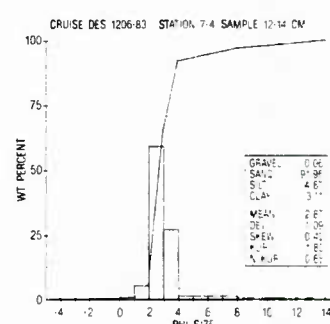
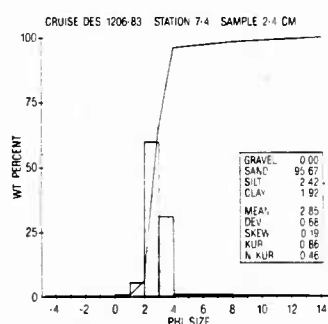
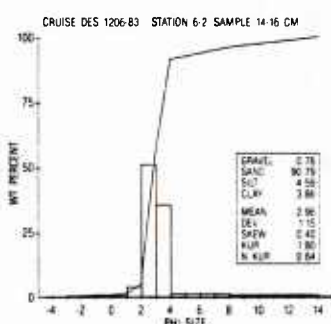
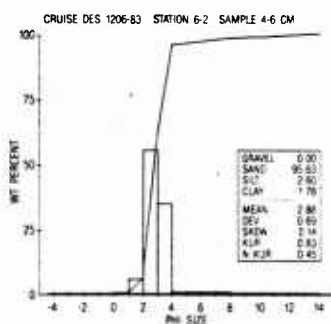
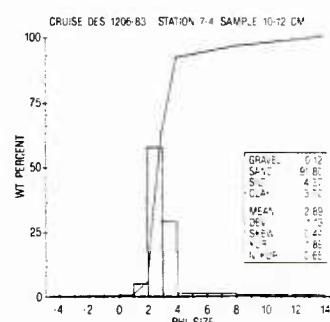
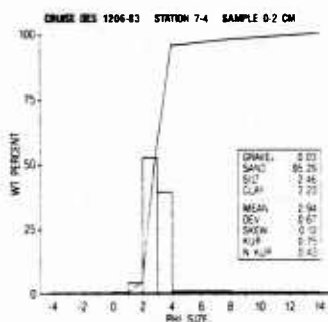
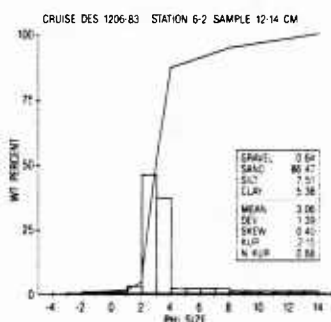
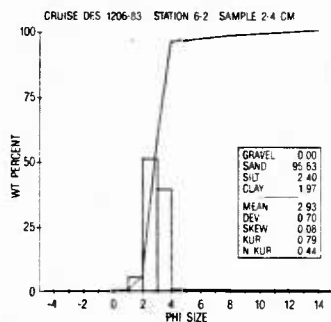
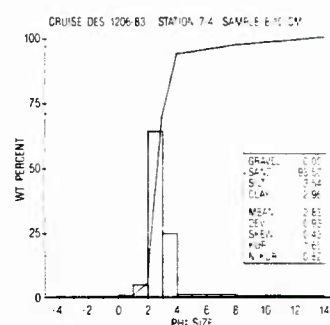
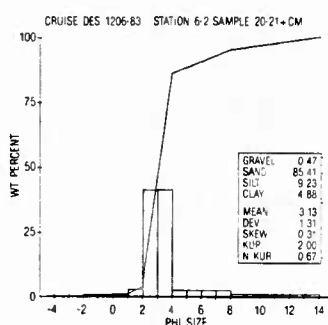
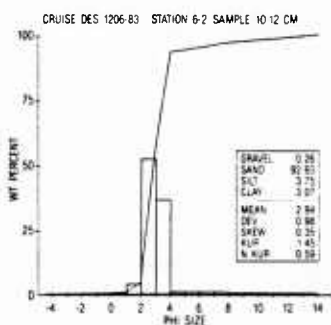
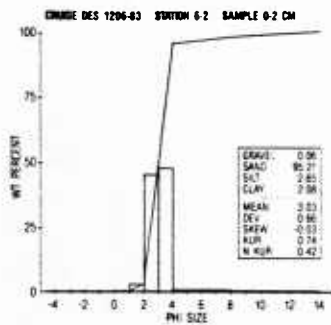
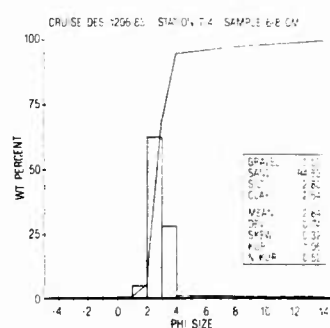
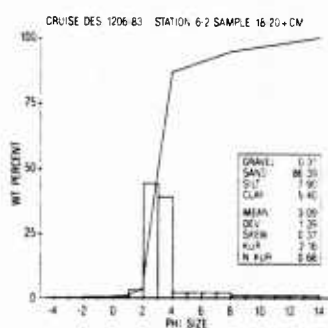
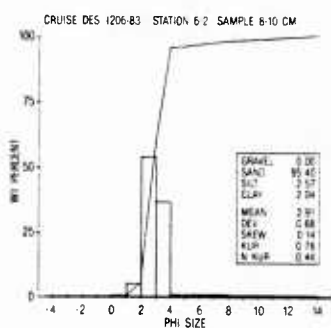
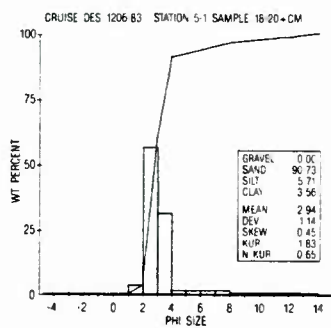
Depth (cm)	Vp (m/sec)	Vp Ratio	Alpha (dB/m)	Attenu- ation k	Mean Grain Size(0)	% Pors.	Depth (cm)
WATER	1525.7	0.998	0.0	0.000			WATER
0.0	1749.5	1.144	431.6	1.079			0.0
1.0	1697.0	1.110	92.0	0.230	2.94	39.7	1.0
2.0	1701.2	1.112	99.7	0.249			2.0
3.0	1705.5	1.115	103.7	0.259	2.85	39.8	3.0
4.0	1710.7	1.119	112.1	0.280			4.0
5.0	1708.8	1.117	107.8	0.270	2.77	40.1	5.0
6.0	1708.3	1.117	116.5	0.291			6.0
7.0	1709.2	1.118	130.5	0.326	2.84	40.9	7.0
8.0	1706.4	1.116	135.5	0.339			8.0
9.0	1701.7	1.113	146.0	0.365	2.83	41.8	9.0
10.0	1696.2	1.109	157.4	0.394			10.0
11.0	1695.2	1.108	146.0	0.365	2.89	42.3	11.0
12.0	1698.4	1.111	157.4	0.394			12.0
13.0	1686.3	1.103	198.4	0.496	2.87	42.9	13.0
14.0	1664.5	1.088	206.5	0.516			14.0
15.0	1645.4	1.076	198.4	0.496	3.26	47.5	15.0
16.0	1665.4	1.089	163.5	0.409			16.0
17.0	1676.3	1.096	157.4	0.394	2.95	43.8	17.0
18.0	1709.2	1.118	157.4	0.394			18.0
19.0					2.91	42.0	19.0
20.0							20.0
21.0					2.94	41.3	21.0

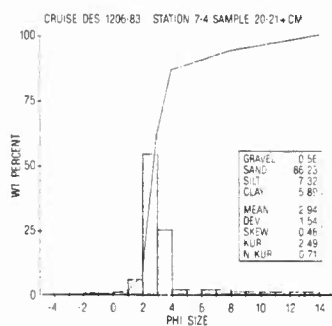
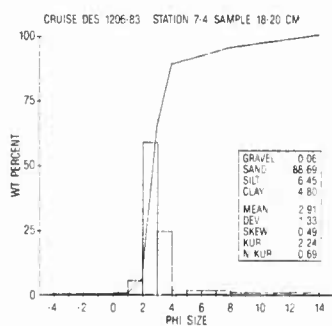
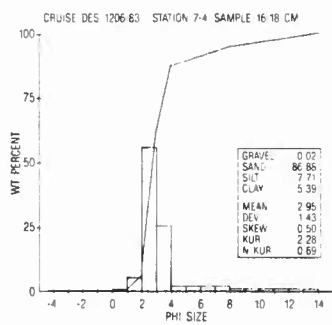
Appendix B. Sediment grain size distribution data



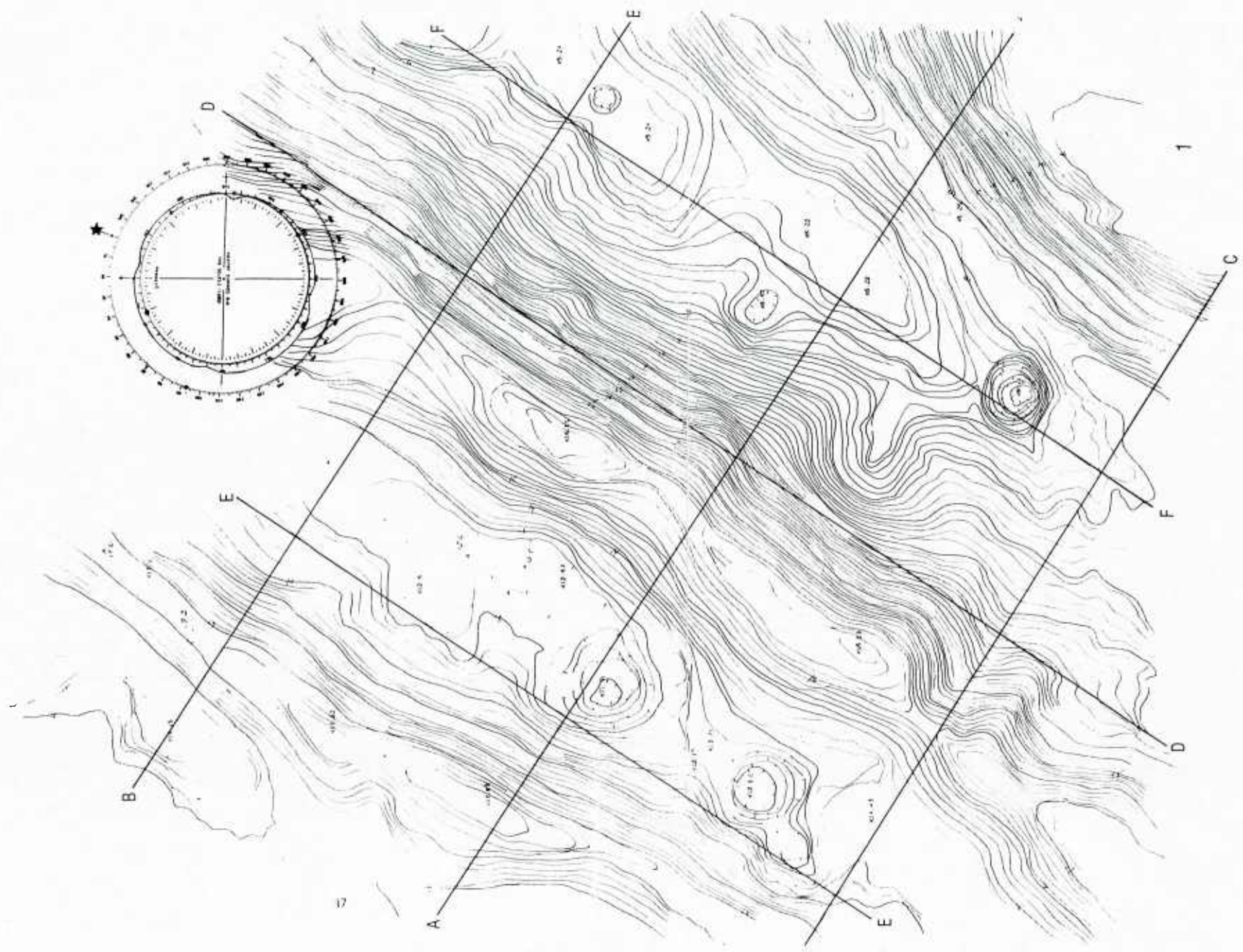


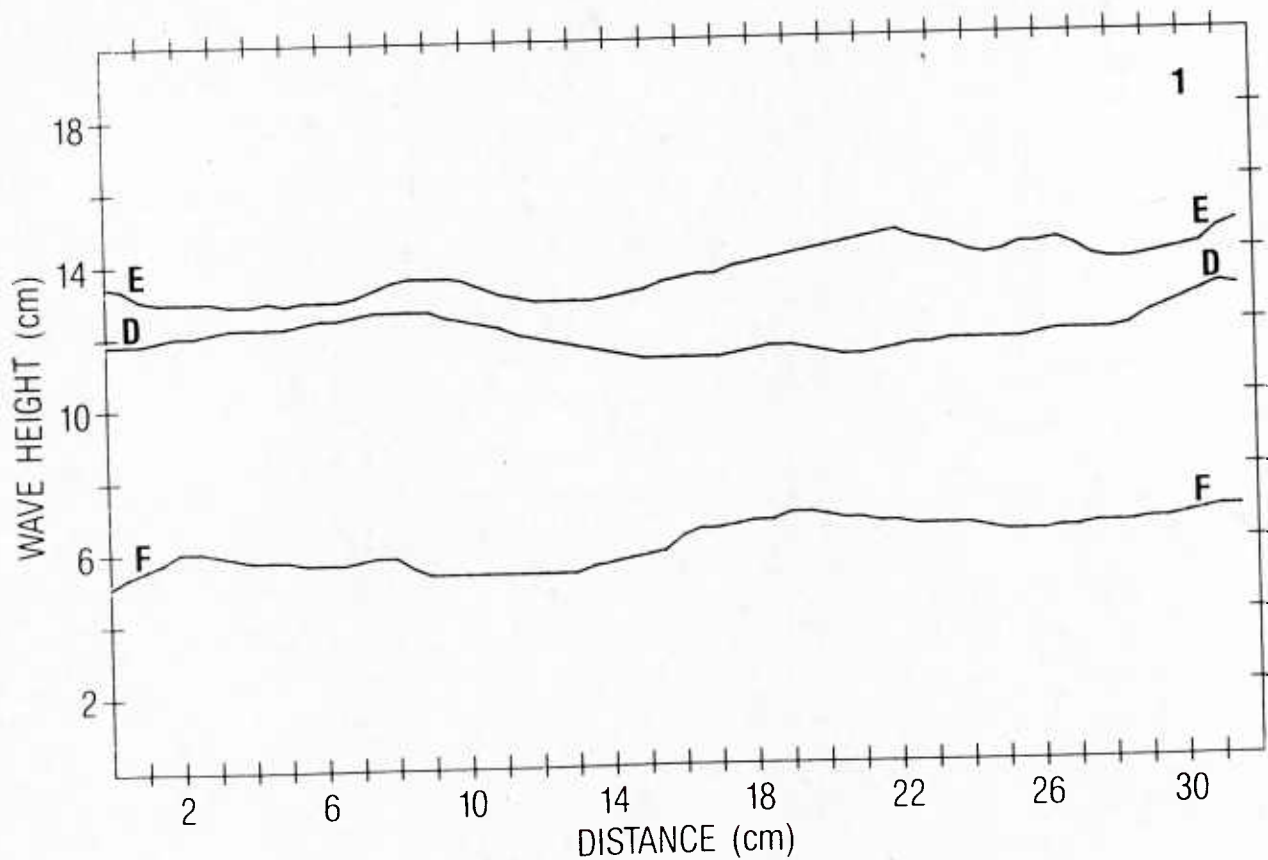
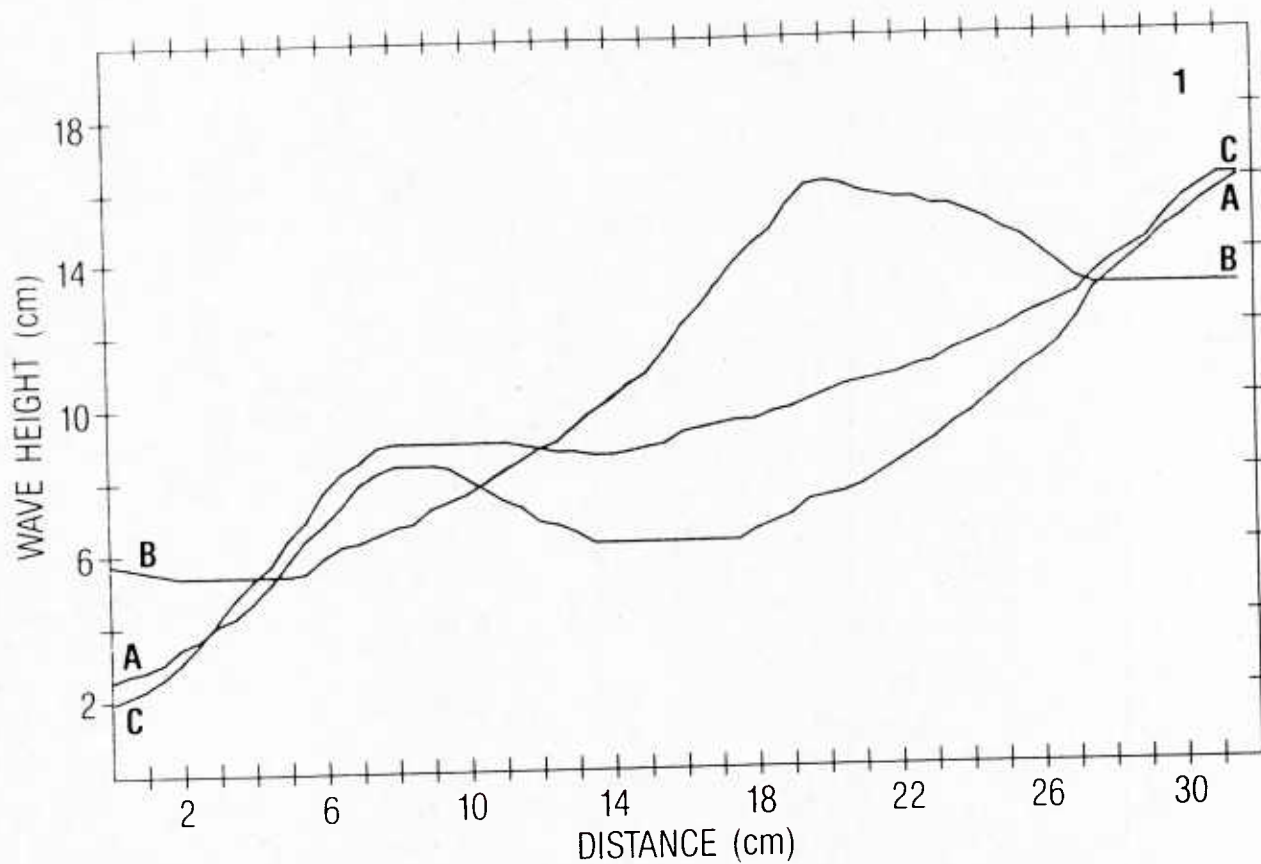


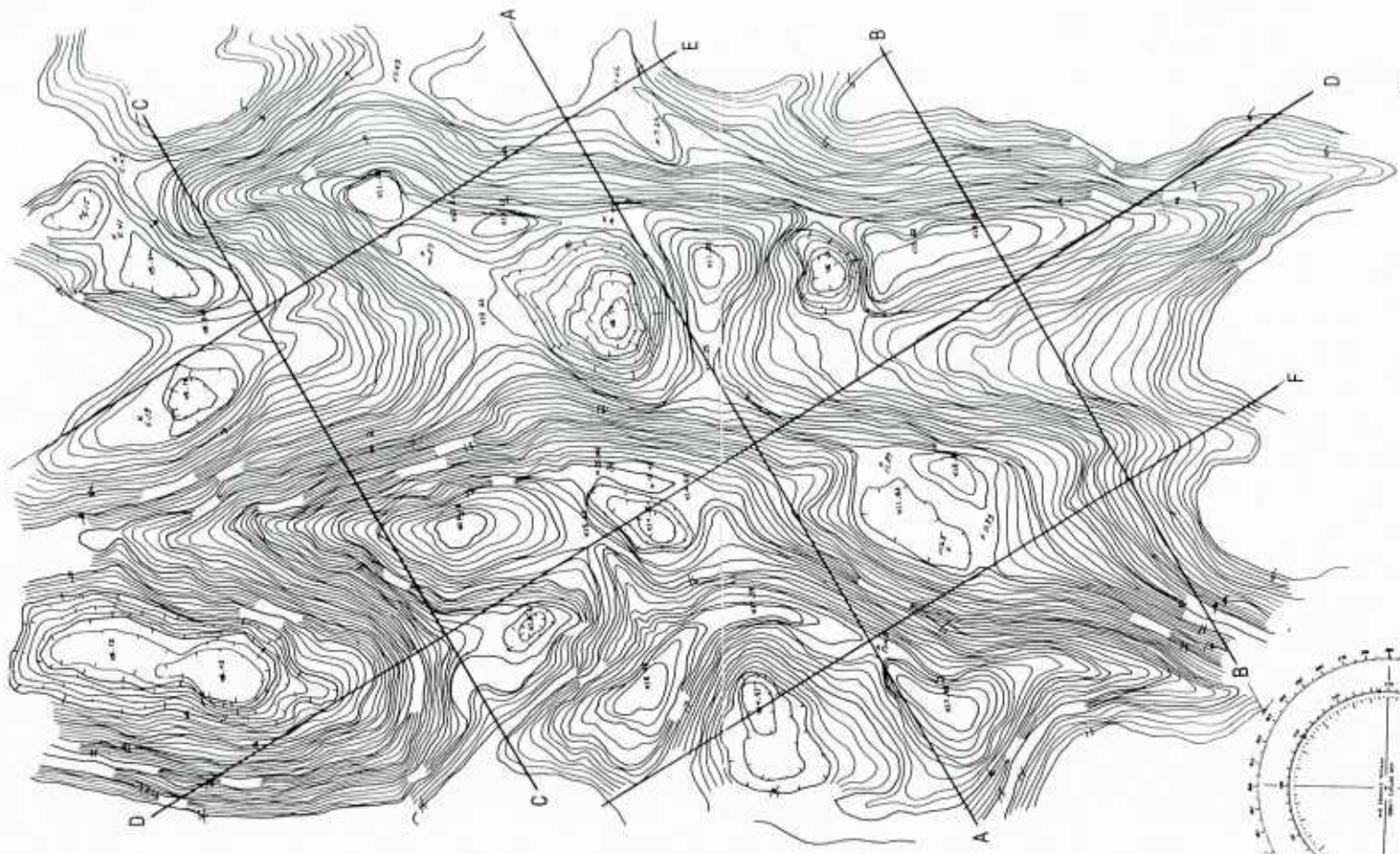




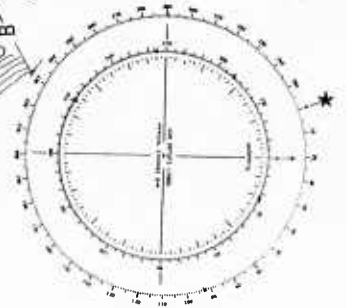
Appendix C. Sediment roughness contours and roughness profiles of cross-sectional lines

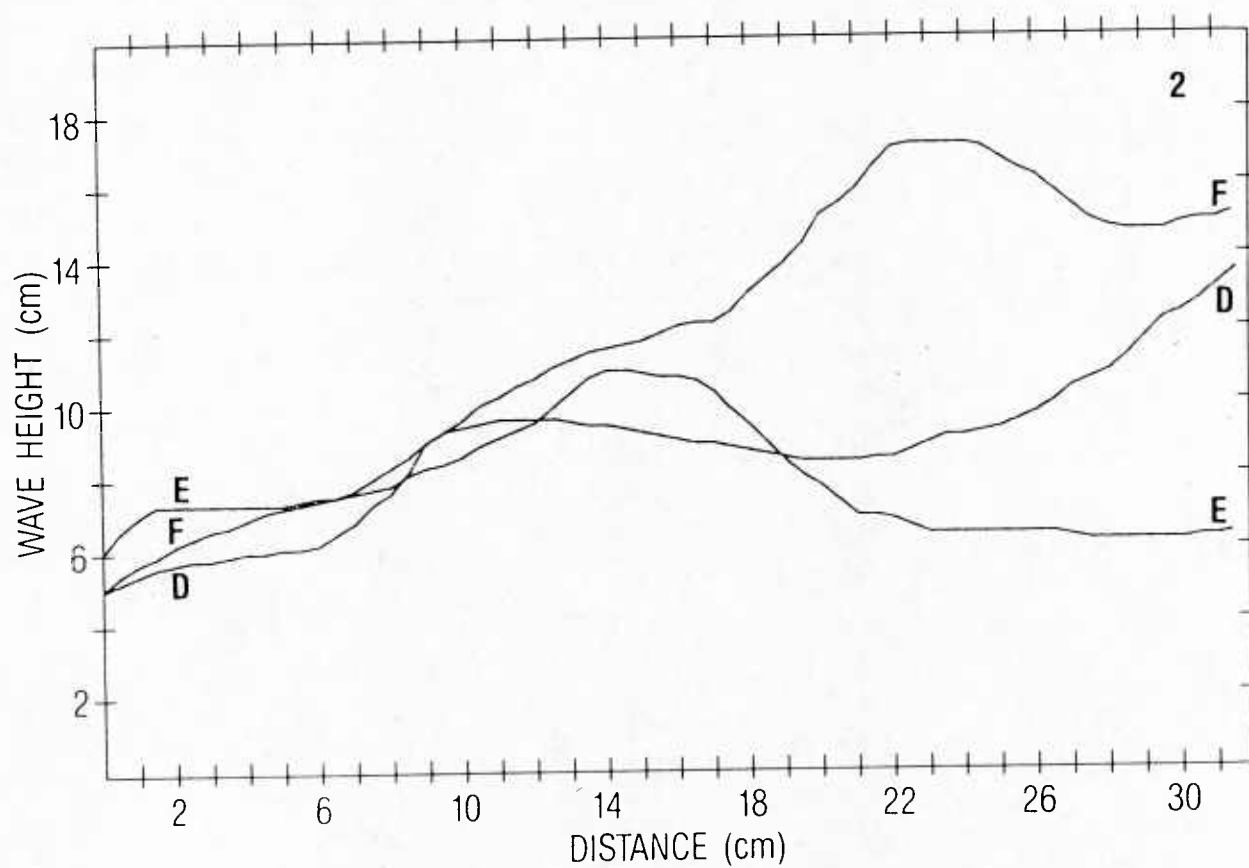
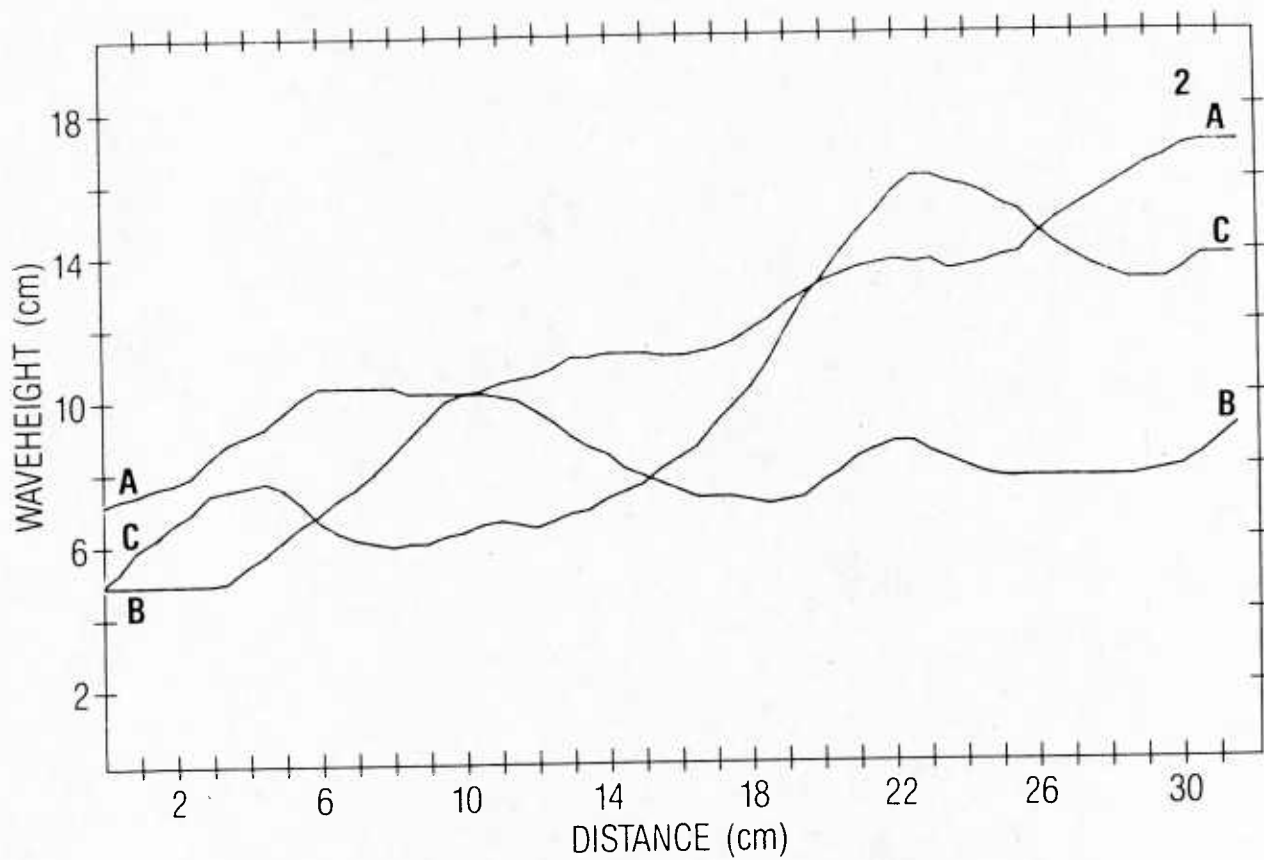


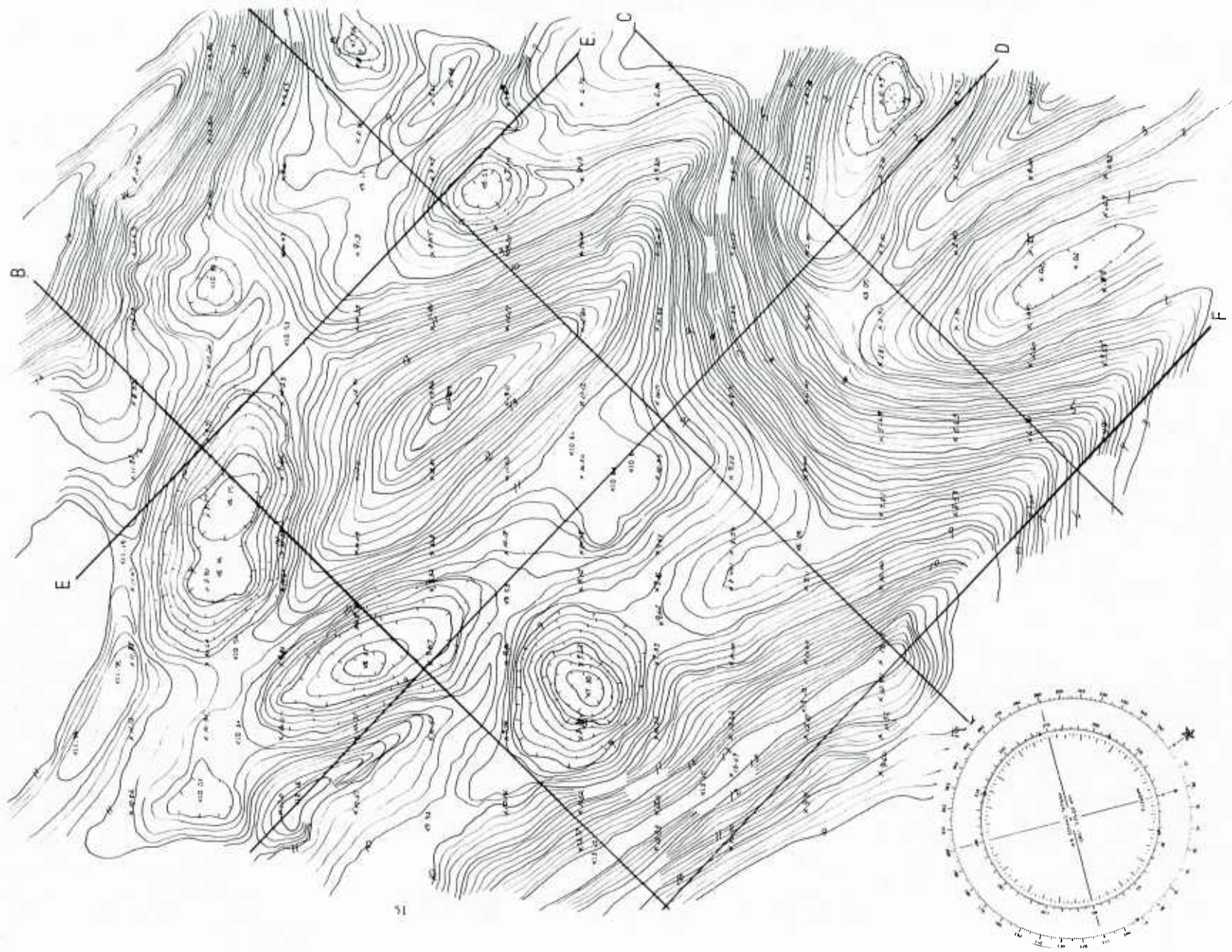


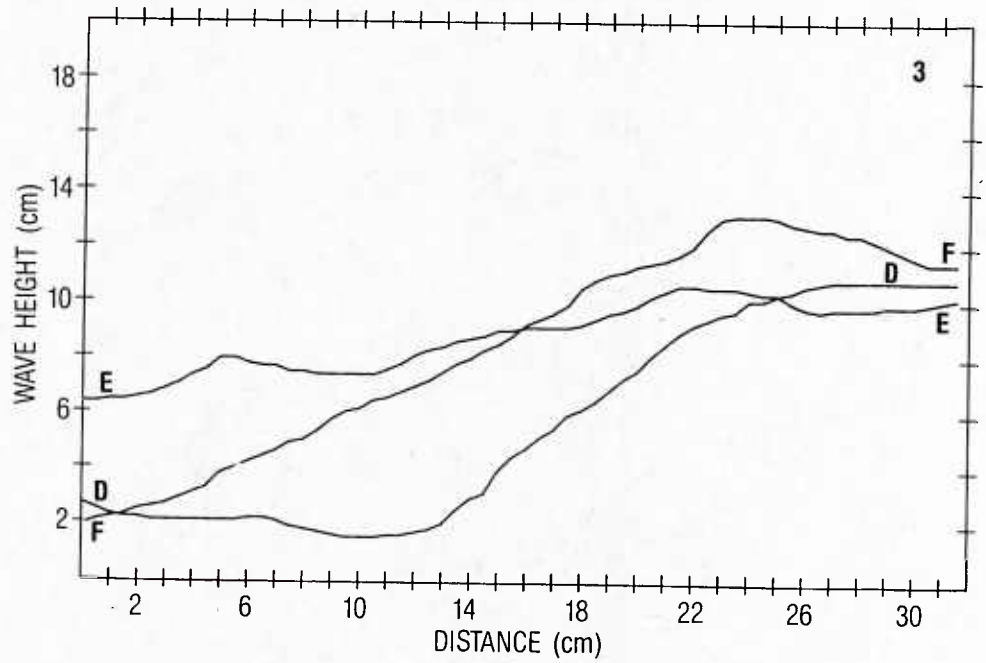
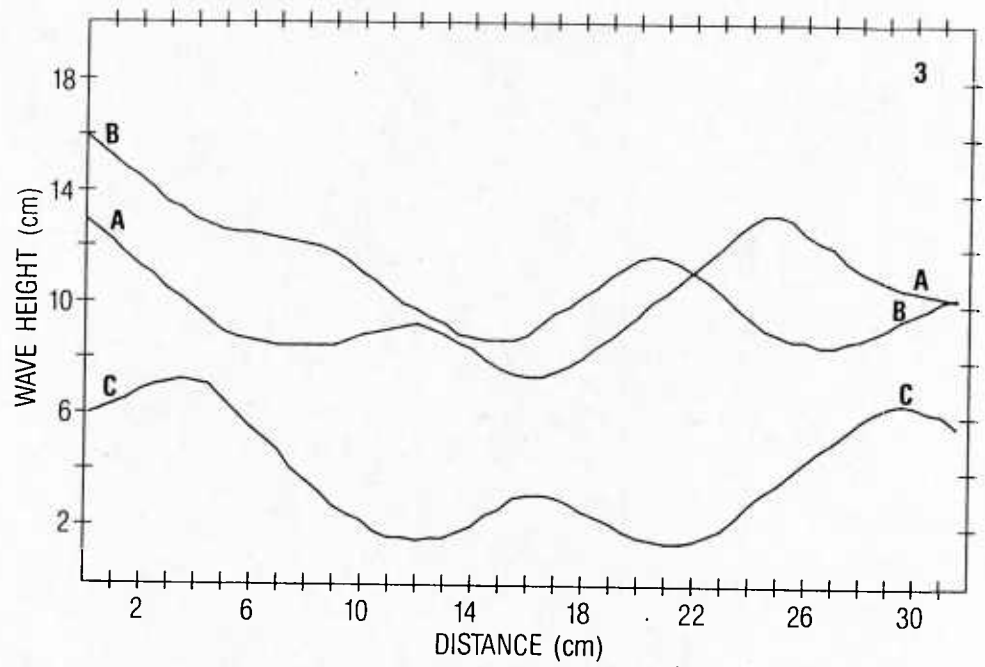


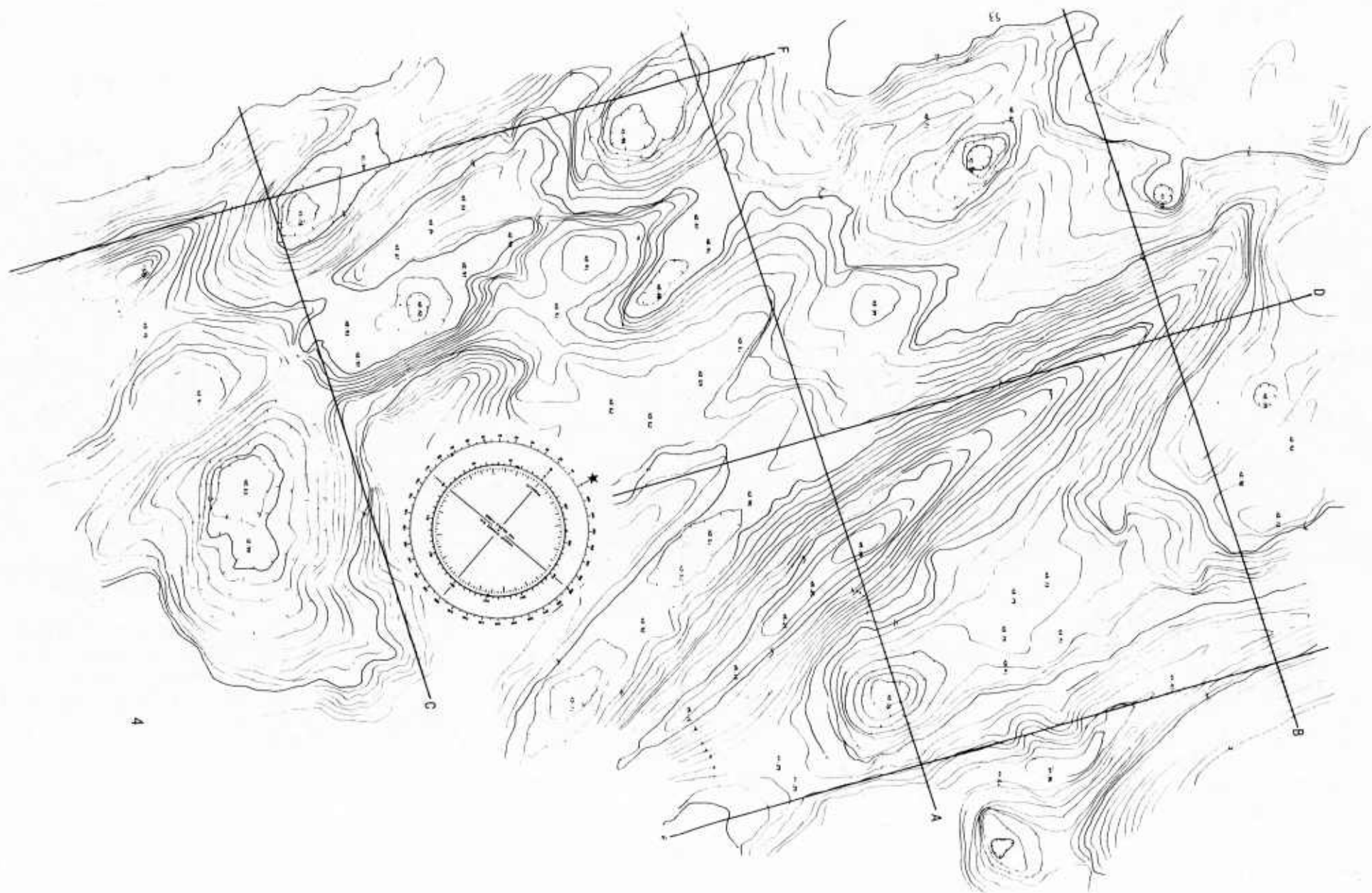
2

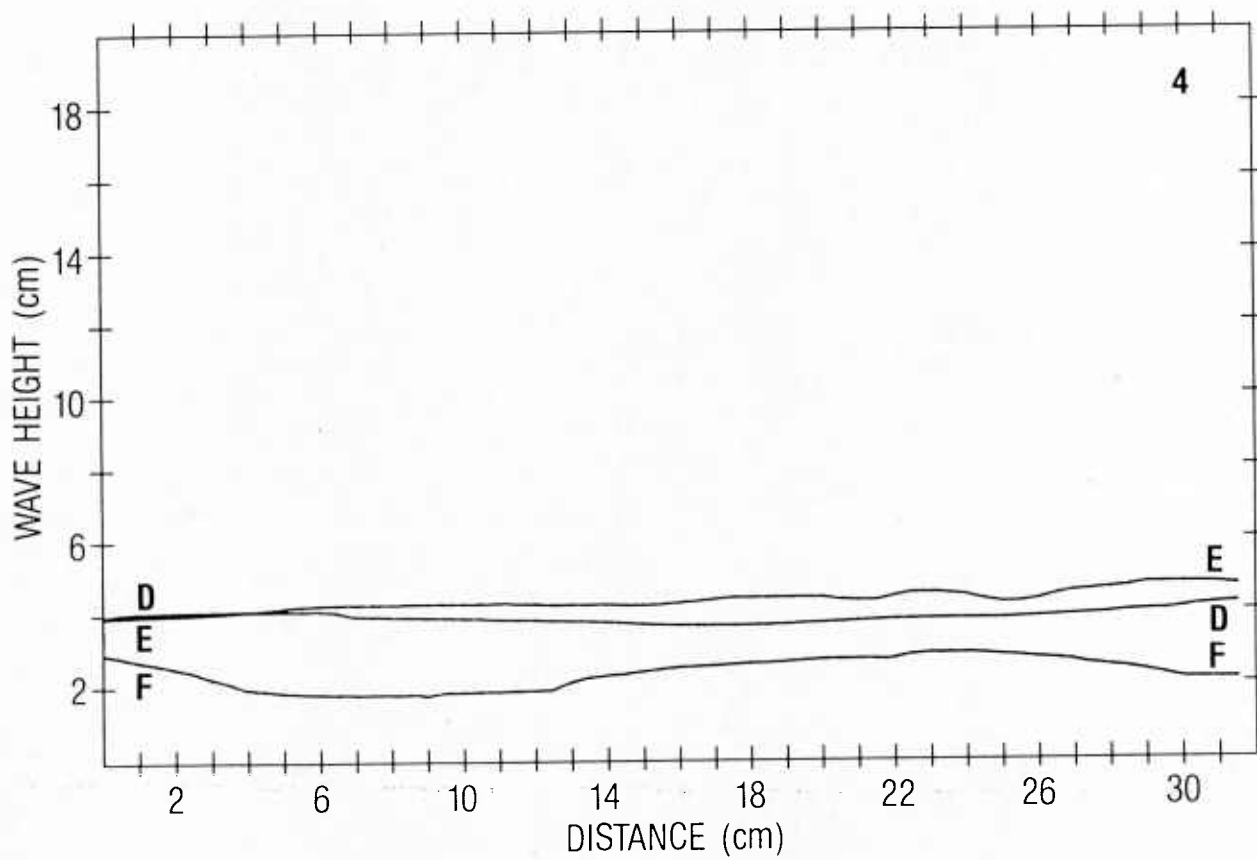
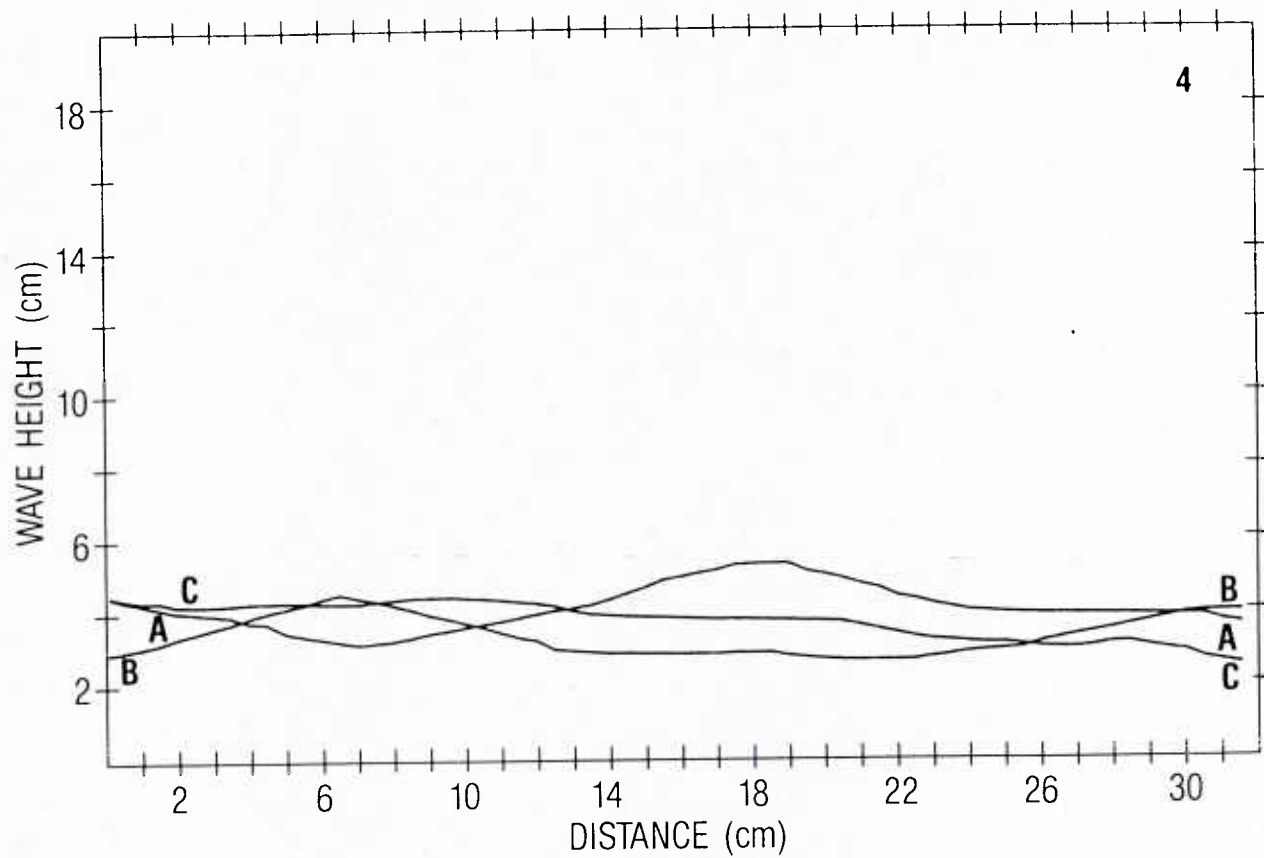


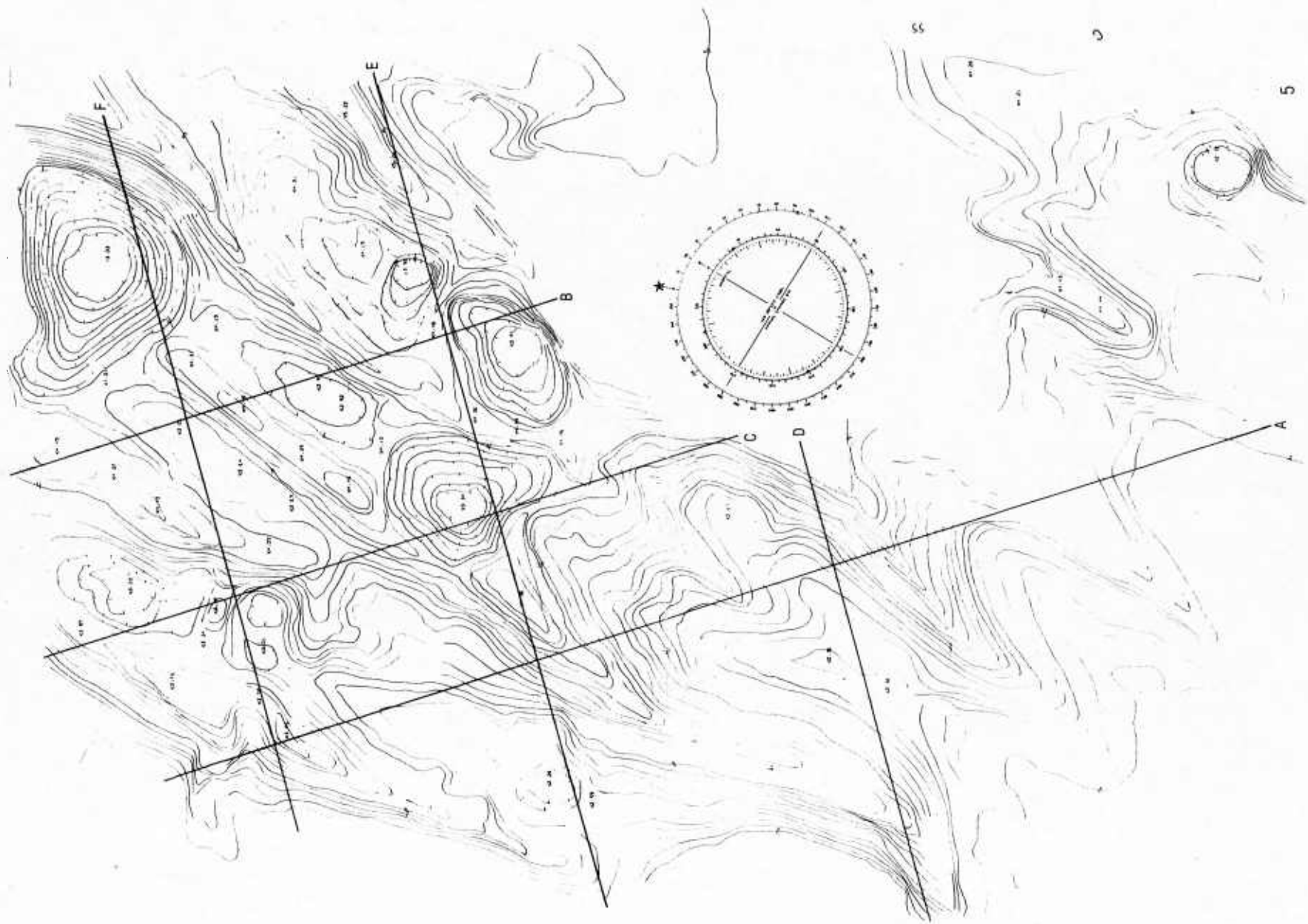


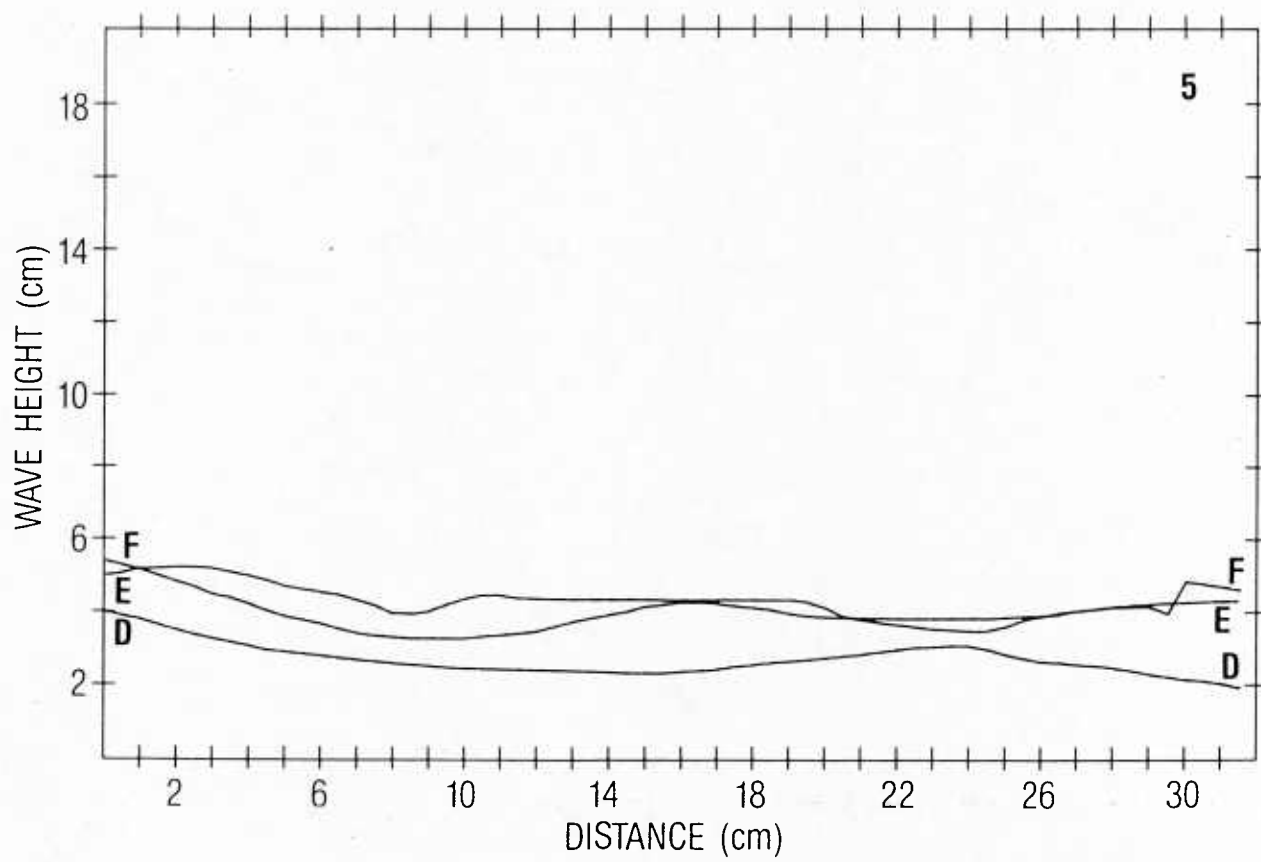
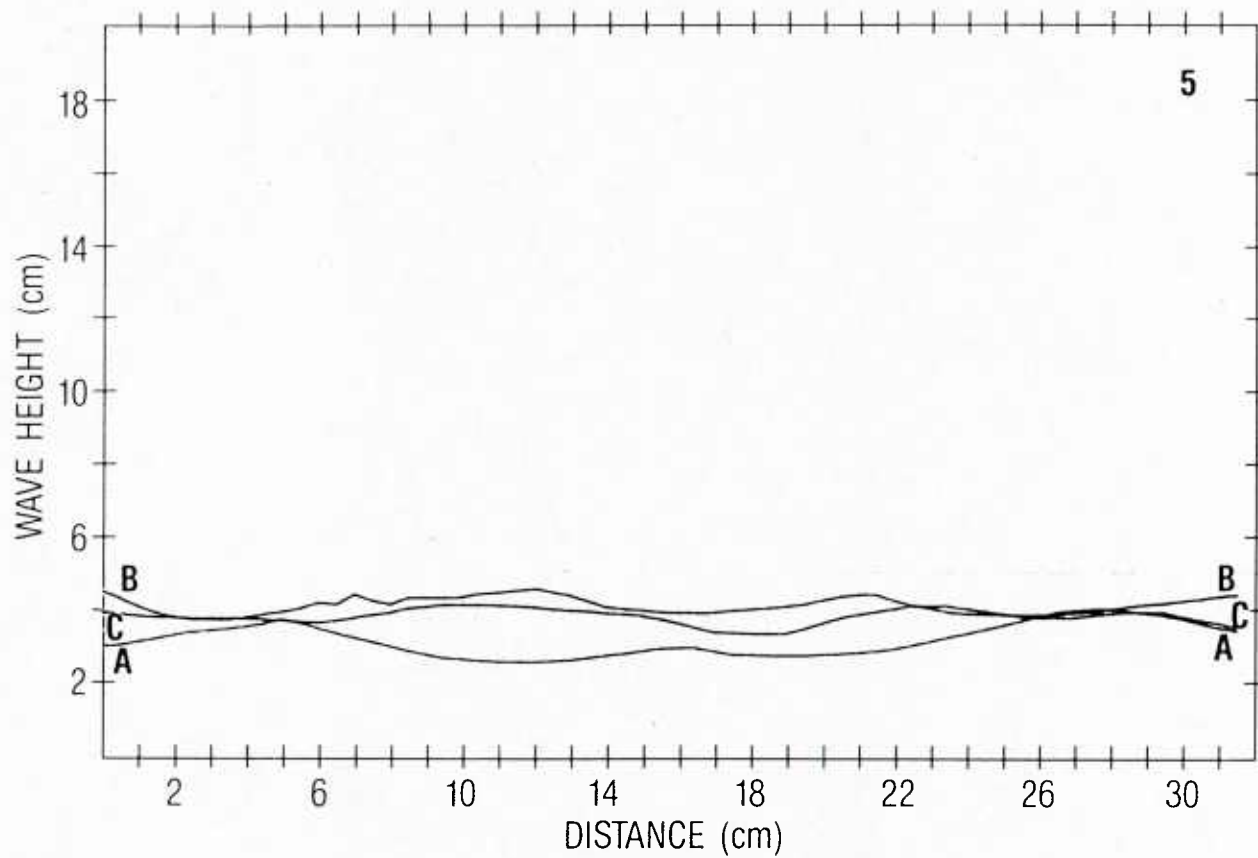


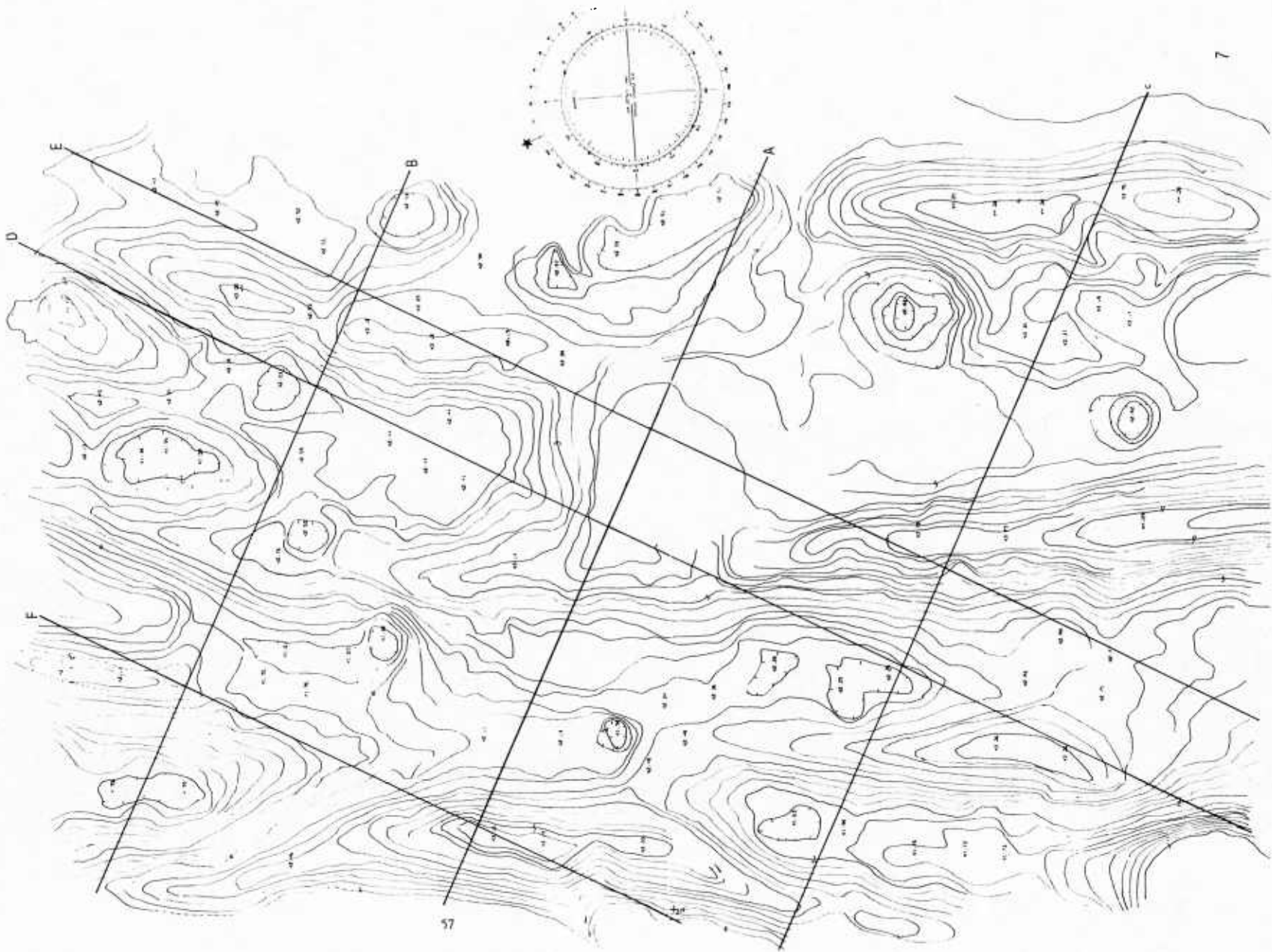


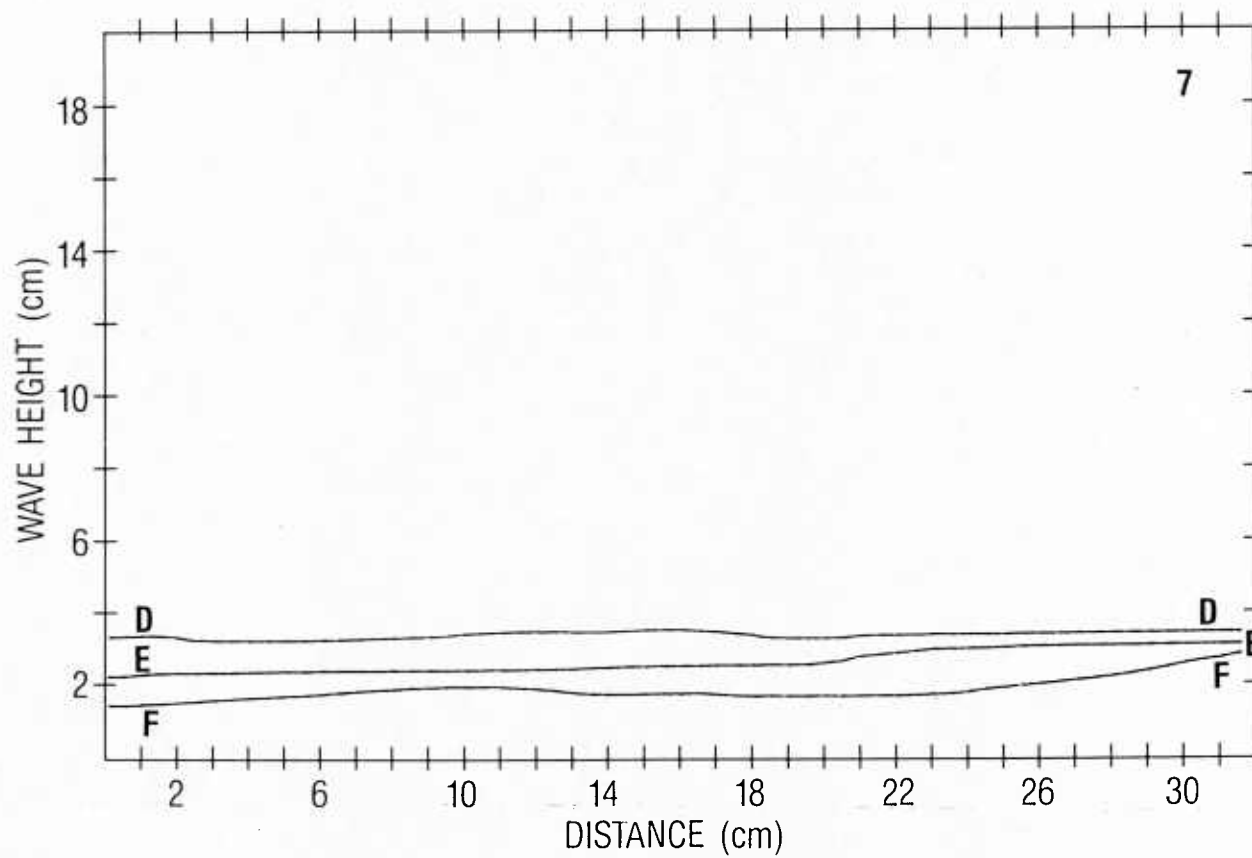
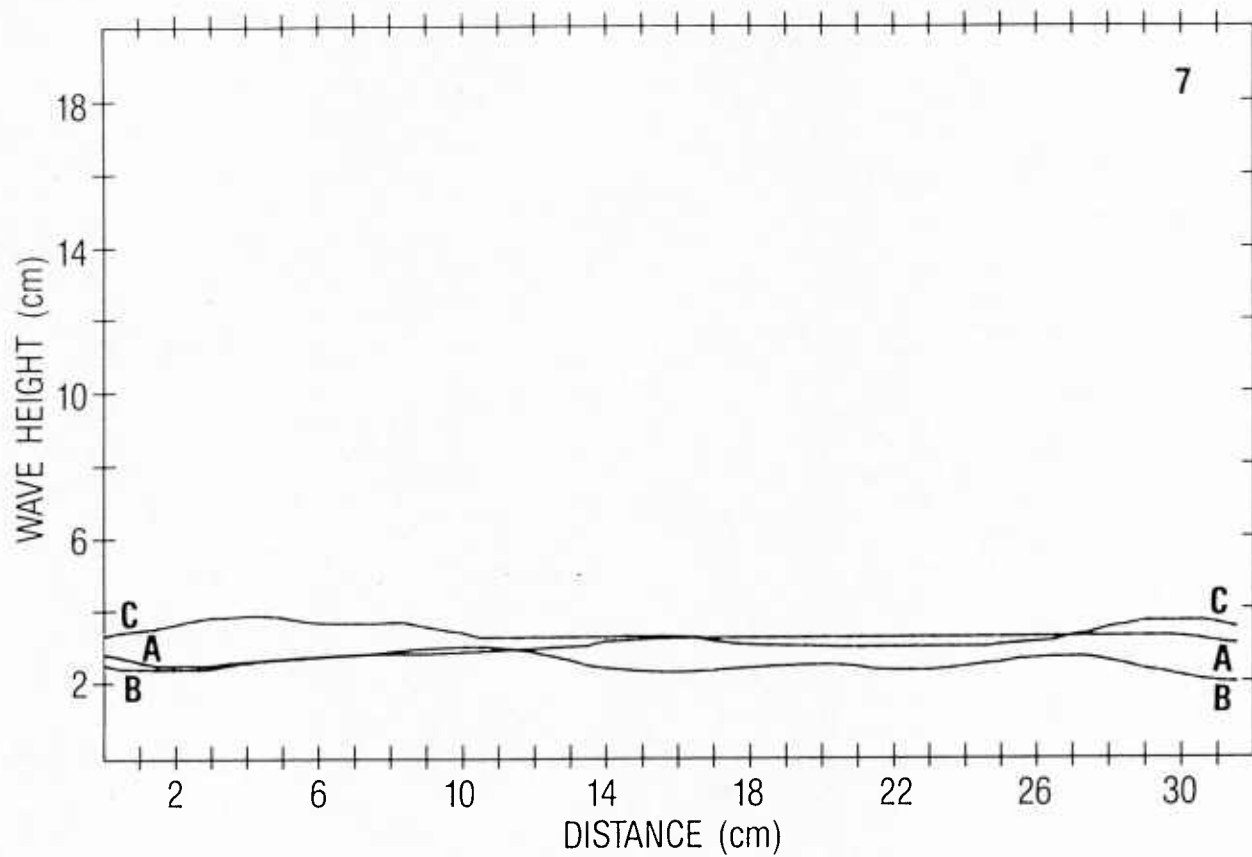


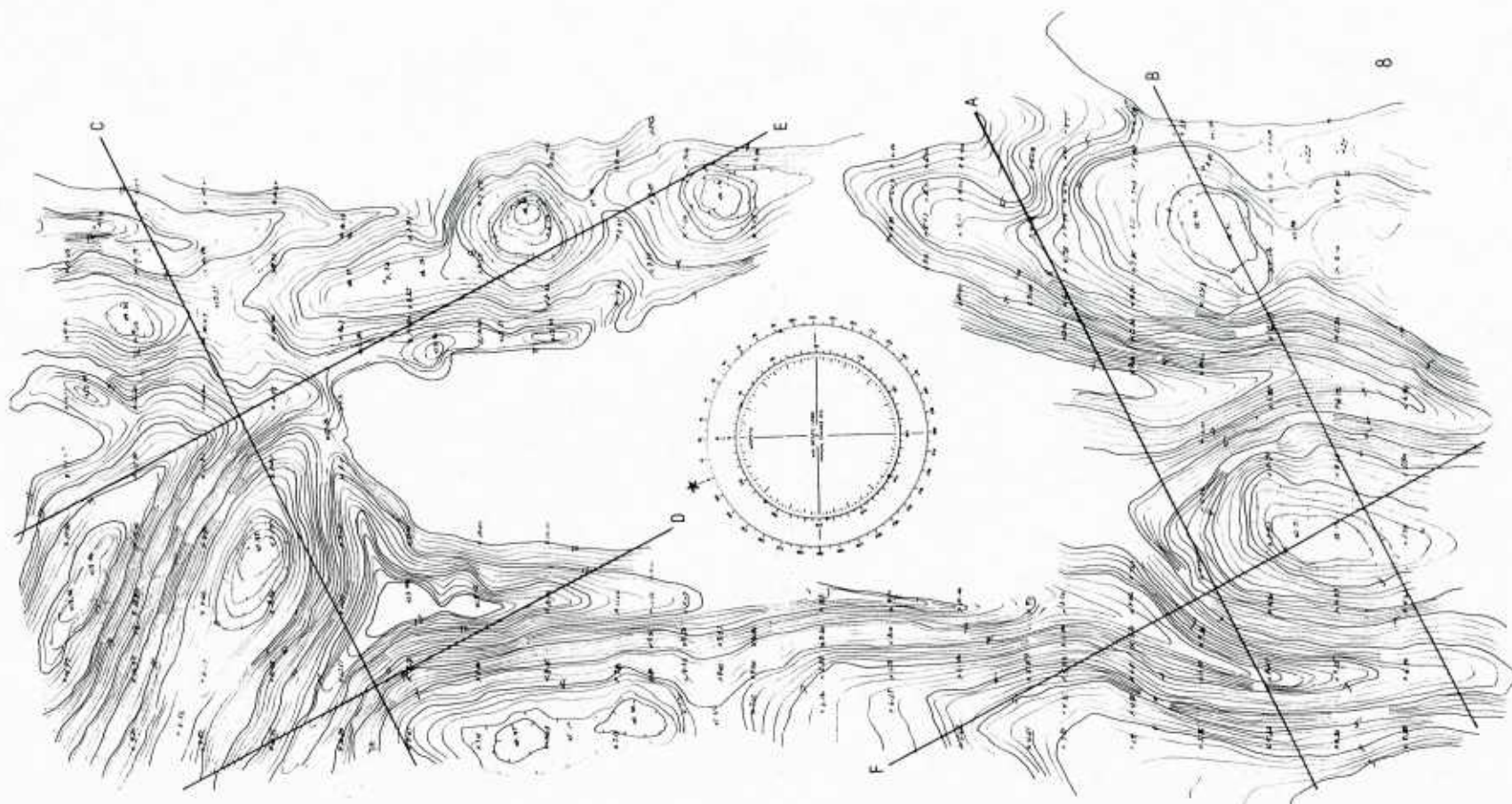


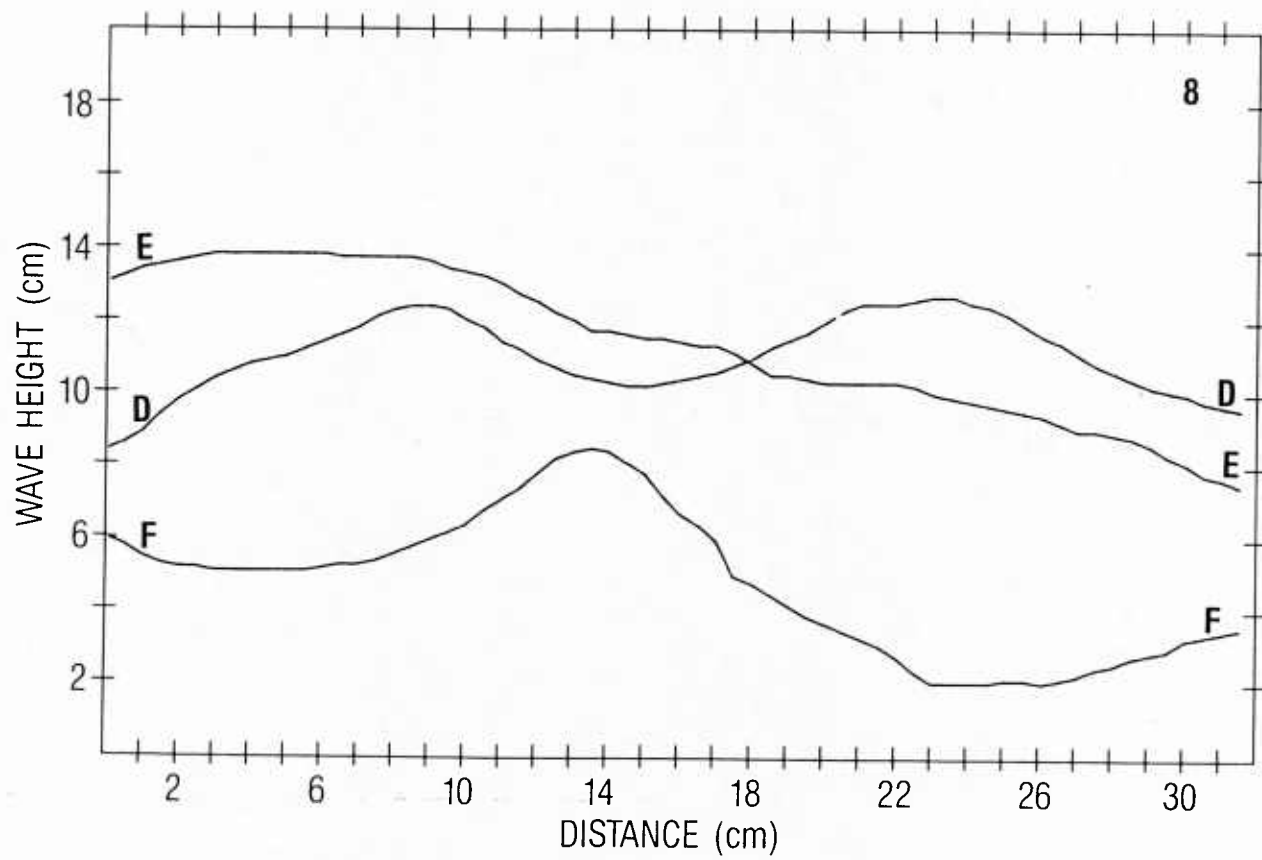
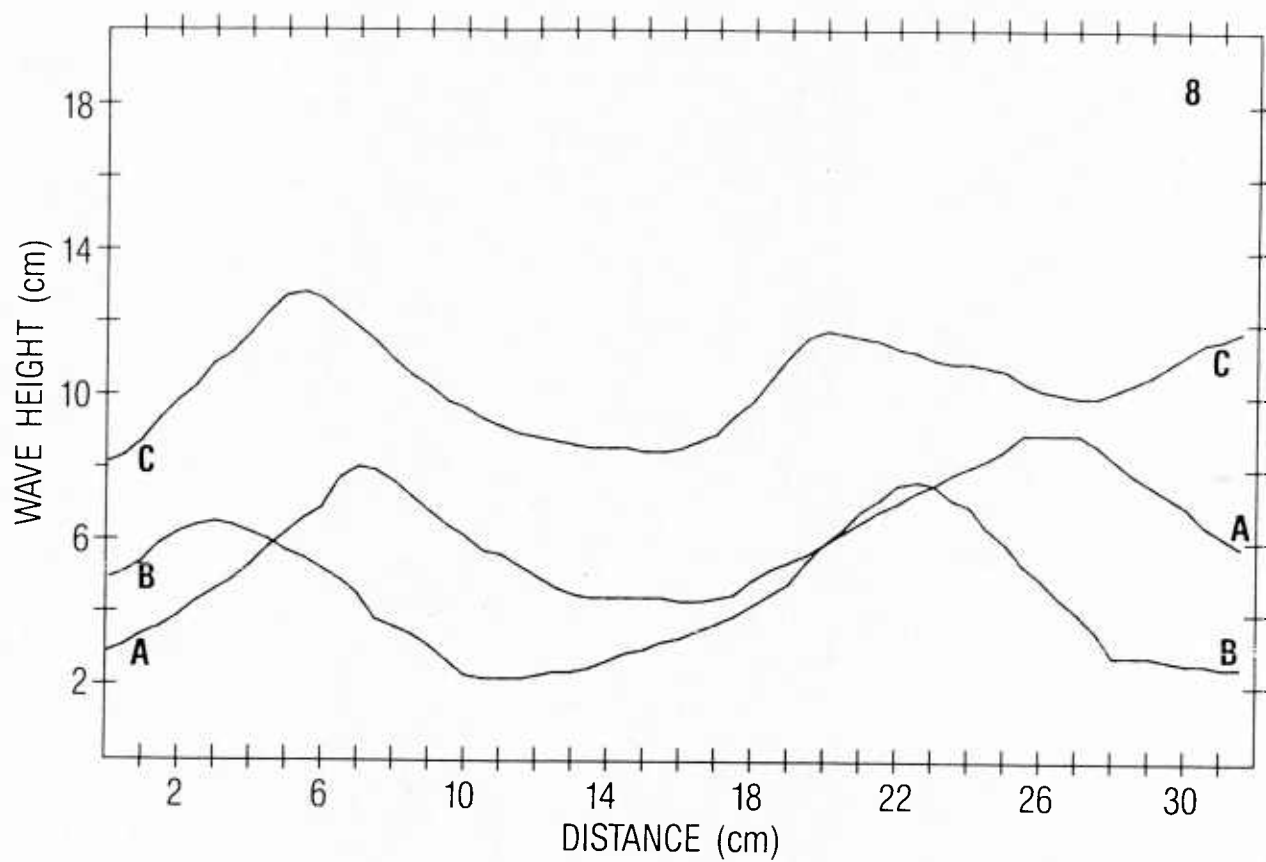


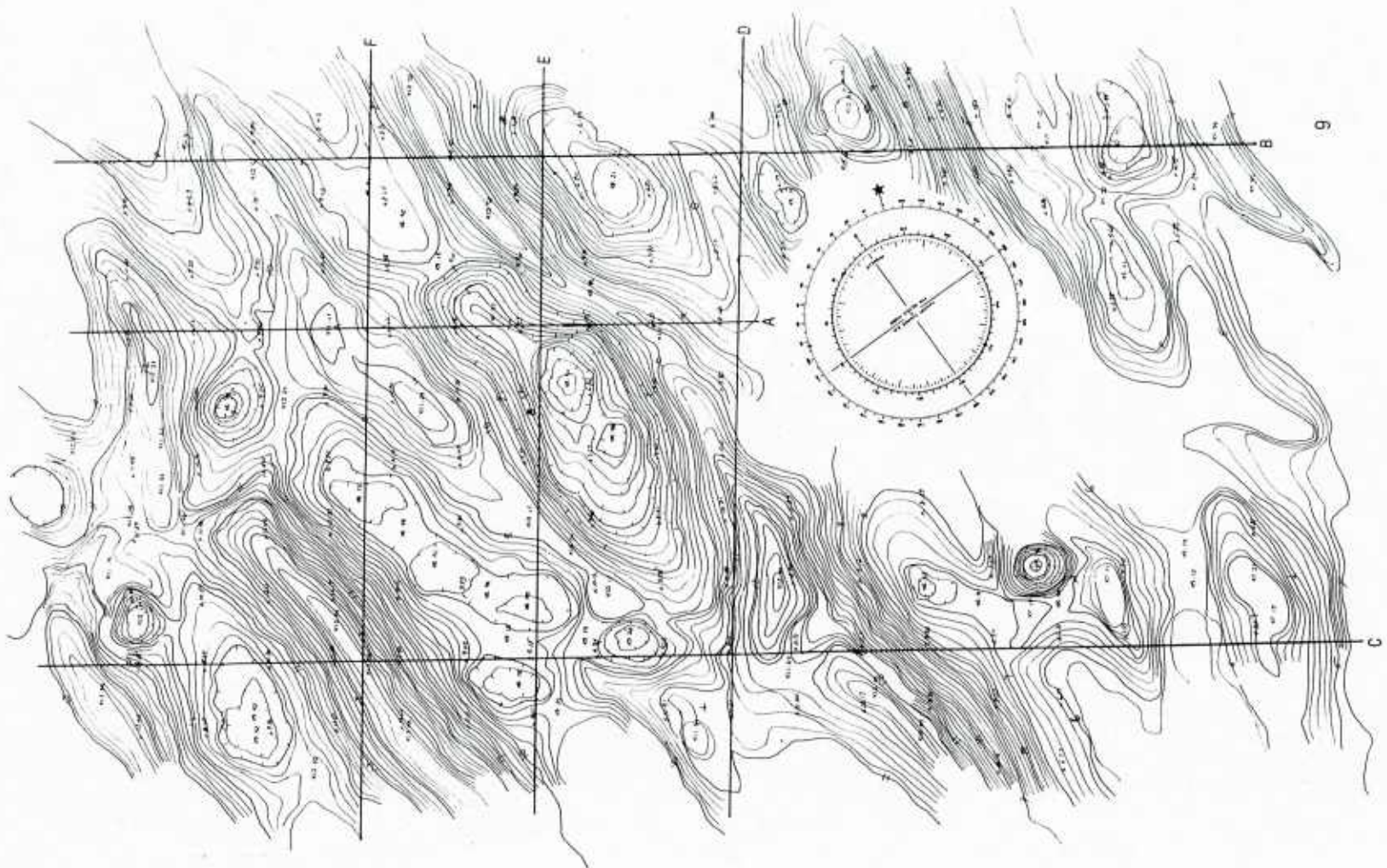


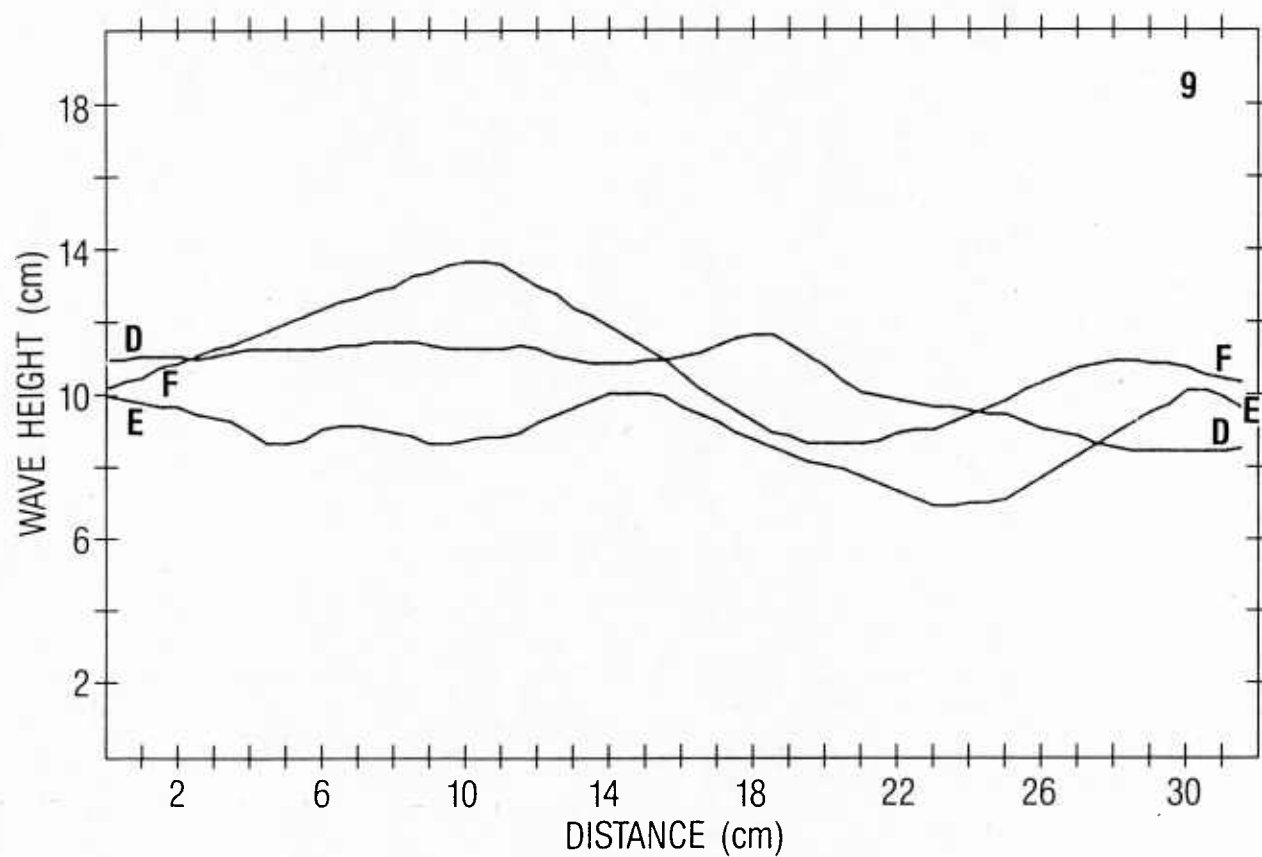
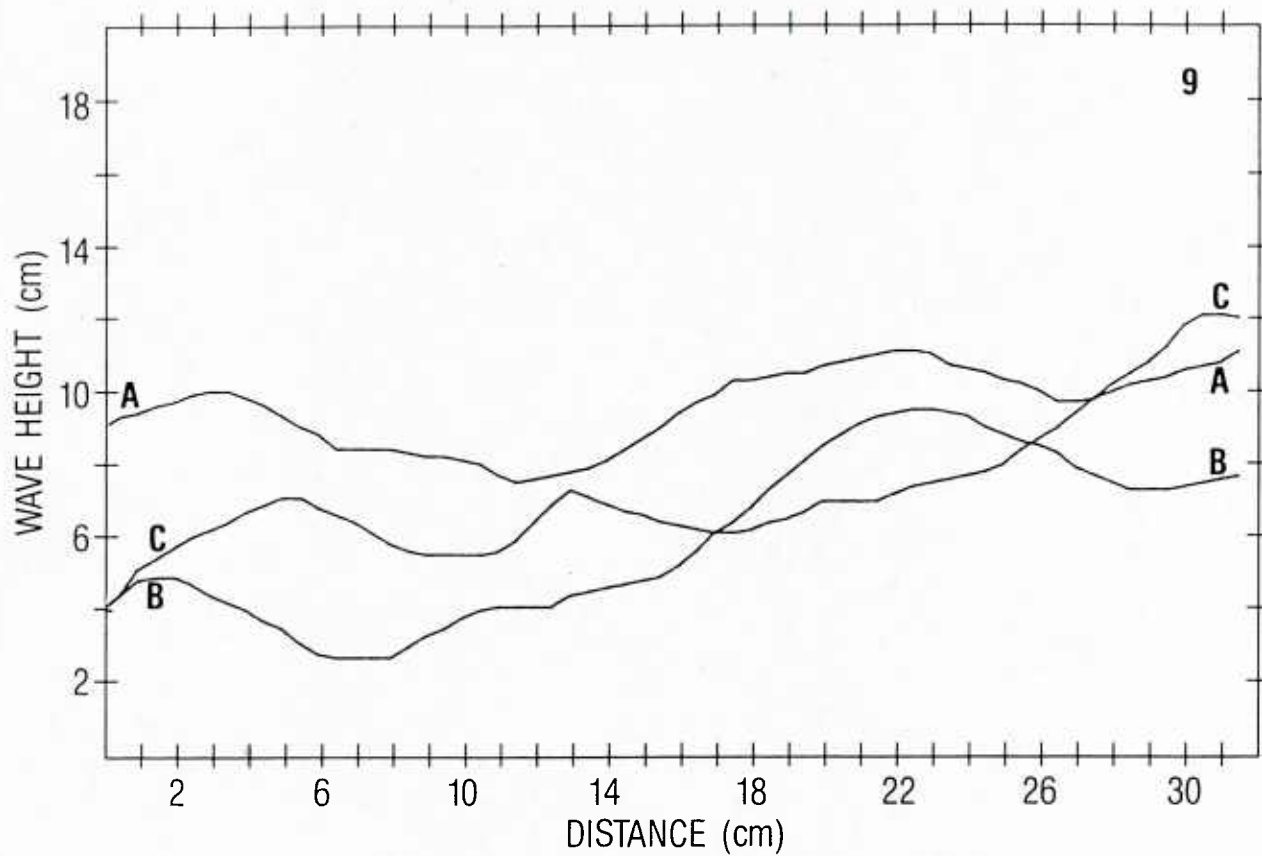


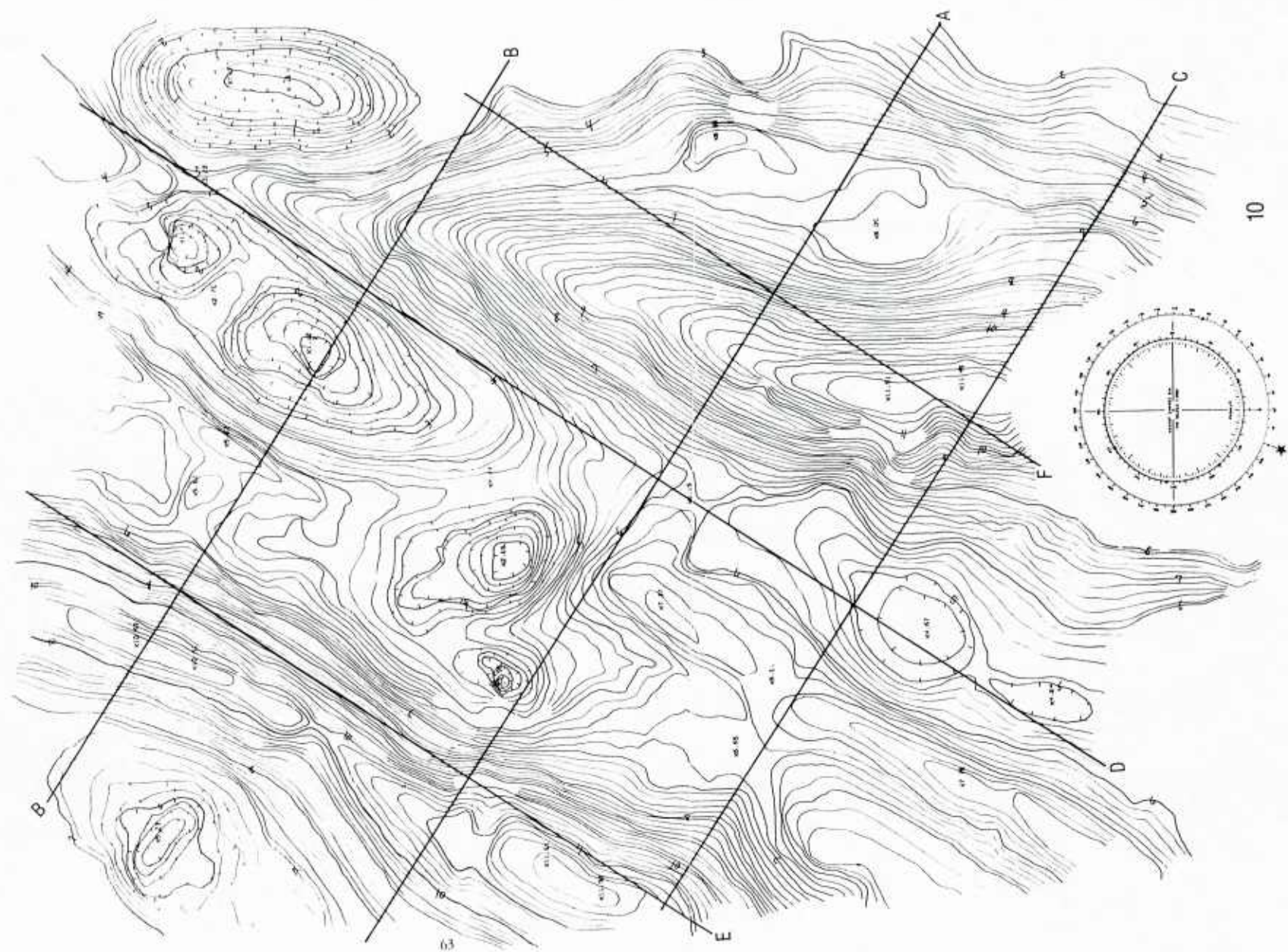


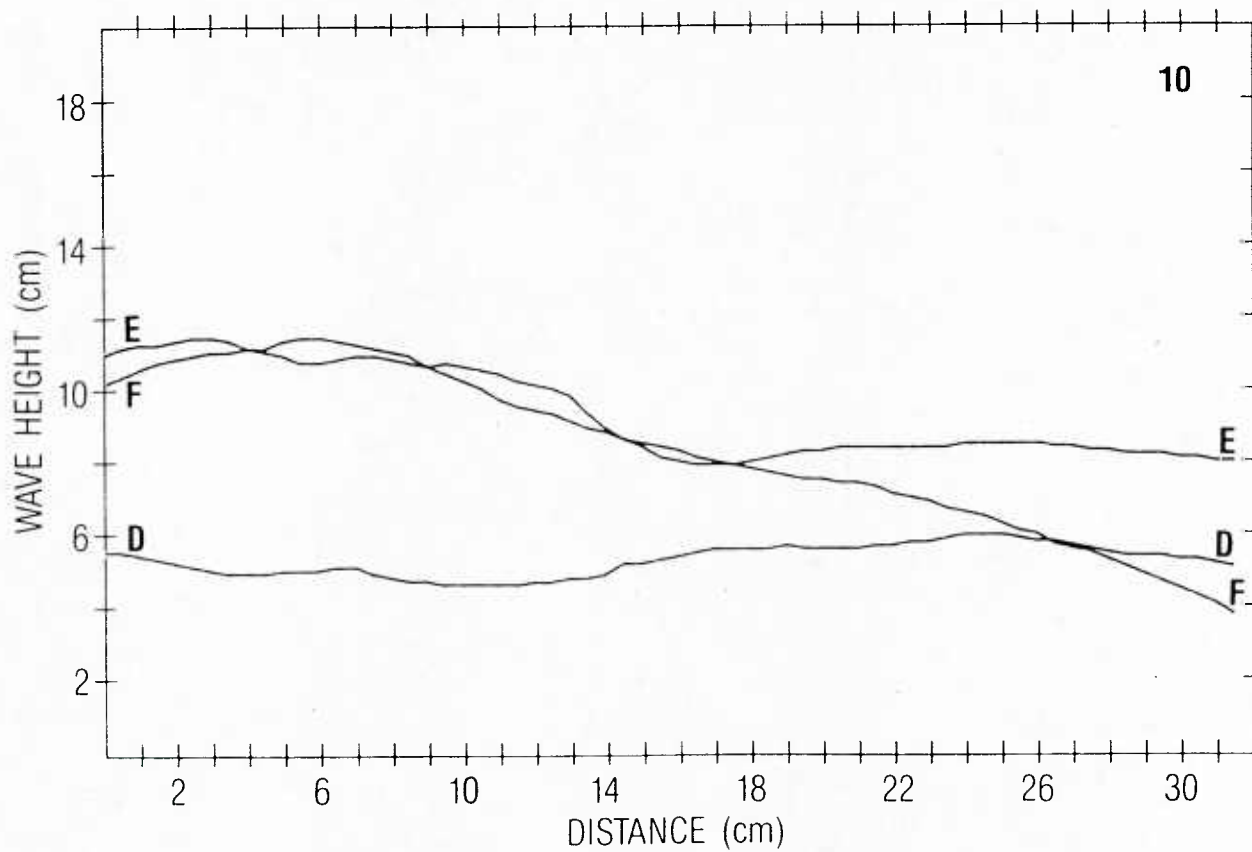
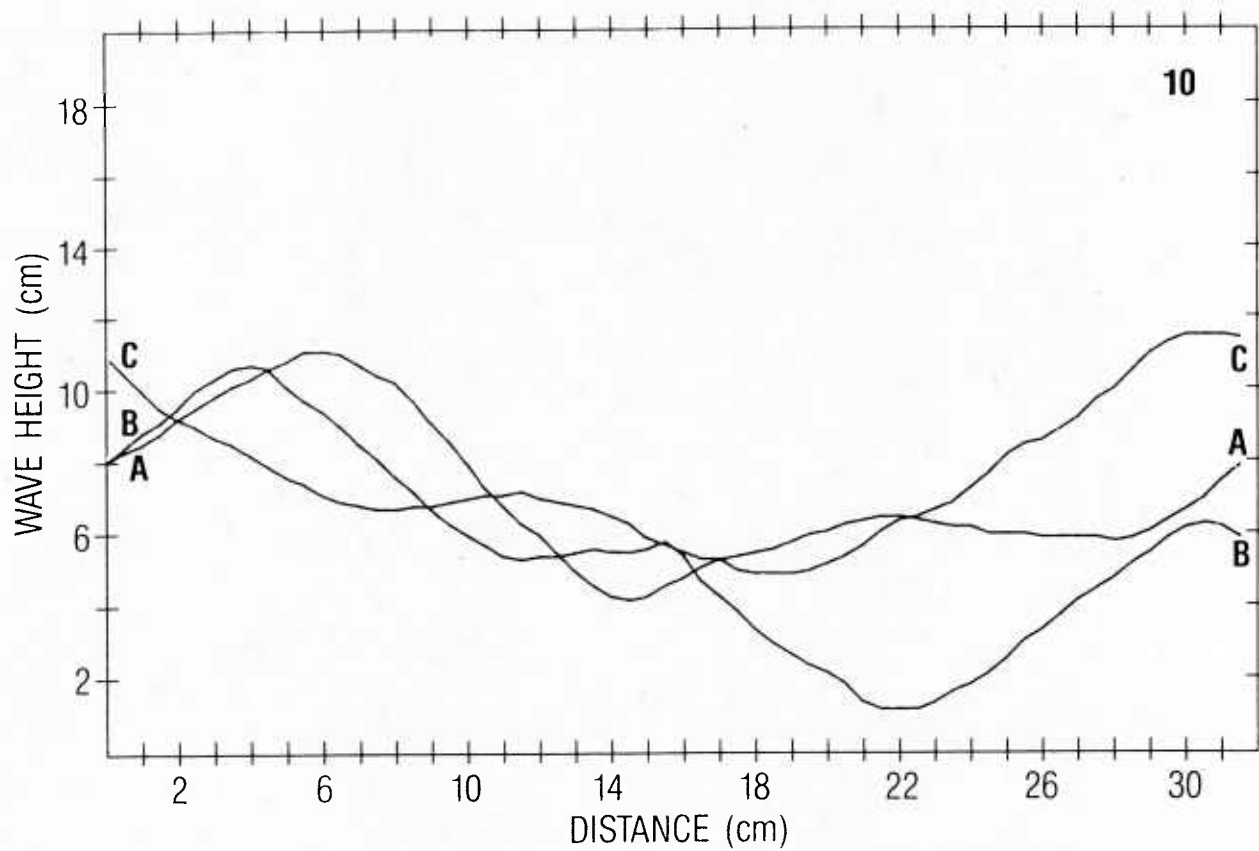


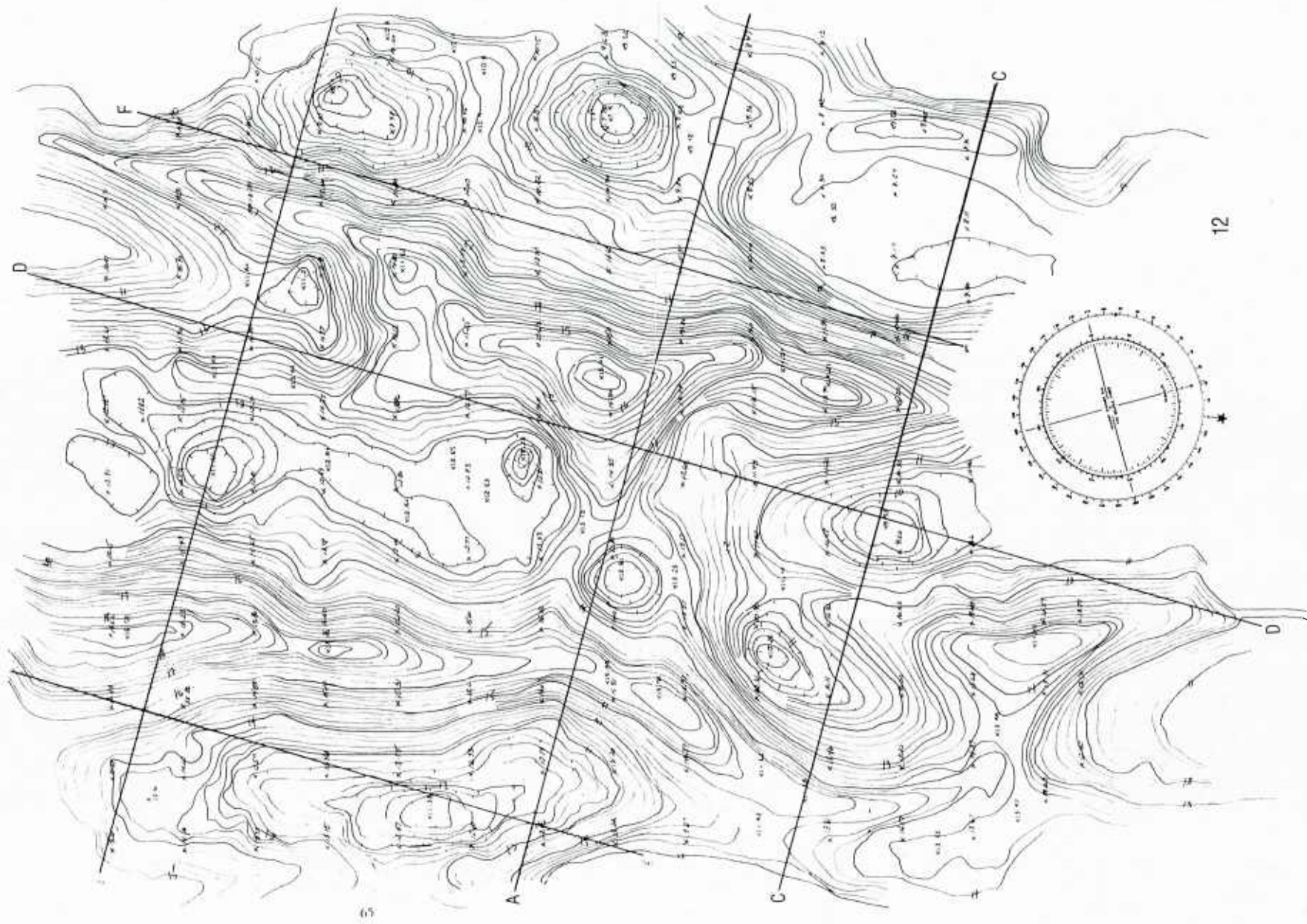


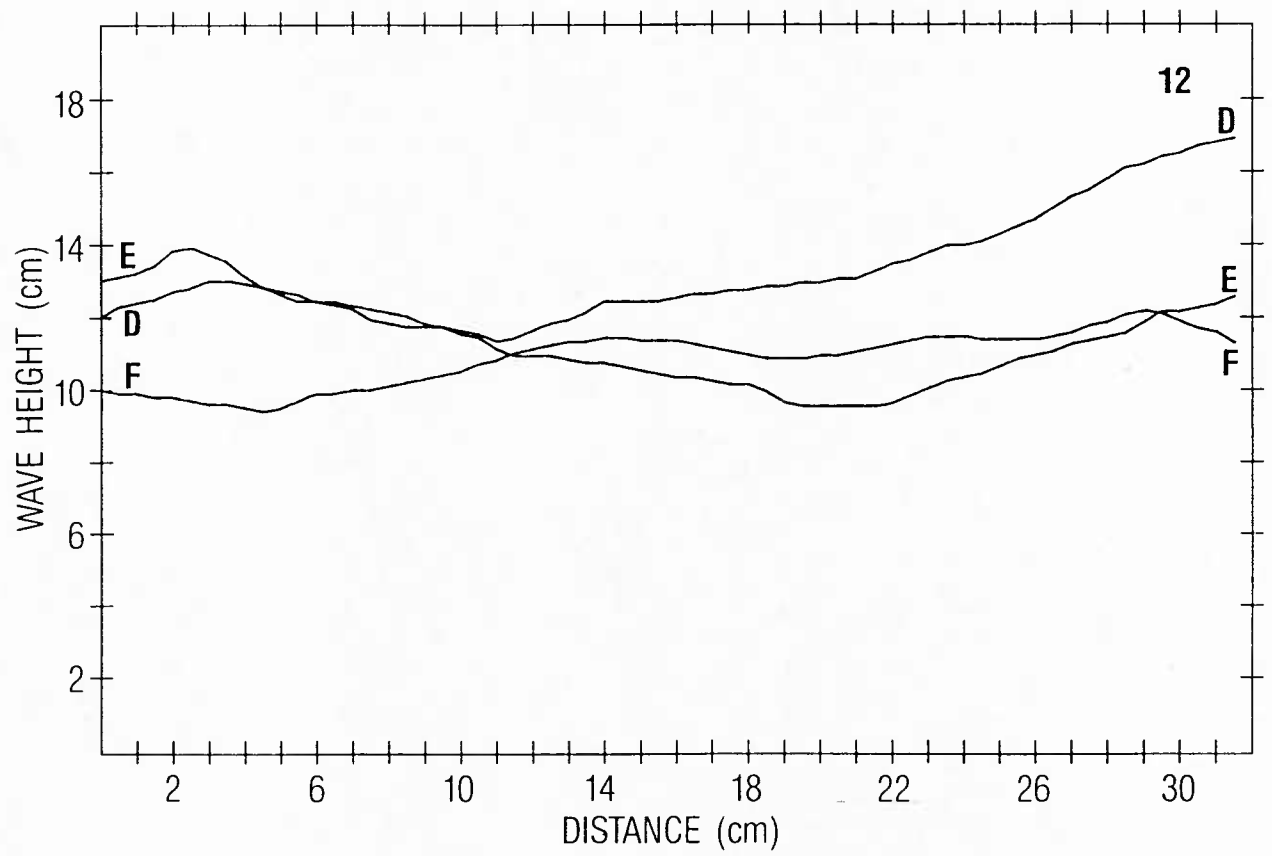
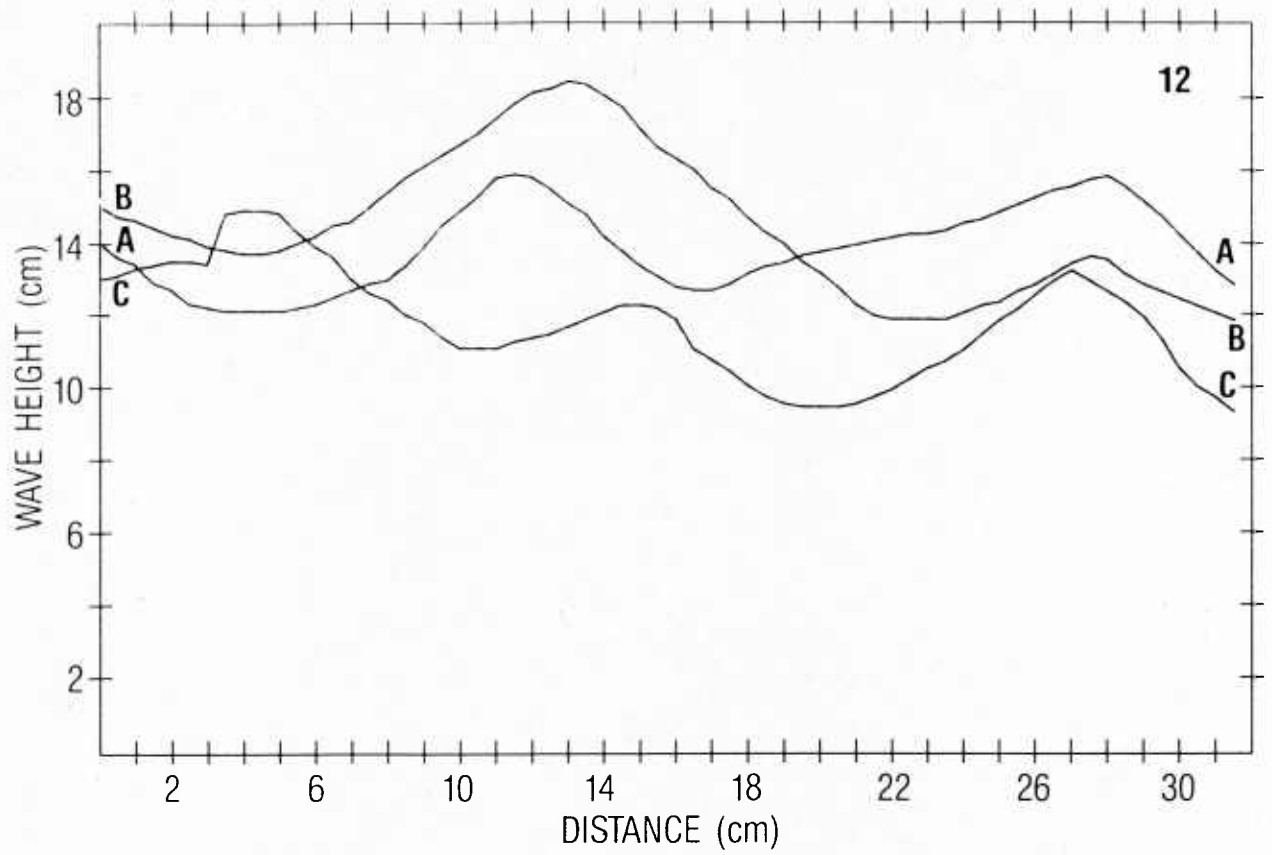


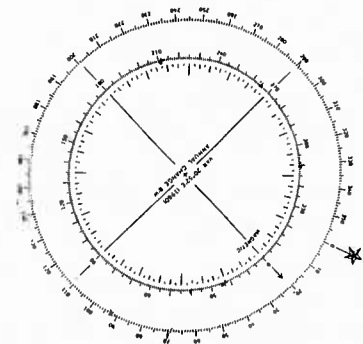
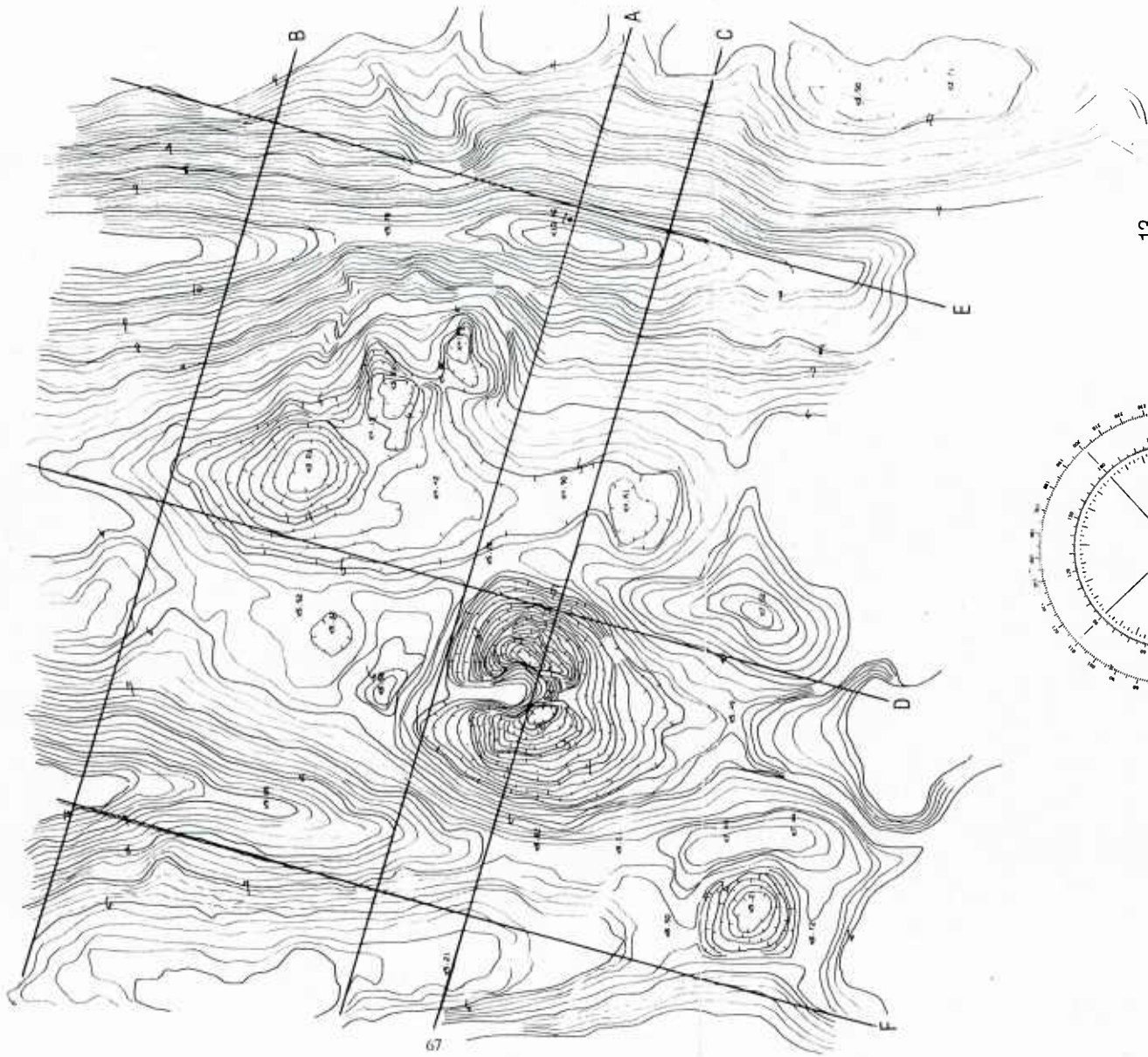


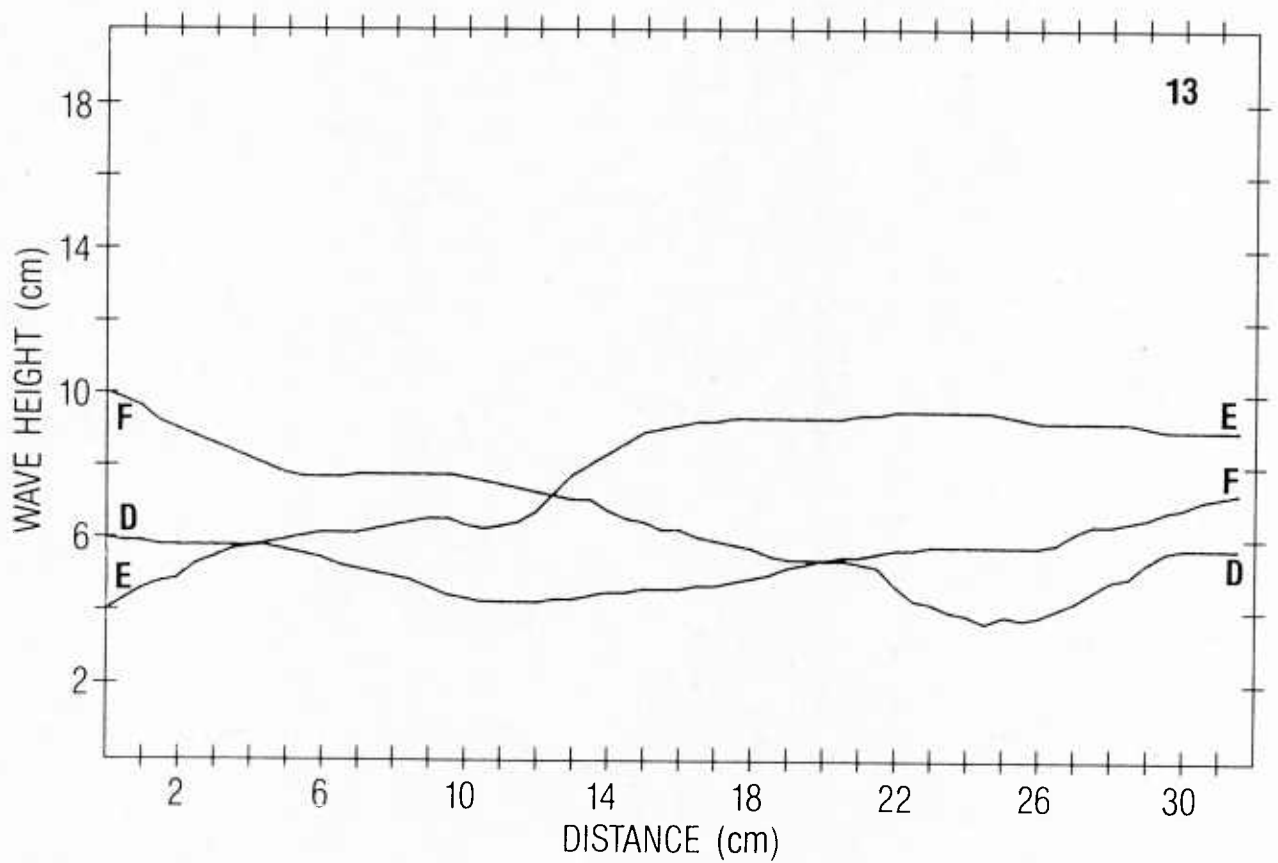
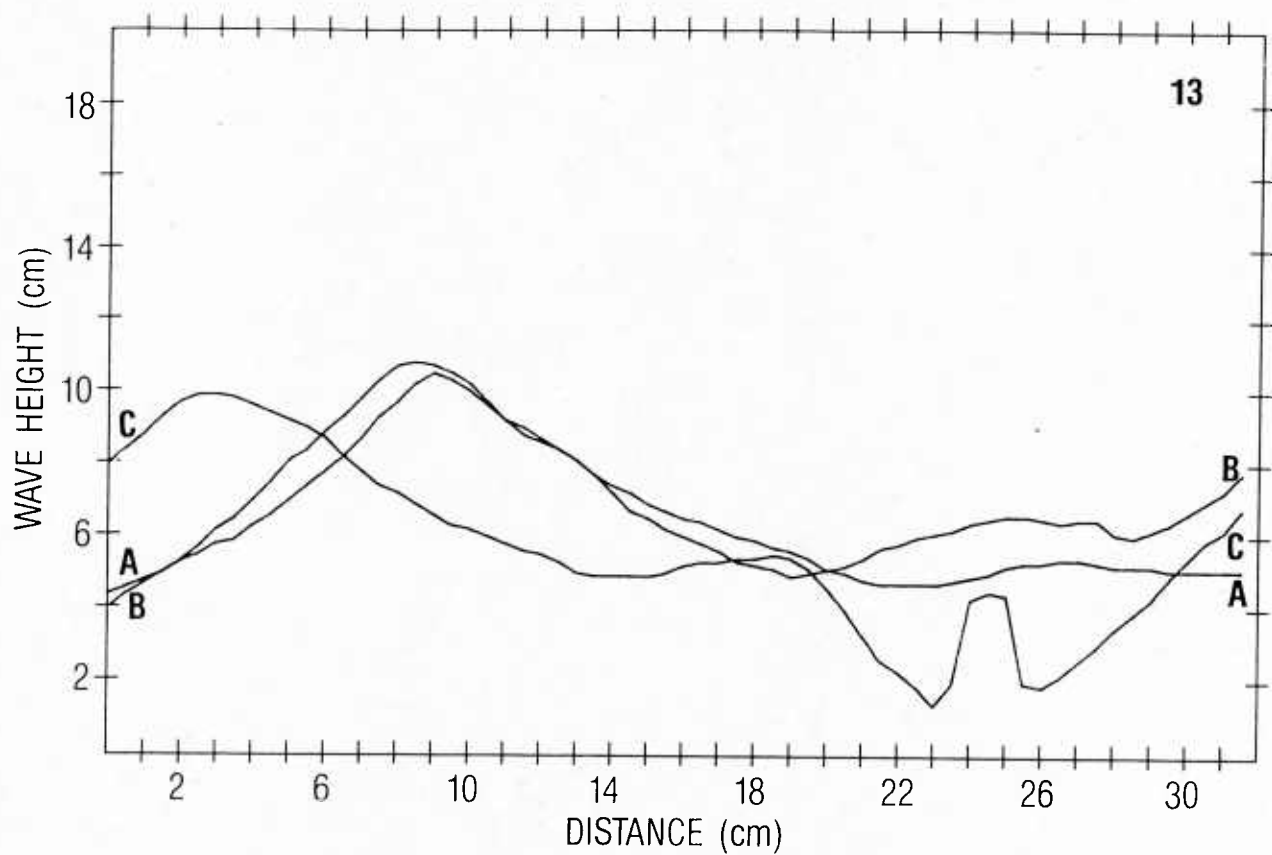




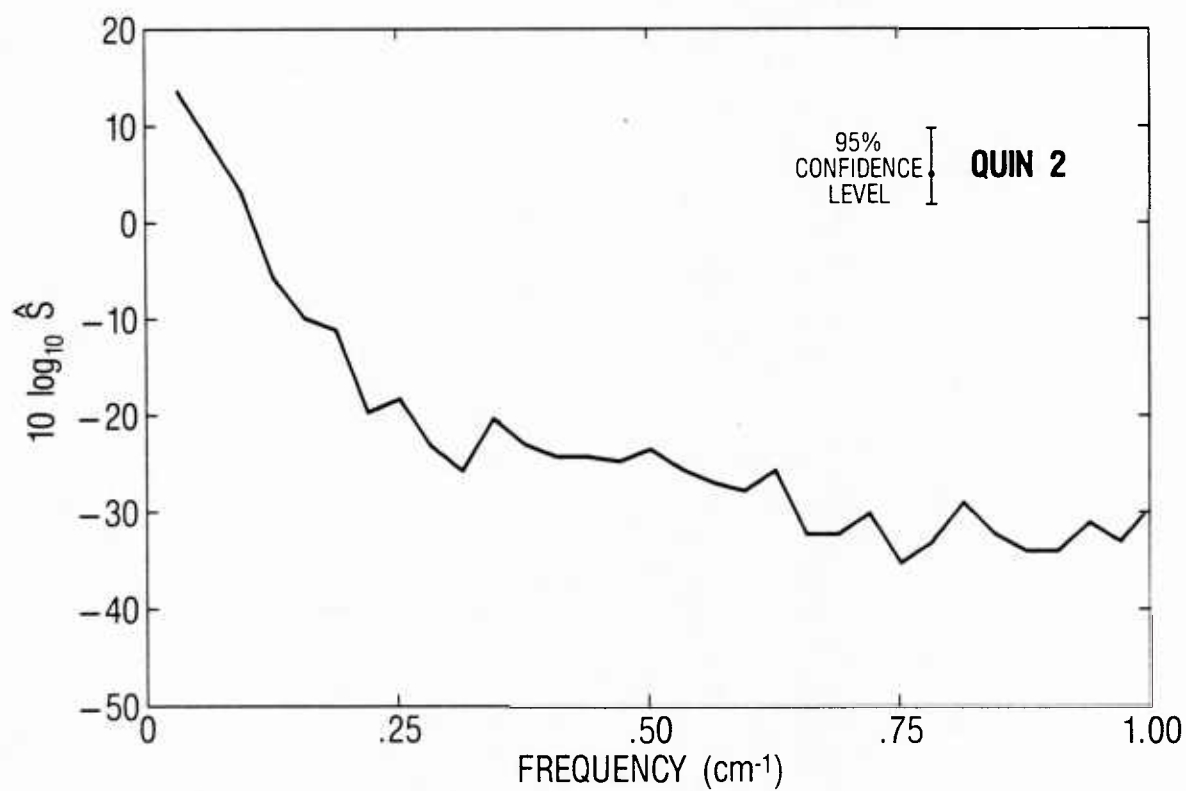
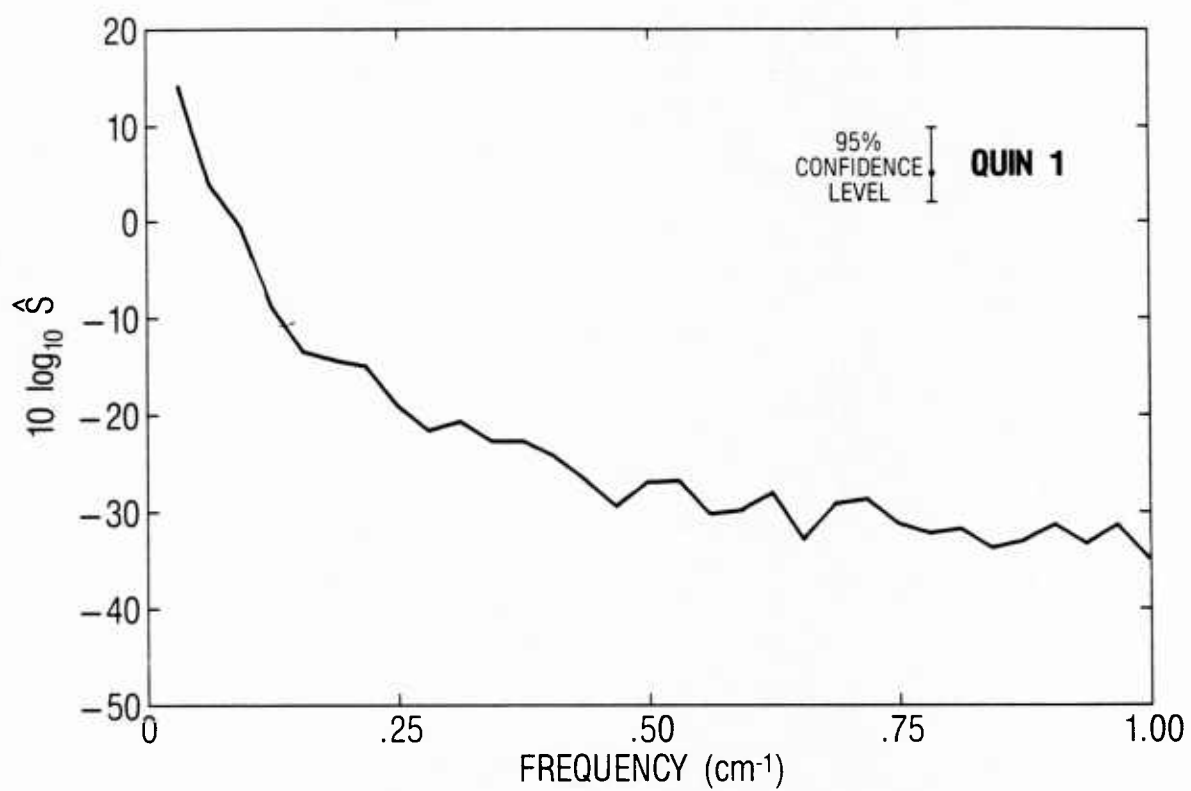


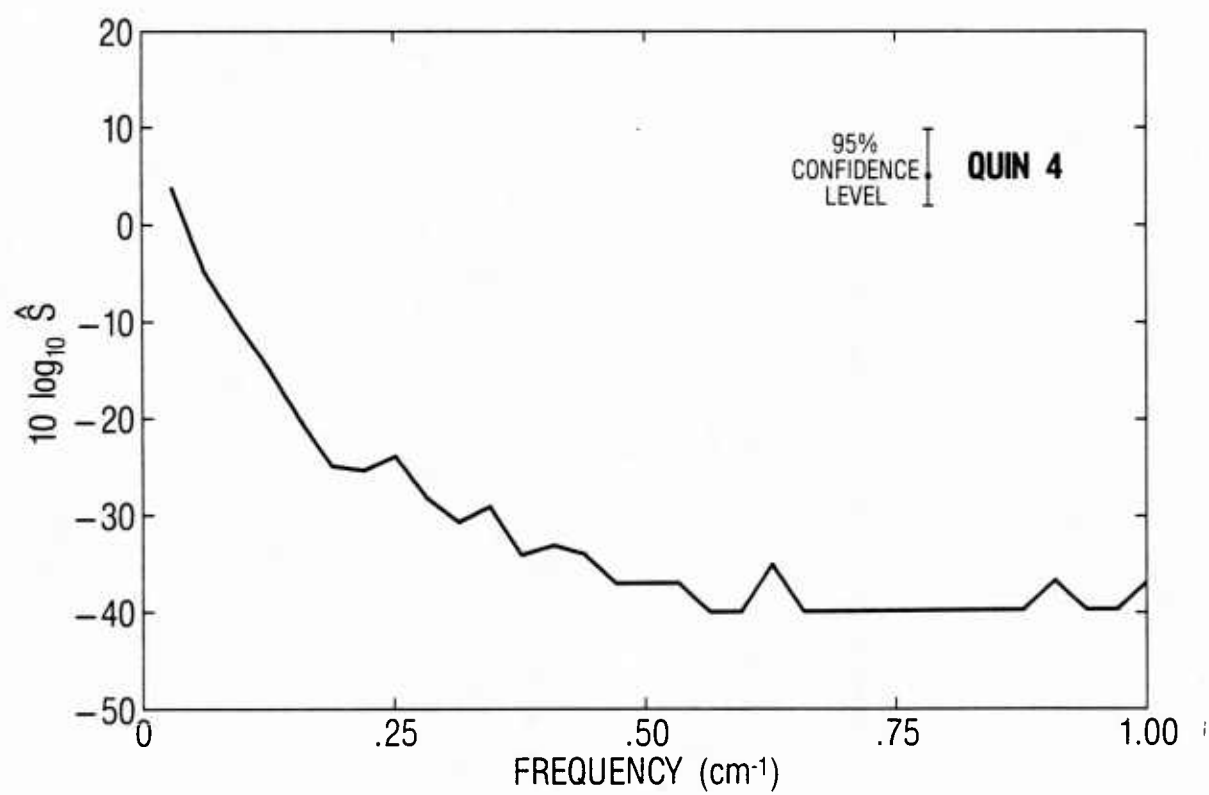
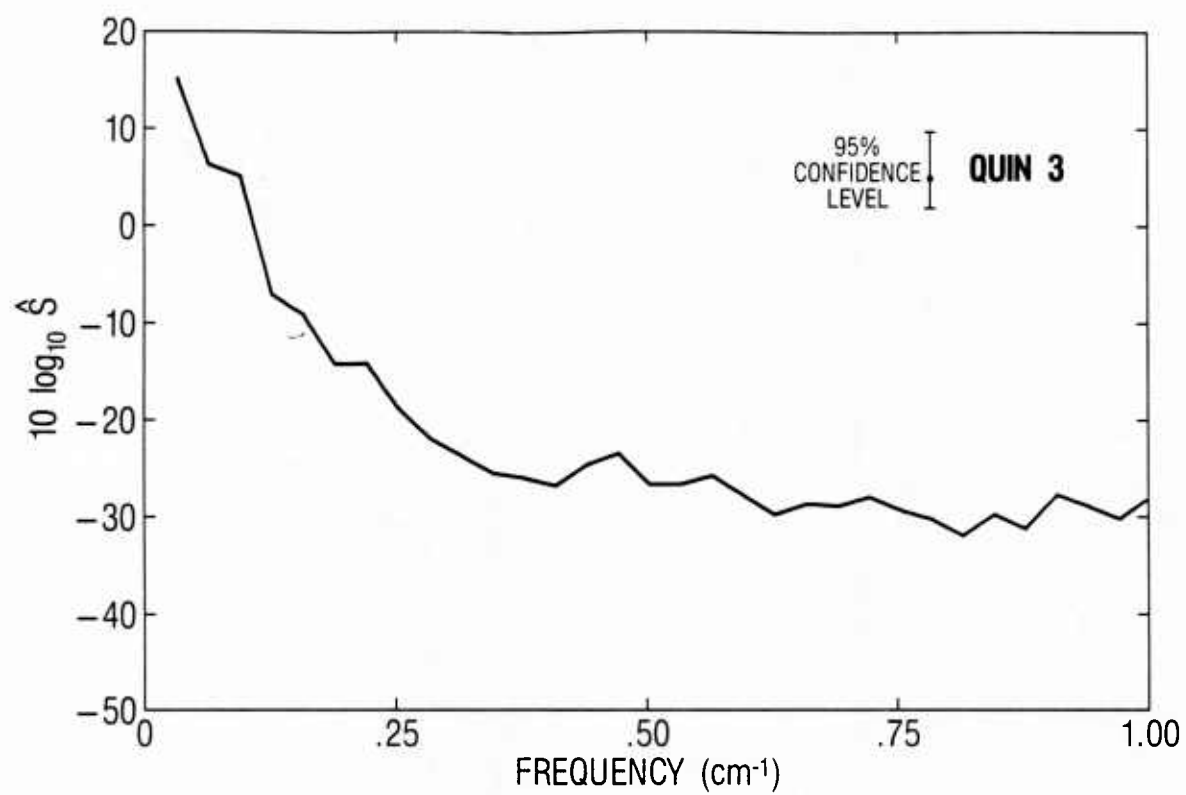


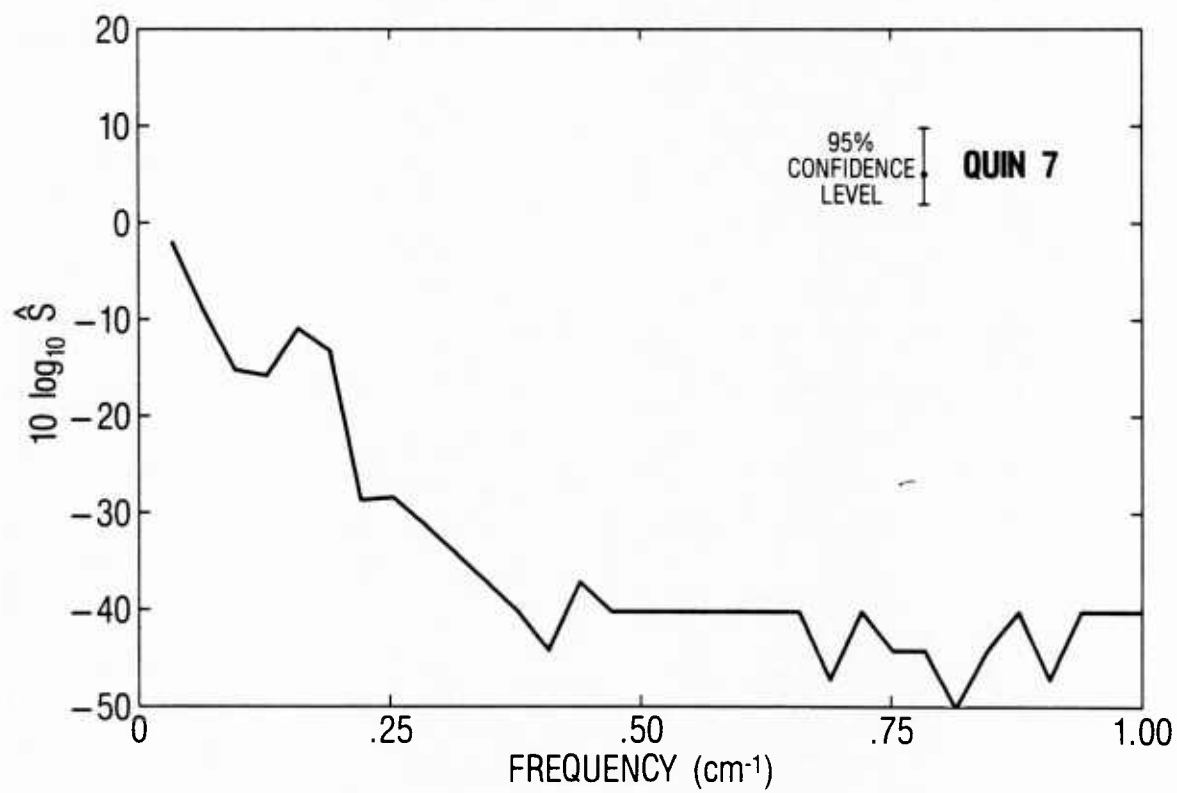
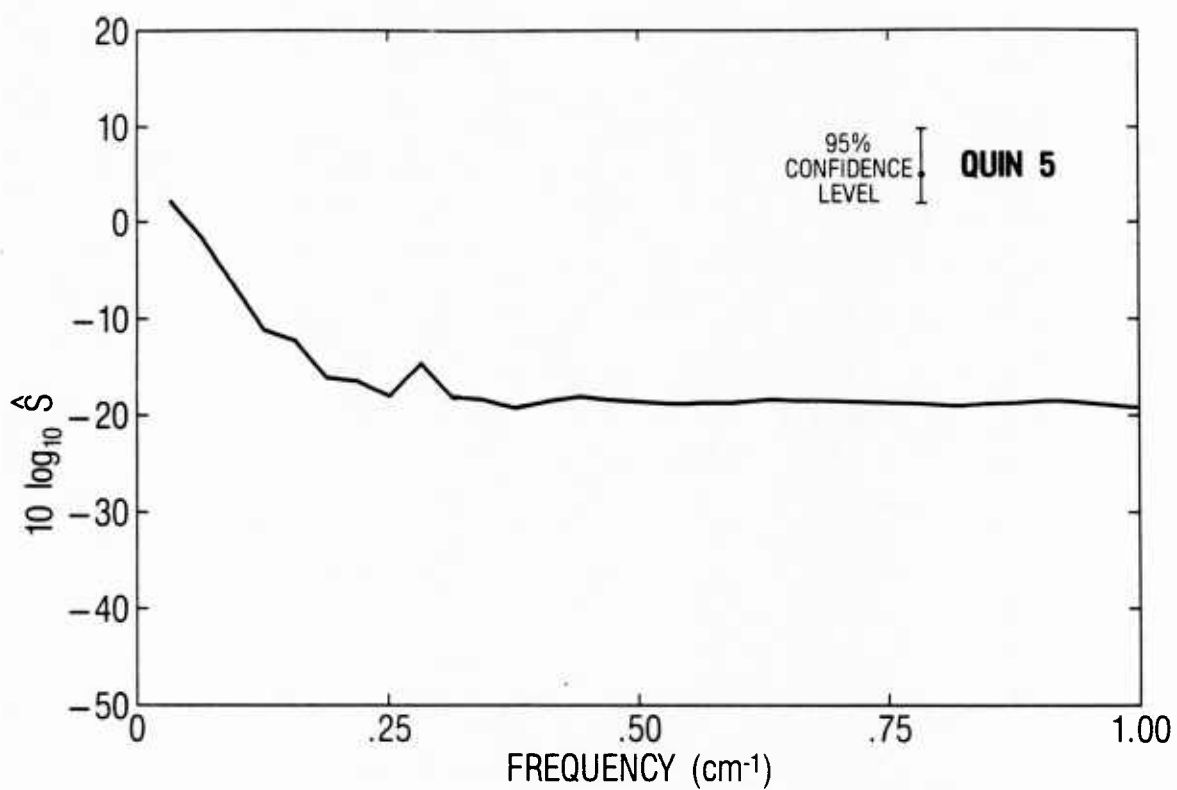


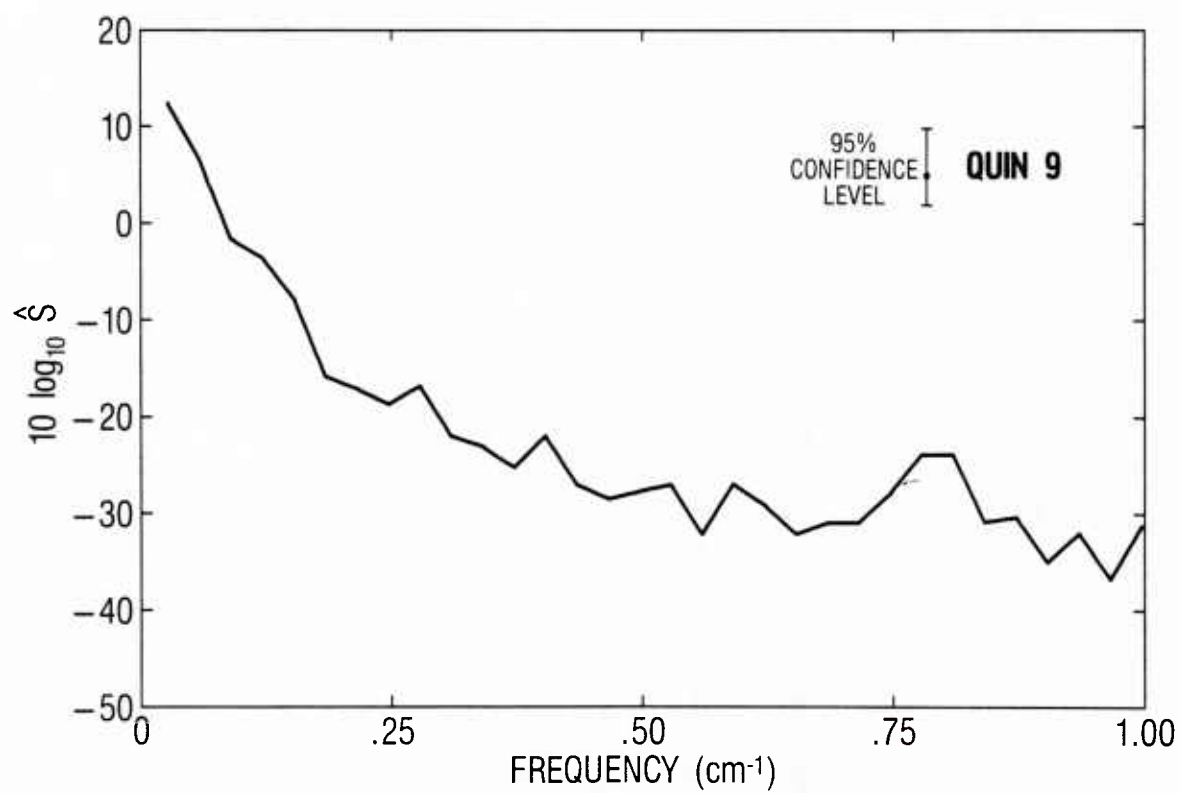
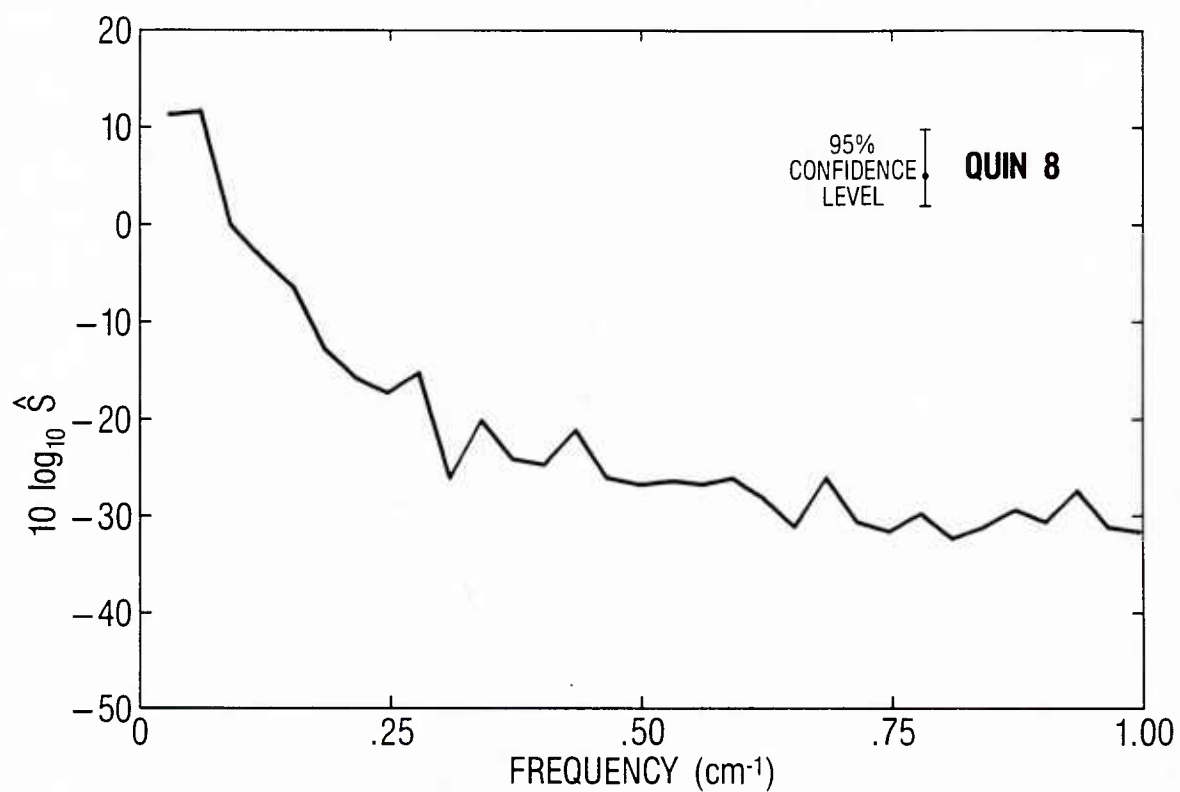


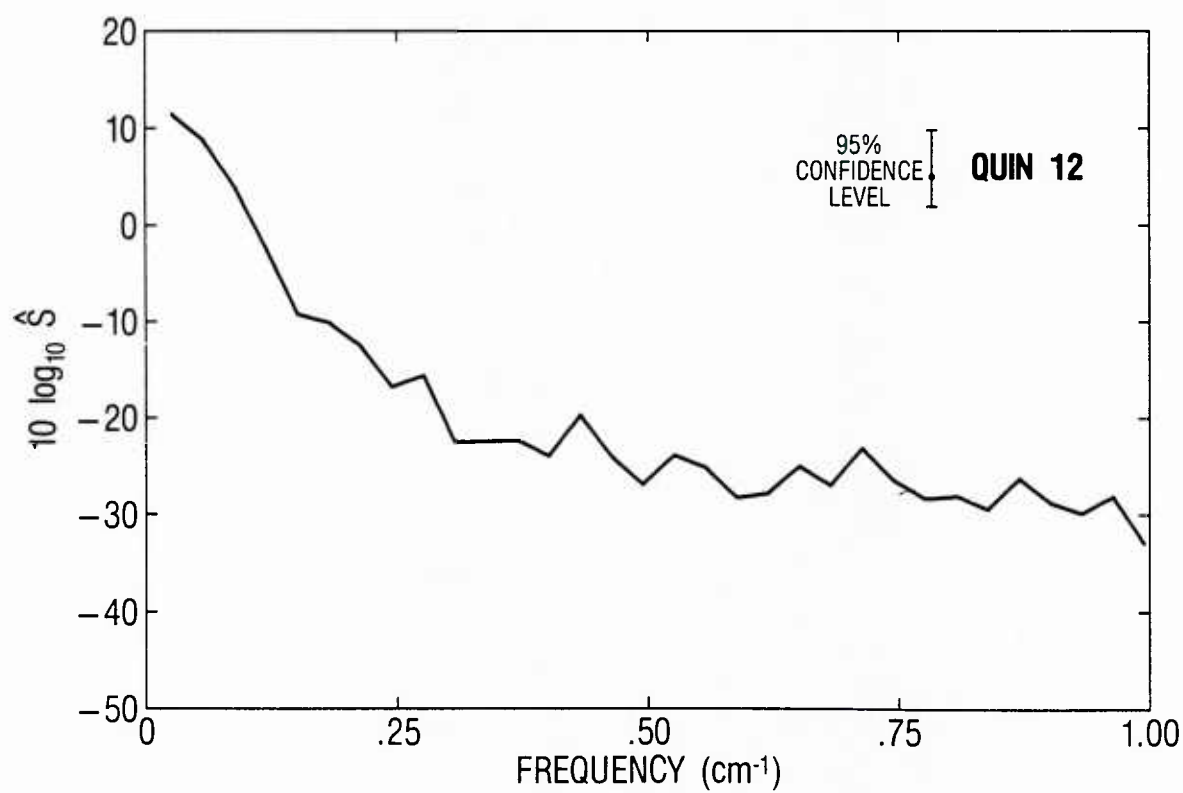
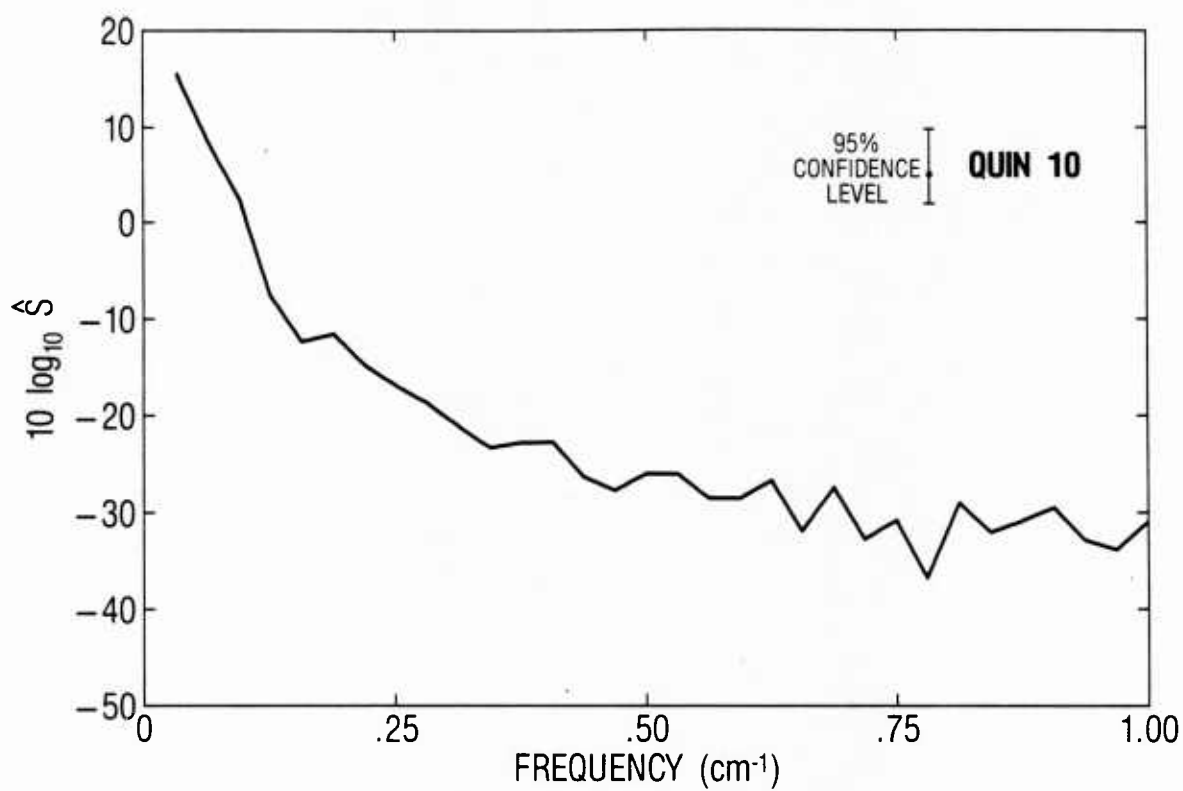
Appendix D. Power spectral density functions from individual photographs

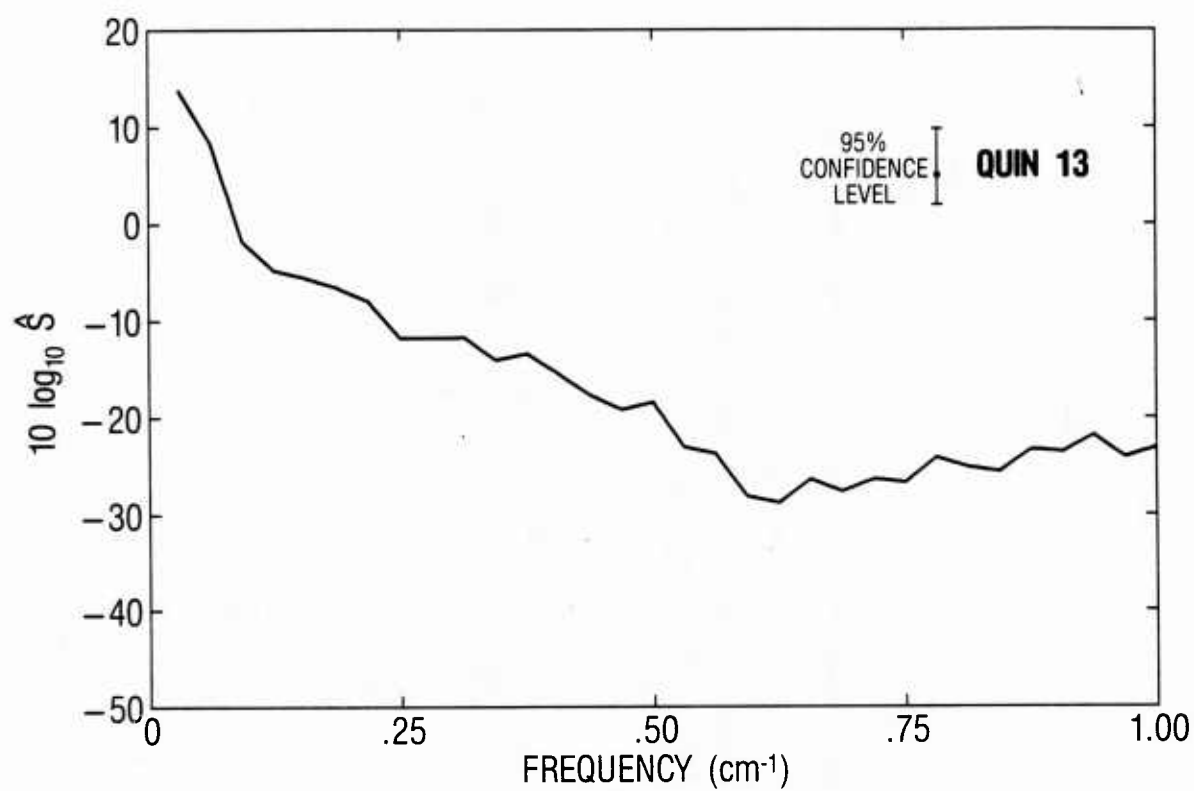












DUDLEY KNOX LIBRARY - RESEARCH REPORTS



5 6853 01015975 9

U224784